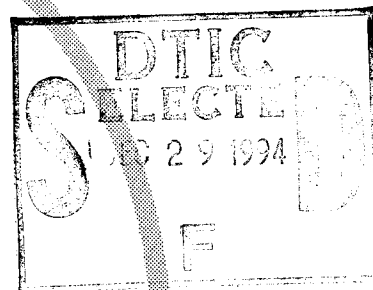# Precision Landing Systems Mathematical Modeling Study Report for Andrews Air Force Base, Runway 19L Camp Springs, Maryland
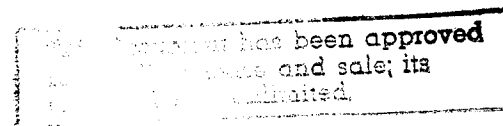
Jesse Jones

November 1994

DOT/FAA/CT-TN93/35

This document is available to the public
through the National Technical Information
Service, Springfield, Virginia 22161.

19941223 045

NOTICE

This document is disseminated under the sponsorship of the U.S. Department of Transportation in the interest of information exchange. The United States Government assumes no liability for the contents or use thereof.

The United States Government does not endorse products or manufacturers. Trade or manufacturers' names appear herein solely because they are considered essential to the objective of this report.

Technical Report Documentation Page

1. Report No. DOT/FAA/CT-TN93/35	2. Government Accession No.	3. Recipient's Catalog No.
4. Title and Subtitle Precision Landing System Mathematical Modeling Study Report for Andrews Air Force Base, Runway 19L, Camp Springs, MD		5. Report Date November 1994
		6. Performing Organization Code ACD-330
7. Author(s) Jesse Jones, ACD-330, and Elliott Rushton and Ronald Lockhart, Raytheon Service Co.		8. Performing Organization Report No. DOT/FAA/CT-TN93/35
9. Performing Organization Name and Address U.S. Department of Transportation Federal Aviation Administration Technical Center Atlantic City International Airport, NJ 08405		10. Work Unit No. (TRAIS)
		11. Contract or Grant No. T06031
12. Sponsoring Agency Name and Address		13. Type of Report and Period Covered Technical Note June - July, 1993
		14. Sponsoring Agency Code

15. Supplementary Notes

This effort was performed in cooperation with FAA Technical Center (ACD-330) personnel and project personnel from Raytheon Service Company in Pleasantville, New Jersey.

16. Abstract

This technical note describes Microwave Landing System (MLS) and Precision Distance Measuring Equipment (DME/P) mathematical modeling performed for runway 19L, Andrews Air Force Base (ADW), Camp Springs, Maryland. This study evaluates the effects of scattering and shadowing from selected buildings, hangars, aircraft, and terrain. Results are provided as plots illustrating the predicted multipath levels, separation angles, and the resulting error plots from the worst case contributors.

Scenarios were modeled to determine the effects of the multipath sources in the modeled environment. These resulting errors were analyzed and compared to error tolerances (FAA-STD-022d) to determine if the errors are acceptable. The effects of the ADW environment were analyzed and evaluated. It was determined that the proposed site will perform satisfactorily with no changes.

17. Key Words Andrews Air Force Base (ADW), Microwave Landing System (MLS), Precision Distance Measuring Equipment (DME/P), Mathematical Modeling	18. Distribution Statement This documentation is available to the public through the National Technical Information Service, Springfield, Virginia 22161	
19. Security Classif. (of this report) Unclassified	20. Security Classif. (of this page) Unclassified	21. No. of Pages 128	22. Price

Form DOT F 1700.7 (8_72)   Reproduction of completed page authorized

TABLE OF CONTENTS

TABLE OF CONTENTS (CONTINUED)

APPENDIXES

LIST OF ILLUSTRATIONS

v

EXECUTIVE SUMMARY

The United States Air Force plans to install a Microwave Landing System (MLS) to serve runway 19L at Andrews Air Force Base, Camp Springs, Maryland. The quality of approach guidance provided by an MLS may be adversely affected by terrain and objects in the approach environment. A computer-based mathematical model was used to study MLS performance in the proposed environment. Based on this study, the MLS is predicted to perform well within applicable tolerances and provide satisfactory service to runway 19L.

1. INTRODUCTION.

1.1 Purpose of Report.

The purpose of this effort was to quantify the magnitude of the derogation that may be caused to the guidance provided by the proposed Microwave Landing System (MLS) and Precision Distance Measuring Equipment (DME/P) installations by characteristics of the environment of runway 19L at Andrews Air Force Base (ADW), Camp Springs, Maryland.

1.2 Overview of Report.

The quality of guidance provided by a MLS-DME/P installation at an airport may be derogated by multipath interference caused by shadowing (blockage) or scattering from objects in the approach environment. Objects such as buildings, aircraft, irregular terrain and trees are examples of such multipath sources. These multipath signals can translate into errors in the position information provided to the approaching aircraft by the MLS-DME/P installation. The Federal Aviation Administration (FAA) has established safety tolerances on the magnitude and frequency of the errors that may be present in these guidance signals.

A computer-based mathematical model has been established for evaluating the effects of characteristics in the approach environment on the guidance quality provided by the MLS-DME/P installation. This model has been repeatedly used to predict these effects and has been used for siting proposed MLS-DME/P installations.

This mathematical modeling study was performed to determine if the proposed installation (location, equipment type, orientation) will provide satisfactory service at ADW. Several scenarios simulating the environment present at this site were modeled to ascertain the magnitude of the error present in the provided guidance signals. The error predicted by the model is analyzed and compared to error tolerances specified in FAA-STD-022d.

Appendixes are included to present the graphical results obtained from this modeling study. Appendixes A, B, and C present selected graphs from modeling performed on the MLS azimuth (AZ), elevation (EL), and DME/P subsystems, respectively. Appendixes D through H contain data used to represent features of the airport environment pertinent to this modeling effort, such as irregular terrain and selected hangars. Introductions to the operation of the MLS, as well as the MLS-DME/P mathematical model are included as appendixes I and J, respectively. These appendixes give a brief overview to the theory of operation of the actual MLS operating systems, and how the model is utilized to predict their performance.

1

2. REFERENCES.

Airport Layout Plan: Master Plan, Andrews AFB (No reference #), December 1970

Airport Topography Map: Master Plan with 5' contours on TAB #C-1, Andrews AFB (No reference #), December 1970

Construction Drawings for Existing Buildings:

Hangar Maint., (SAM-2), Drawing #AW-3901-47, F-3307, A-1280

Addition to Hangar #3640, Code Ident. #80091, Y&D Drawing #1120191, F-5881, A-3640

Addition to Hangar #3640, Code Ident. #80091, Y&D Drawing #1120195, F-5885, A-3640

ADAL Aircraft Maint. Hangar, Code Ident. #80091, NAVFAC Drawing #3048743, A-3635

ADAL Aircraft Maint. Hangar, Code Ident. #80091, NAVFAC Drawing #3048749, A-3635

ADAL Aircraft Maint. Hangar, Code Ident. #80091, NAVFAC Drawing #3048750, A-3635

Aerial Port Training Facility, Code Ident. #80091, NAVFAC Drawing #3003864, A-3623

Aerial Port Training Facility, Code Ident. #80091, NAVFAC Drawing #3003807, A-3623

Aircraft Maintenance Facilities (NAS, NASVR), Spec. #ENG 49-080-60-22, Drawing #AW-16-06-879, F-4102, A-3158

Aircraft Maintenance Facilities, NAS Hangar Building, Spec. #ENG 49-080-60-22-(24), Drawing #AW-3901-40, F-4120, A-3158

Aircraft Maintenance Facilities, NAS Hangar Building, Spec. #ENG 49-080-60-22-(24), Drawing #AW-3901-40, F-4121, A-3158

US Naval Air Facility - Replace Roof Hangar 12 Building 3188, Code Ident. #80091, NAV Drawing #5830, A-3158

First Increment - NARTU Hangar Building, Spec. #ENG 49-080-59-62-(59), Drawing #AW-39-01-39, A-3148

Hangar Maintenance, Organization Addition, Building #3129, Code Ident. #80091, NAVFAC Drawing #1309301, A-3129

Hangar Maintenance, Organization Addition, Building #3129, Code Ident. #80091, NAVFAC Drawing #1309308, A-3129

Hangar, Motor Service Shop, Motor Pool and Paint Storage, Spec. #ENG 49-080-54-42-(34), Drawing #16-01-214, F-2149, A-3119

Hangar (Type H-2) 2 Story Lean-To, Spec. #ENG 49-080-54-42-(34), Drawing #AFD-51-301, F-2169, A-3119

Hangar (Type H-2) 2 Story Lean-To, Spec. #ENG 49-080-54-42-(34), Drawing #AFD-51-301 Modified, F-2170, A-3119

Hangar-Alert, Building 3032, Drawing #39-01-18-2, F-1071, A-3032

Construction of Refueling Vehicle Open Storage, Drawing #F1070, F-1070

Relocation of Nosedock, Code Ident. #80091, NAVFAC Drawing #1292606, F-6028, A-1915

Relocation of Nosedock, Code Ident. #80091, NAVFAC Drawing #1292611, F-6033, A-1915

Hangar Maintenance, Org. (CRT-2), Spec. #ENG 49-080-60-8-(8), Drawing #AW-16-01-360, F-3352, A-1914

Hangar Maintenance, Org. (CRT-2), Spec. #ENG 49-080-60-8-(8), Drawing #39-01-45, F-3360, A-1914

Hangar Maintenance, Org. (CRT-3) (CRT-4), Spec. #ENG 49-080-60-6-(6), Drawing #AW-16-01-361, F-3902, A-1754

Hangar Maintenance, Org. (CRT-3&4), Code Ident. #ENG 49-080-60-6-(6), Drawing #39-01-46, F-3909, A-1754

Hangar Maintenance, Org., Spec. #ENG 49-080-59-15-(16), Drawing #16-01-341, F-2725, A-1734

Hangar Maintenance, Org., Spec. #ENG 49-080-59-15-(16), Drawing #39-01-36, F-2733, A-1734

Hangar and Shops, Type Res. #1A, Spec. #ENG 49-080-55-80-(1), Drawing #39-01-22, F-1867, A-1714

Hangar Maintenance, Org. (SAM-2), Spec. #ENG 49-080-60-7-(7), Drawing #16-01-362, F-3300, A-1280

MLS and DME/P Multipath, Simulation Model User's Manual, Vol. 1 - Operating Instructions, DOT/FAA/CT-TN91/47, I, February 1992

MLS Mathematical Modeling Test Plan, Andrews AFB, MD, June 18, 1993

Obstruction Data Sheet: NOAA Obstruction Data Sheet #561

Preparation of Test and Evaluation Documentation, FAA-STD-024B, April 30, 1993

Runway Profile Drawings: NOAA Obstruction Chart #561

Site Selection Report Microwave Landing System (MLS), Runway 19L Andrews AFB, MD (ADW), June 18, 1993

3. MODELING STUDY DESCRIPTION.

3.1 Mission Review.

The proposed MLS-DME/P installation is intended to continue to provide precision landing service to runway 19L after the decommissioning of the precision approach radar (an AN/GPN-22) that presently provides that service. The airport diagram is shown in figure 1.

3.2 MLS-DME/P Equipment Sites.

The MLS AZ station will be located on the extended centerline of runway 19L, 2,285 feet (ft) past the stop end. The DME/P site is 50 feet (ft) west and abeam of the AZ station. The MLS EL station will be placed 400 ft west and abeam of a point on centerline, 922.6 ft from the threshold of runway 19L.

The MLS-DME/P mathematical model uses a cartesian reference system that has the runway surface on centerline at the stop end as the origin. The orientation of the coordinate axes is indicated in figure 2. The elevation at the origin of the reference coordinate system is 253 ft above mean sea level (m.s.l.). The phase centers of the MLS AZ, MLS EL, and DME/P antennas were modeled at the proposed locations of:

	X	Y	Z
MLS AZ:	-2285.0 ft	0.0 ft	9.75 ft
MLS EL:	8832.4 ft	400.0 ft	29.00 ft
DME/P:	-2285.0 ft	50.0 ft	18.30 ft

4

SEPTEMBER 1991
ANNUAL RATE OF CHANGE
0.1°W

38°50'N

VAR 10.1°W

161 x 150

250
x 500

999 x 200

861

MA-1A MOD

300 x 800

ELEV
279

ELEV 274

189.9°

101

480

6

7

10

FIELD
ELEV
281

BAC-
12

11

189.9°

3

FIRE STATION

1

38°49'N

2

301

3

9300 x 200

4

9755 x 150

2

12

5

5

13

7

14

PASSENGER
TERMINAL

009.9°

009.9°

15

9

8

16

BASE
OPS

17

ELEV
269

CONTROL
TOWER

502

TANKS

18

STATE RAMP

19

BAC-12
2

38°48'N
AERO CLUB

ELEV
255 9

ELEV
253

300 x 800

HOT CARGO

MA-1A MOD

1L

250
x 500

1R

1000 x 200

1000 x 150

HANGARS ARE NUMBERED

76°53'W

76°52'W

76°51'W

38°47'N

AIRPORT DIAGRAM

CAMP SPRINGS, MARYLAND
ANDREWS AFB/NAF (KADW)

FIGURE 1.   AIRPORT DIAGRAM FOR ADW, CAMP SPRINGS, MARYLAND

5

FIGURE 2. COORDINATE SYSTEM USED TO MODEL
PROPOSED INSTALLATION FOR 19L

3.3 MLS Approach Procedure and Orbit.

The United States Air Force plans to develop an MLS Category I
approach using a straight in AZ, 3° glide path, 50 ft threshold
crossing height, with a 200 ft decision height.

3.4 Impact of Other Systems.

There were concerns of the effects of existing or proposed landing
aids on the proposed MLS-DME/P installations. Two possible
conflicts exist; one concerning the MLS EL station in proximity of
the proposed Instrument Landing System (ILS) glide slope, and
another concerning the MLS AZ in proximity of the existing Approach
Lighting System (ALS).

As shown in figure 3, the location of the MLS EL station does not
penetrate the critical area for the proposed glide slope station
for runway 19L, and is not expected to cause a problem. The ILS
glide slope array also will not affect the guidance provided by the
MLS EL station, due to its location behind the EL station.

As illustrated in figure 4, the proposed location of the MLS AZ
shelter will not cause blockage of the light beam emanating from
the ALS. Since the approach lights are below the MLS AZ station's
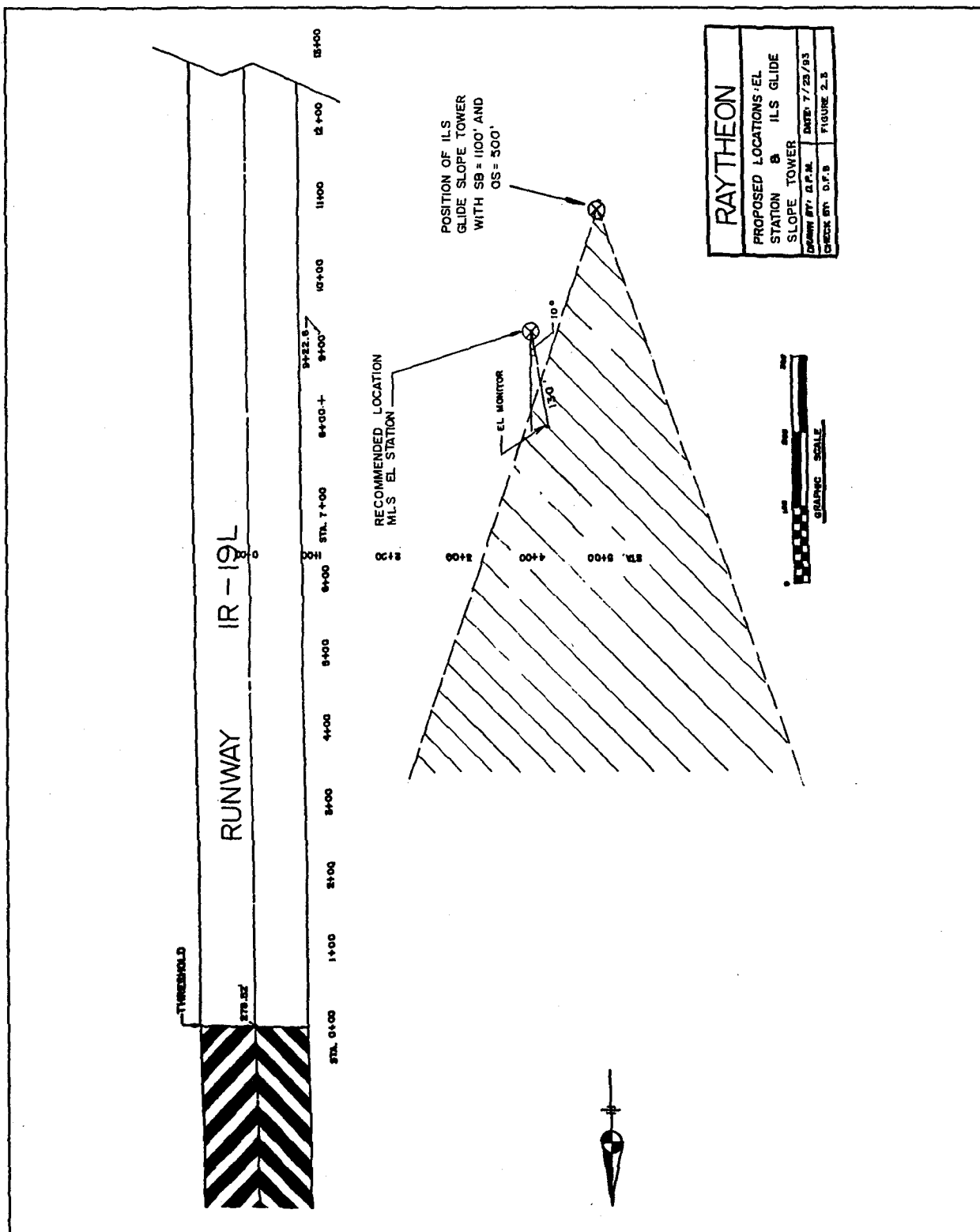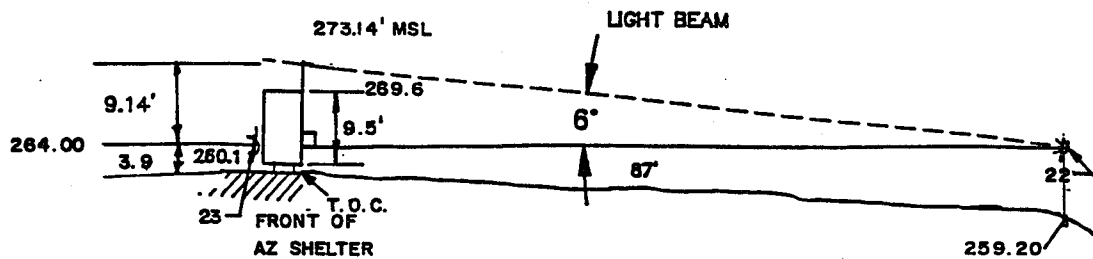phase center, they will not affect the MLS AZ signal.

FIGURE 3. MLS EL STATION RELATIVE TO PROPOSED
ILS GLIDE SLOPE CRITICAL AREAS

7

ANDREWS AIR FORCE BASE
MLS

LIGHT BEAM OBSTRUCTION CALCULATIONS:

$87'$ TAN $6° = 9.14'$

FORWARD APPROACH LIGHT ELEV. = 264.00 (FROM FIELD SURVEY)
ADD HEIGHT OF BEAM OVER SHELTER + __9.14__
LIGHT BEAM ELEV. = __273.14'__ MSL

TOP OF AZ FOUNDATION = 260.1 (PROPOSED)
HEIGHT OF SHELTER = __9.5'__ (FROM ALLIED INFO.)
TOP OF SHELTER = __269.6'__

THEREFORE THE MLS AZ SHELTER WILL NOT OBSTRUCT
THE ADJACENT APPROACH LIGHT.

RAYTHEON	
NON — BLOCKING OF LIGHT BEAM	
DRAWN BY: D.P.M.	DATE: 7/23/93
CHECK BY: D.F.B.	FIGURE 2.5

FIGURE 4. MLS AZ SHELTER RELATIVE TO APPROACH LIGHT BEAM.

4. TEST DESCRIPTION.

The six scenarios listed below were modeled for this study, and consisted of three approaches and three orbits. The designed approach glide path angle (GPA) is 3.0°. Orbit flight paths were modeled at a range of 10 nautical miles (nmi) from the DME/P station. The altitudes of the orbit scenarios are relative to the elevation of the origin of the reference coordinate system, and correspond to the minimum vectoring altitude (MVA) at 10 nmi, the 3° GPA intercept at 10 nmi, and the 4° GPA intercept altitude at 10 nmi.

Scen. #	Scen. Type
1	2° Approach
2	3° Approach
3	4° Approach
4	1747' Orbit (MVA)
5	2624' Orbit
6	3492' Orbit

4.1 Test Schedule and Location.

The modeling study was performed at the Raytheon Service Company (RSC) office in Pleasantville, NJ, under a contract with the FAA. The Airborne Systems Technology Branch (ACD-330) provided technical oversight and direction to this effort. The workstation used was an IBM compatible 486/66Mhz machine (running DOS 6.0) with 16MB of RAM, in cooperation with a Hewlett Packard LaserJet Series IV printer with 4MB of RAM. Modeling activities took place between June 11 and July 28, 1993.

4.2 Participants.

Jesse Jones (FAA)	MLS Math Modeling Project Manager
Elliott Rushton (RSC)	Modeler, Writer
Ron Lockhart (RSC)	Writer
Ray Anderson (RSC)	Site Surveyor

4.3 Mathematical Model Description.

The model used to estimate the quality of the guidance provided by the proposed MLS-DME/P installation was the MLS-DME/P Multipath Simulation Model, version 3.0. The Fortran 77 source code was compiled using the F77 Lahey 32-bit compiler for DOS. Further detail on the mathematical model is available in appendix J.

4.4 Test Objective.

The test objective was to predict the performance of the proposed system installed at the specified location. If necessary, results obtained through this modeling study, and additional work, may be used to evaluate the performance of alternative equipment sites at ADW.

4.5 Testing Categories.

Following an on-site study of the environment present for the proposed MLS-DME/P installation, several buildings and terrain areas were chosen as possible contributors of multipath error to the transmitted guidance signals, based on size and orientation.

4.5.1 Buildings Modeled for Multipath and Shadowing Effects.

The performed modeling study used data collected from site visits, as well as data extracted from base maps, construction drawings, etc. The airport structures were represented in the model as perfectly electrically conducting plates, similarly located and oriented. The sections of data generated from these sources of information are in appendixes D and F (multipath buildings and shadowing buildings, respectively).

The plates used to represent the airport structures in the modeled environment were assigned reference numbers. Modeling was performed on hangars #12 through #15, with the rooftops included to establish the total effect of the structures. Once it was determined that the rooftops had no impact on the resulting error due to multipath, they were removed from the study. The wall heights were increased to evaluate the shadowing effects of the entire hangar structure. Scatterers #21 through #28 represent the hangars with rooftops. Scatterers #11 through #14 represent these hangars with increased wall heights, without rooftops, for shadowing purposes only. The following table correlates the scatterer numbers with the buildings or hangars they represent (see (figure 5).

Scatterer no.	Description From Base Map		
1	hangar	01	
2	hangar	02	
3	hangar	03	
4	hangar	04	
5	hangar	05	
6	hangar	06	
7	hangar	10	
8,9,10	hangar	11	
11	hangar	12	
12	hangar	13	
13	hangar	14	
14	hangar	15	
15,16	bldg.	3629	
17,18	bldg.	3001	
19	bldg.	2487	
20	bldg.	1915	
21	hangar	12	
22	hangar	12	roof
23	hangar	13	
24	hangar	13	roof
25	hangar	14	
26	hangar	14	roof
27	hangar	15	
28	hangar	15	roof

4.5.2 Terrain Modeled for Multipath and Shadowing Effects.

The modeling study used topographical data obtained from a site survey performed by project personnel. Figure 6 shows the approximate modeled terrain structure used to simulate the effects of the irregular terrain in the region of the MLS EL station. This modeled structure is based on data collected on the surveyed structure measured in the region of the proposed EL station. The data used to model the terrain is listed in appendix H. Illumination of plates one through four is negligible due to their location behind the MLS EL station, thus these plates are not considered to be contributors of multipath error.

The modeled earth is assumed to have a complex dielectric constant of 80-j54 and a roughness factor of 6.52×10^{-2}. This dielectric constant was chosen to maximize the effects of ground reflections so that the results would show a worst-case result. The roughness value is a typical value for grass-covered ground.

4.5.3 Aircraft Modeled for Multipath and Shadowing Effects.

Following analysis of the ADW runway and taxiway layout, three locations were chosen to place aircraft during the modeling

11
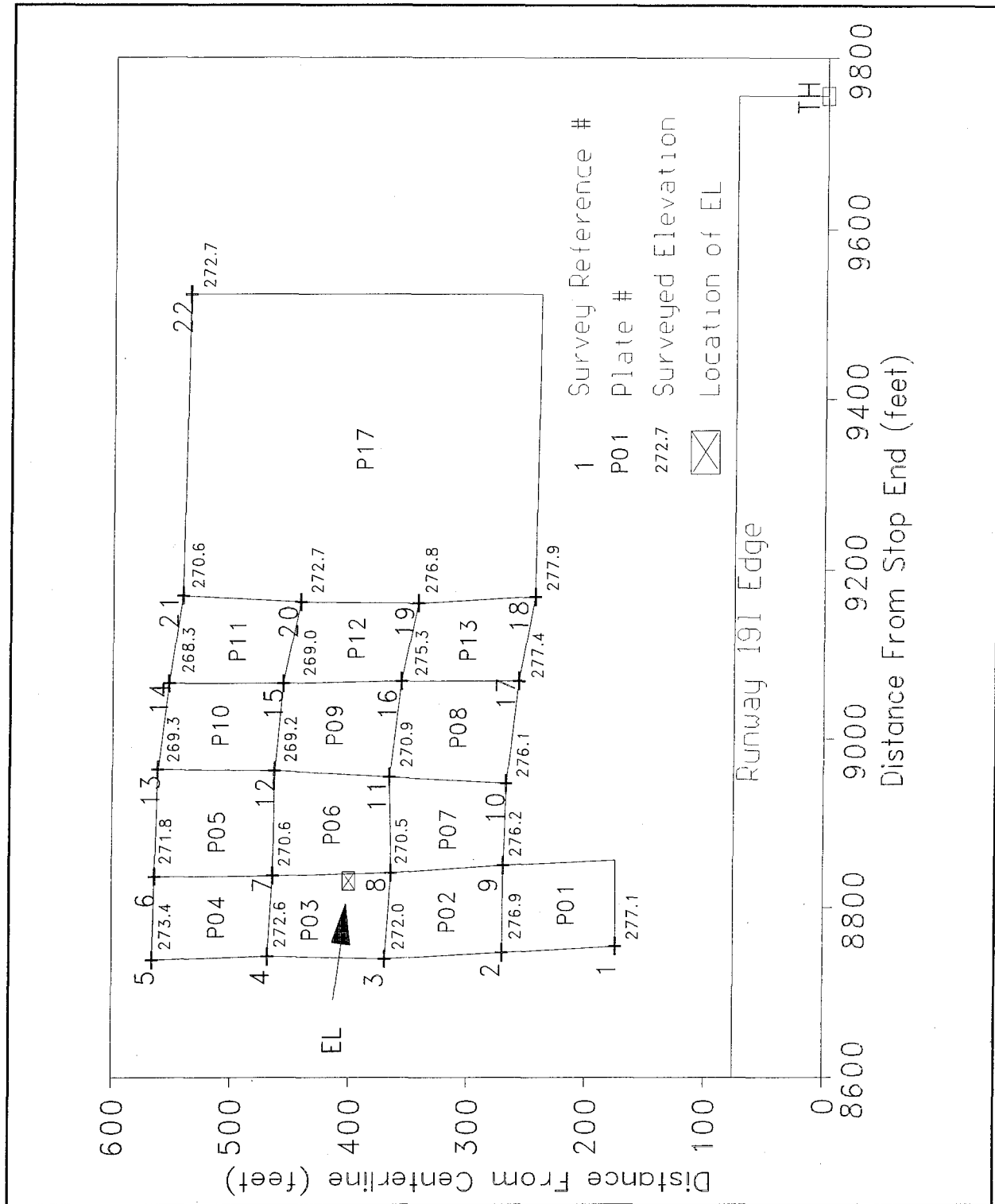
FIGURE 5. SURVEYED DATA POINTS COLLECTED IN THE REGION OF THE PROPOSED MLS EL SITE AND PLATES USED TO REPRESENT TOPOGRAPHIC STRUCTURE
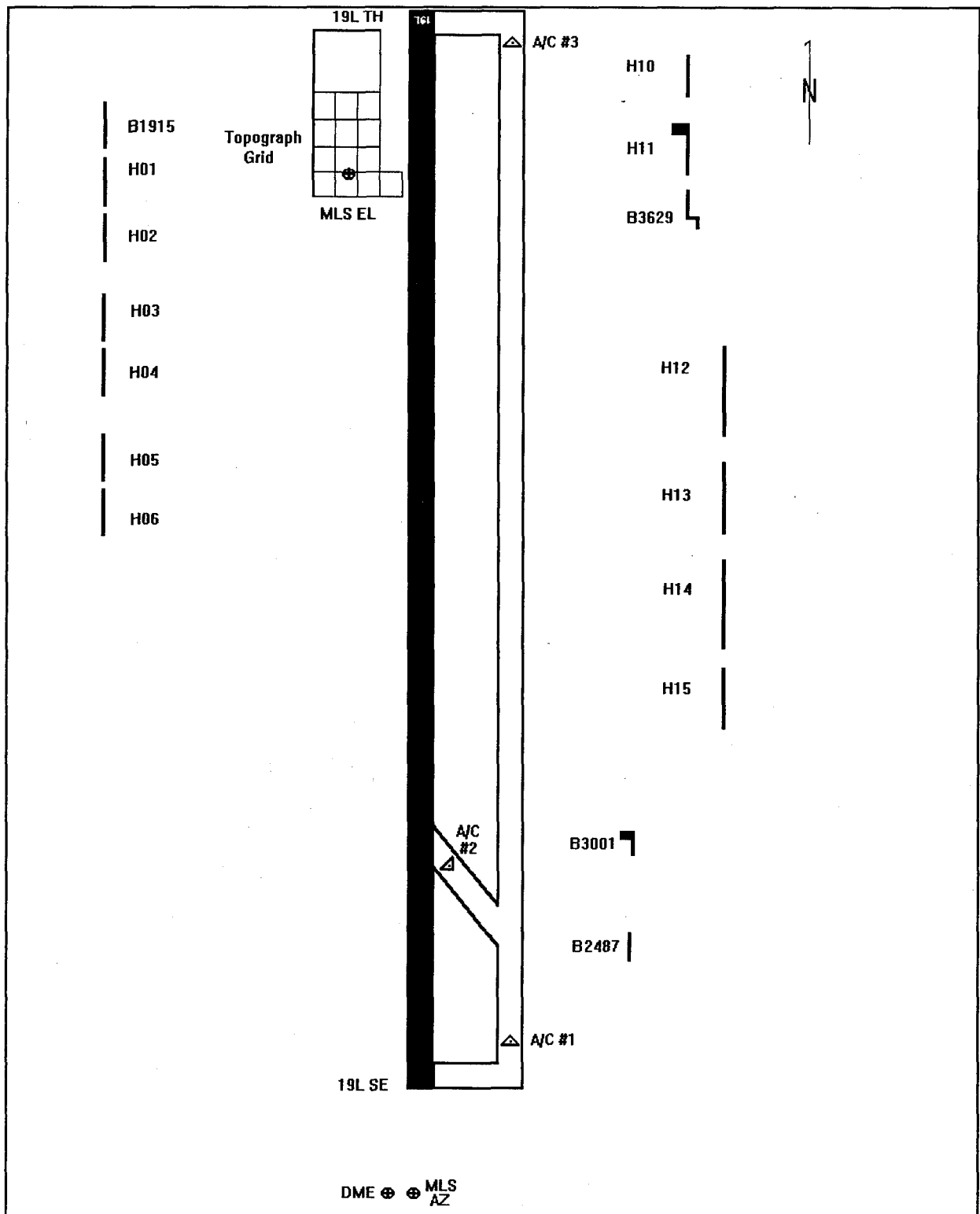
FIGURE 6.   MODELED HANGARS, BUILDINGS, AIRCRAFT,
AND TOPOGRAPHY FOR ADW

studies. The data generated for use in the input files for this modeling study are in appendix E. It is likely that aircraft could be in these positions during a precision approach to runway 19L. Since large aircraft have been proven to have an effect on provided guidance, it is necessary to quantify this effect. The C5A Galaxy is assumed to be the largest aircraft in use at ADW, and thus should result in the largest disturbance of the provided guidance information. The C5A Galaxy was modeled in positions as indicated in figure 5. Appendix E contains data tables concerning the coordinates of the three modeled aircraft.

4.6 Data Collection and Analysis Method.

Initially, the study included three sets of scatterers representing buildings, in addition to three aircraft. Each set of scatterer data was included in each of six scenarios. This amounts to 18 unique computer modeling runs. Following the generation of results, the graphical plots were analyzed and the 10 highest magnitude multipath contributors were selected from the 28 scatterers modeled (since the model can simulate the effects of up to 10 scatterers at one time). These 10 scatterers were compiled into data files (including the aircraft) and the final 6 scenarios were run. The 10 scatterers chosen are listed as follows:

Scatterer no.	Description From Base Map	
1	hangar	01
2	hangar	02
3	hangar	03
4	hangar	04
5	hangar	05
6	hangar	06
11	hangar	12
12	hangar	13
13	hangar	14
14	hangar	15

5. MODEL TEST DATA AND ANALYSIS.

The results of the modeling study are presented in this section. Before presenting the graphs, the different types of graphs are discussed. The discussed graphs, multipath, shadowing, and guidance error, are presented in appendixes A, B, and C. The graphs are organized according to the three functional parts of the proposed installation to which they refer, MLS AZ (appendix A), MLS EL (appendix B), or DME/P (appendix C). Within the respective appendix, graphs are presented according to scenario. The results from the three types of approach scenarios are first, followed by results from the three partial orbit scenarios for each subsystem.

14

The captions associated with each graph describe the data presented.

5.1 Multipath Plots.

The propagation model calculates signal levels at the aircraft of all the most prominent multipath signals from the AZ, EL, and DME/P uplink transmitters. The signal level at the DME/P transponder is calculated for the multipath signals from the DME/P airborne interrogator (downlink). The six most dominant multipath contributors are listed in each plot along with a single symbol associated with that obstacle. This multipath signal strength is calculated for each receiver position, and plotted as a ratio of multipath to direct signal strength in decibels (dB) (MLS and DME/P Multipath Simulation Model User's Manual, p. 65). Figures A-1 in appendix A and B-1 in appendix B are examples of the multipath plots for the modeled MLS AZ and EL subsystems, respectively. Figures C-1 and C-3 in appendix C are examples of the multipath plots for the modeled DME/P subsystem uplink and downlink results.

The propagation model also determines the separation angle between the direct beam and each multipath signal received from the AZ and EL systems. This parameter can have a significant effect on the total guidance received since the receiving system has an ability to identify multipath signals that are out-of-beam. A multipath signal is considered to be out-of-beam if its separation angle is greater than approximately 1.7 transmitter beam widths. In-beam signals are those whose separation angles are less than 1.7 beam widths. This parameter is used to facilitate analysis of multipath signals and their affect on the guidance provided by the installation (MLS and DME/P Multipath Simulation Model User's Manual, pp. 65-66). Figures A-2 and B-2 are examples of the separation angle plots for the modeled MLS AZ and EL subsystems, respectively.

For the DME/P system, a similar phenomenon occurs to the received pulse shape due to multipath effects. This shape distortion, however, affects the guidance only when it occurs during the first approximately 300 nanoseconds (ns) of the waveform. This information is presented in plots illustrating the multipath signal time of arrival relative to the direct pulse time of arrival (MLS and DME/P Multipath Simulation Model User's Manual, pp. 65-66). Figures C-2 and C-4 are examples of the time delay plots for the modeled DME/P subsystem uplink and downlink results.

5.2 Shadowing Plots.

Obstacles in the environment of the installation, such as buildings, aircraft, and runway humps, may cause shadowing or signal blockage to occur, distorting the direct signal received on the flight path. These results are plotted relative to the undisturbed direct signal strength in dB (MLS and DME/P Multipath

15

Simulation Model User's Manual, pp. 65-66). Figures A-3 and B-3 are examples of the multipath plots for the modeled MLS AZ and EL subsystems, respectively. Figures C-5 and C-6 are examples of the multipath plots for the modeled DME/P subsystem uplink and downlink results.

5.3 Graphical Representation of Calculated Error.

The mathematical model generates plots of the calculated error from the received-signal characteristics explained above. These error data are presented in four components; static error, dynamic error, path following error (PFE), and control motion noise (CMN). All data are plotted versus receiver position.

The static error plots show the calculated receiver error for each system. This information does not account for the damping of the error that occurs, which depends primarily on aircraft velocity. Examples of static error plots can be seen in figures A-4, B-4, and C-7.

The dynamic error plots present information similar to the static error plots with one difference. The dynamic error has been filtered to account for the effects of aircraft velocity, receiver slew rate limiting, and any other filtering of the received signal that occurs before the information would be displayed to the pilot. Examples of dynamic error plots can be seen in figures A-5, B-5, and C-8.

For the PFE, the error data are passed through a low-pass filter before being plotted versus receiver position. Similarly, the CMN data are obtained by passing the generated data through a high-pass filter before plotting. The FAA places tolerance limits on the magnitude of the excursions of these types of error that may occur in a commissioned installation. Examples of PFE plots can be seen in figures A-6, B-6, and C-9. Examples of CMN plots can be seen in figures A-7, B-7, and C-10.

Within these generated figures, error plots presenting the results for CMN and PFE filtering are shown with tolerance brackets indicated. Figure 7 shows illustrations of the tolerance brackets used in error analysis to evaluate the quality of guidance provided by the installation. The horizontal dashed lines represent the tolerances limits as specified in FAA-STD-022d. The vertical dashed lines at the extents of the tolerances represent the limits of the tolerances in the coverage volume. The third vertical line (within the specified coverage region specified by the tolerance limits) represents the beginning of a "time window" placed around the largest error occurring in the data. The duration of this time window is 40 seconds for the MLS AZ subsystem and 10 seconds for the MLS EL subsystem. The error, if present, cannot violate the tolerance bounds for more than 5 percent of the time during any

16
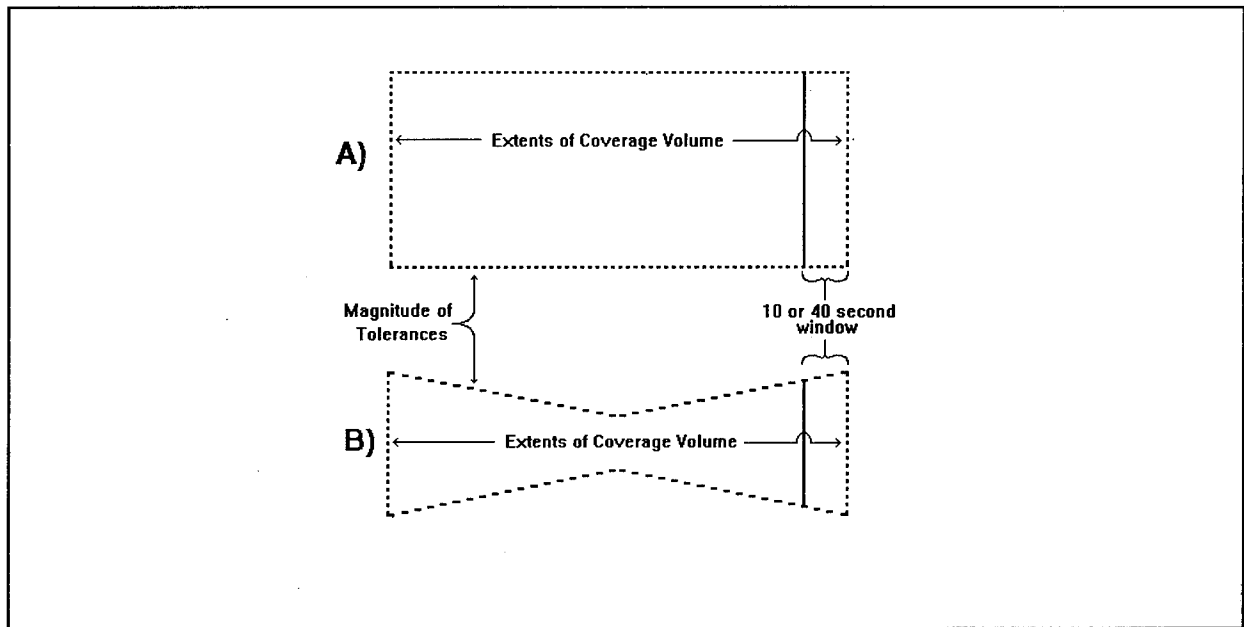
FIGURE 7. COVERAGE VOLUME DEFINING LIMITS OF GUIDANCE ERROR

given time period. If there is no significant error, the window marker lies at the end of the flight path.

5.3.1 Results of Modeling for MLS AZ Station.

The results provided by the modeling study for the effects of the 10 strongest contributors (as listed in section 4.6) and 3 aircraft on the guidance provided by the MLS AZ station are in figures A-1 through A-42. As shown in the multipath plots (figures A-1, A-8, A-15, etc.), buildings #3, #4, #6, #13, #14, and #15 are predicted to be the dominant contributors to the multipath received along the flight paths modeled. However, the separation angles between the resulting multipath and the direct signals from the AZ are sufficiently large and therefore result in minimal error in the lateral guidance.

5.3.2 Results of Modeling for MLS EL Station.

The results provided by the modeling study for the effects of the 10 strongest contributors (as listed in section 4.6), 3 aircraft, and modeled terrain structure on the guidance provided by the MLS EL station are in figures B-1 through B-42. As shown in the multipath plots (figures B-1, B-8, B-15, etc.), aircraft #3 (refer to figure 5) is predicted to be the dominant contributor of the multipath received along the flight paths modeled. However, the relative magnitude difference between the resulting multipath and the direct signals from the EL station is sufficiently large and therefore results in minimal error in the vertical guidance.

17

5.3.3 Results of Modeling for DME/P Station.

The results provided by the modeling study for the effects of the 10 strongest contributors (as listed in section 4.6) and 3 aircraft on the guidance provided by the DME/P station are in figures C-1 through C-60. As shown in the multipath plots (figures C-1, C-3, C-11, C-13, etc.), buildings #4, #5, #6, #13, #14, and #15 are predicted to be the dominant contributors to the multipath received along the flight paths modeled. However, the relative time delays between the resulting multipath and the direct signals from the DME/P are sufficiently large (greater than 300 ns), and therefore result in a minimal error in the range guidance.

6. CONCLUSIONS.

Six scenarios were modeled successfully using the Microwave Landing System (MLS)-Precision Distance Measuring Equipment (DME/P) mathematical model. From these results, the 10 strongest contributors of error due to multipath were selected (see section 4.6). These 10 scatterers, along with 3 carefully-placed aircraft, were compiled into 1 data set which was used in the 6 scenarios once again.

According to the results obtained from this modeling study, the proposed MLS installation at Andrews Air Force Base, runway 19L, is predicted to satisfy FAA-STD-022d tolerances without exception.

7. RECOMMENDATIONS.

None.

Appendix A
MLS Azimuth Modeling Results
List of Illustrations

Results of modeling effort of the six scenarios with the 10 worst-case contributors of multipath on the guidance provided by the MLS AZ are presented in this section.

Figure A-1   MLS AZ multipath relative magnitude plot for
a straight approach (3° GPA) flight path.
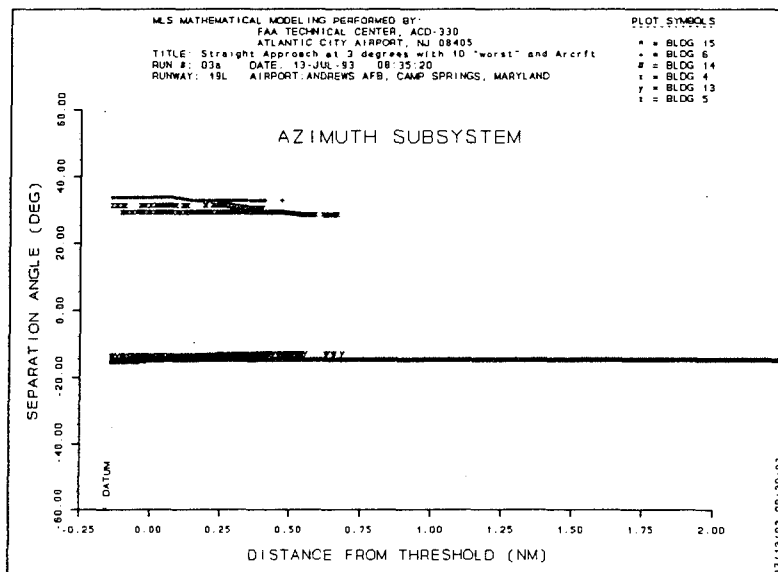
Figure A-2   MLS AZ multipath separation angle plot for
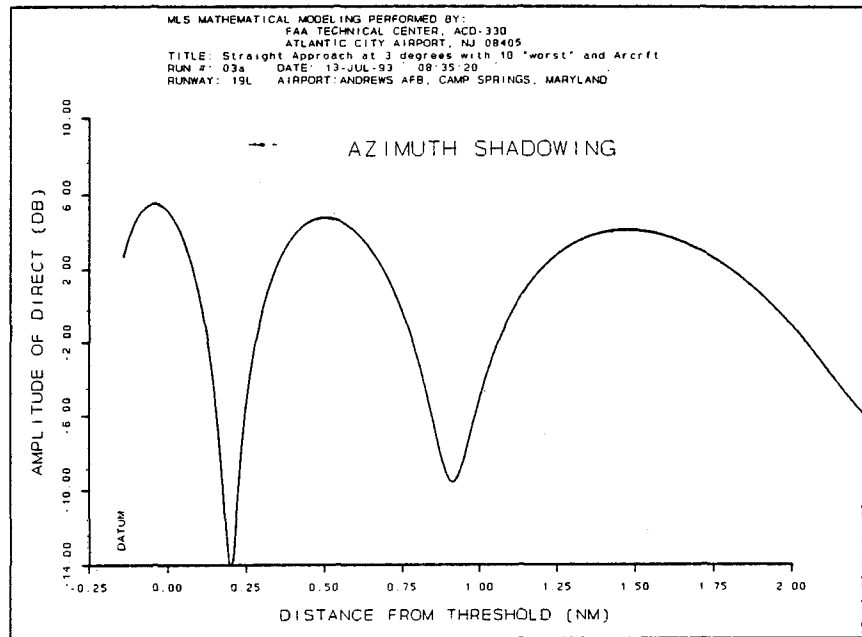a straight approach (3° GPA) flight path.

FIGURE A-3. MLS AZ COMPOSITE MAGNITUDE PLOT FOR A
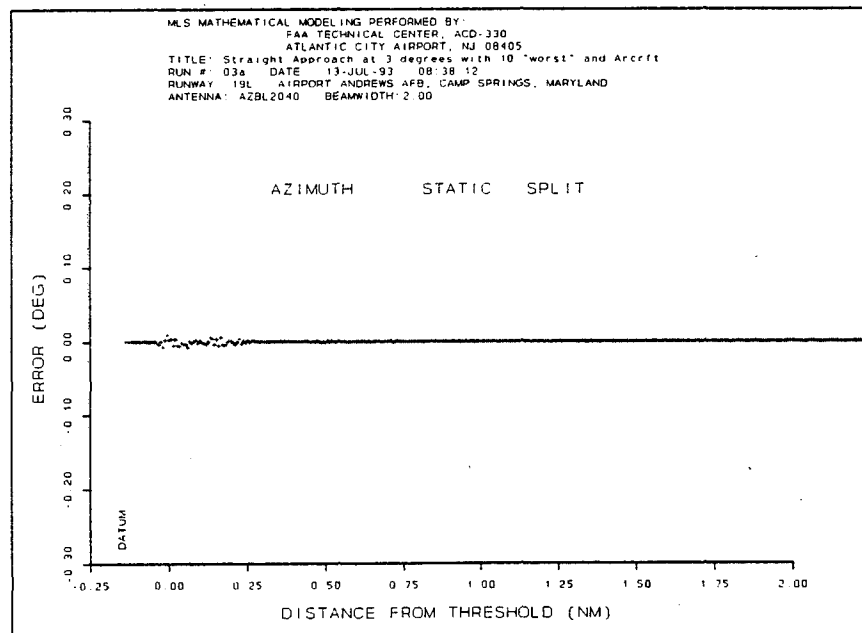STRAIGHT APPROACH (3° GPA) FLIGHT PATH.

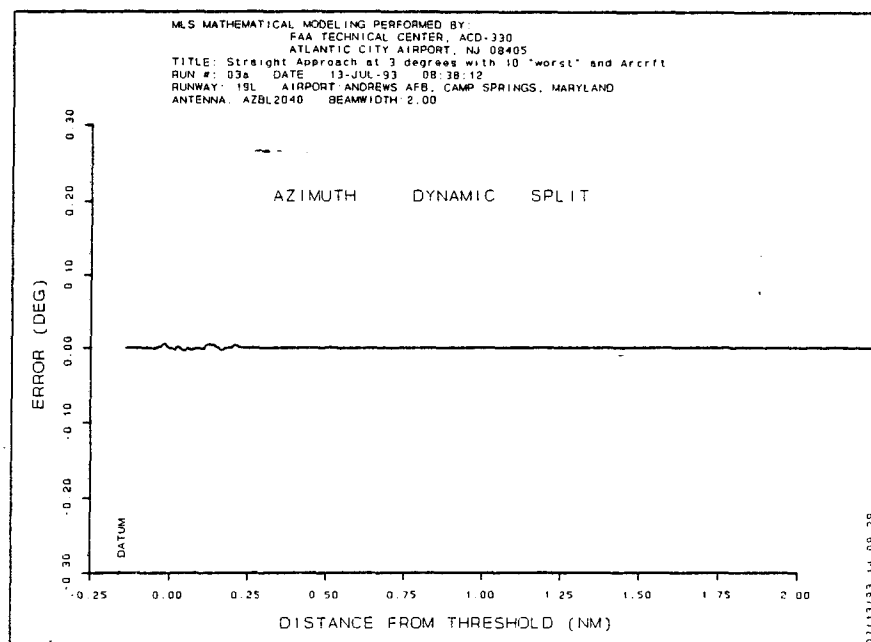FIGURE A-4. MLS AZ STATIC ERROR PLOT FOR A STRAIGHT
APPROACH (3° GPA) FLIGHT PATH.

A-5

MLS MATHEMATICAL MODELING PERFORMED BY:
FAA TECHNICAL CENTER, ACD-330
ATLANTIC CITY AIRPORT, NJ 08405
TITLE: Straight Approach at 3 degrees with 10 "worst" and Arcrft
RUN #: 03a   DATE   13-JUL-93   08:38:12
RUNWAY: 19L   AIRPORT: ANDREWS AFB, CAMP SPRINGS, MARYLAND
ANTENNA: AZBL2040   BEAMWIDTH: 2.00

AZIMUTH   DYNAMIC   SPLIT

**FIGURE A-5.   MLS AZ DYNAMIC ERROR PLOT FOR A
STRAIGHT APPROACH (3° GPA) FLIGHT PATH.**

MLS MATHEMATICAL MODELING PERFORMED BY:
FAA TECHNICAL CENTER, ACD-330
ATLANTIC CITY AIRPORT, NJ 08405
TITLE: Straight Approach at 3 degrees with 10 "worst" and Arcrft
RUN #: 03a   DATE   13-JUL-93   08:38:12
RUNWAY: 19L   AIRPORT: ANDREWS AFB, CAMP SPRINGS, MARYLAND
ANTENNA: AZBL2040   BEAMWIDTH: 2.00
MEAN: 0.00   2*STD DEV: 0.00
TOLERANCE LIMITS VIOLATION (%): 0.00

AZIMUTH   PFE   SPLIT

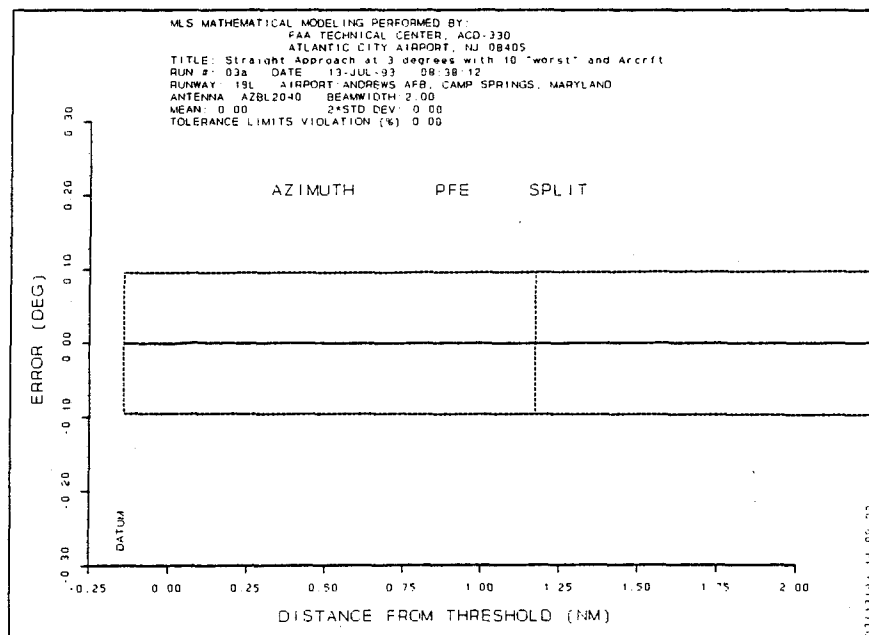**FIGURE A-6.   MLS AZ PATH FOLLOWING ERROR PLOT FOR A
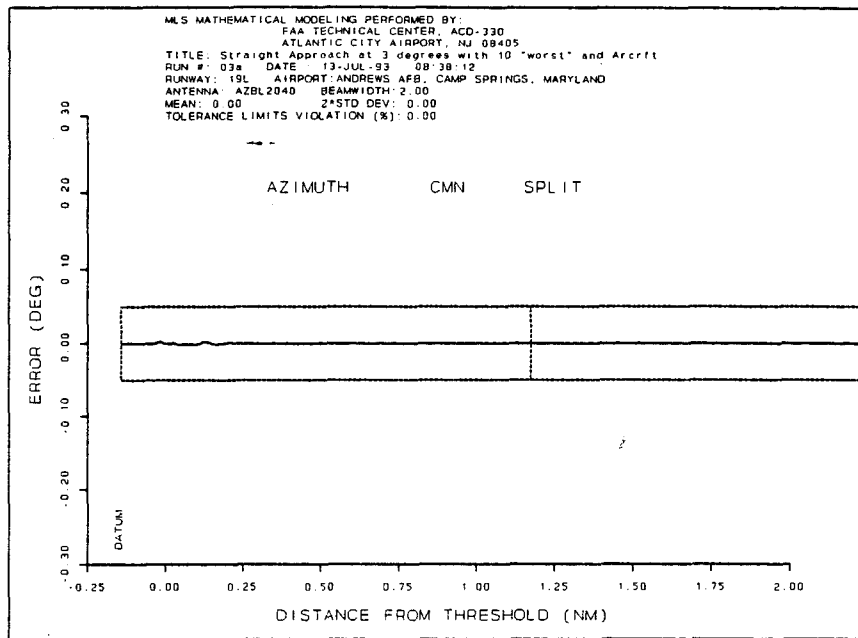STRAIGHT APPROACH (3° GPA) FLIGHT PATH.**

FIGURE A-7. MLS AZ CONTROL MOTION NOISE PLOT FOR A
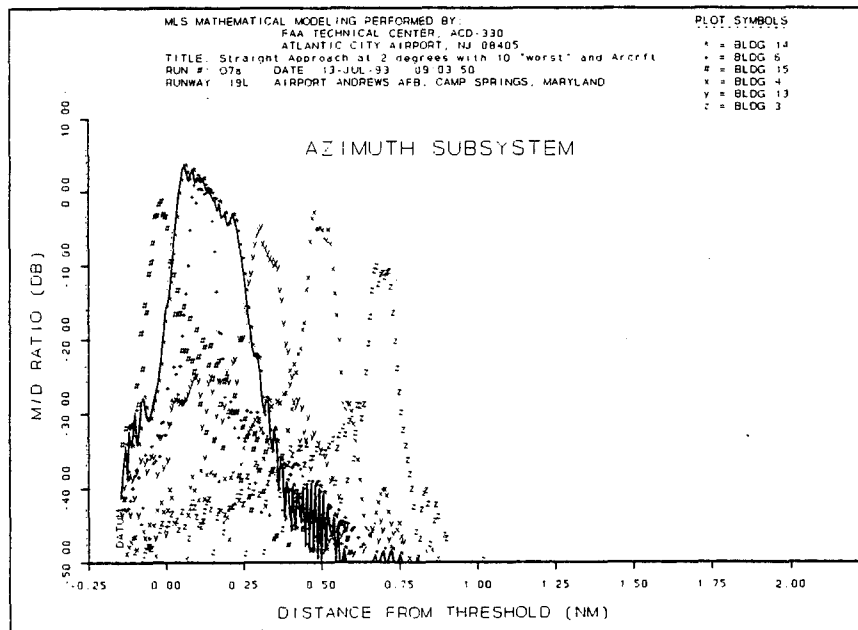STRAIGHT APPROACH (3° GPA) FLIGHT PATH.

FIGURE A-8. MLS AZ MULTIPATH RELATIVE MAGNITUDE
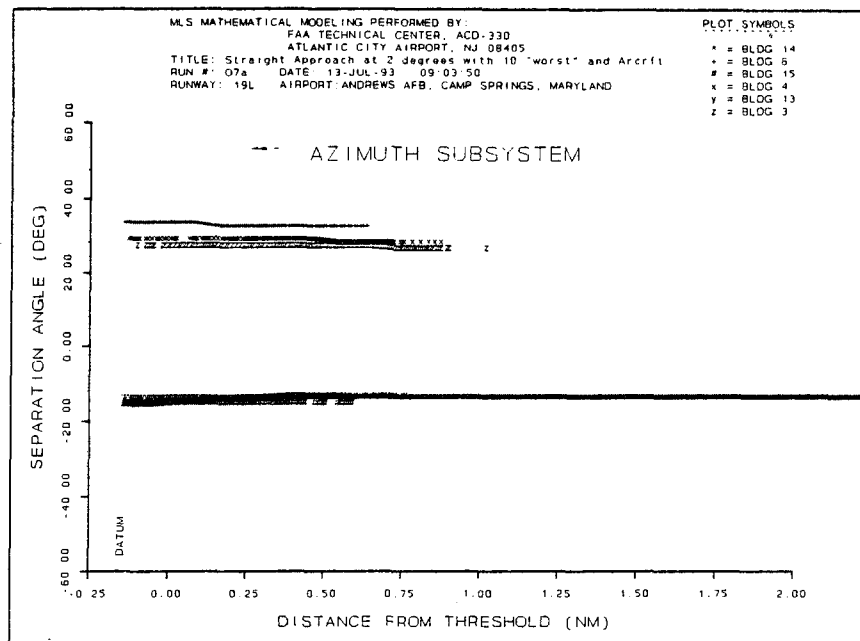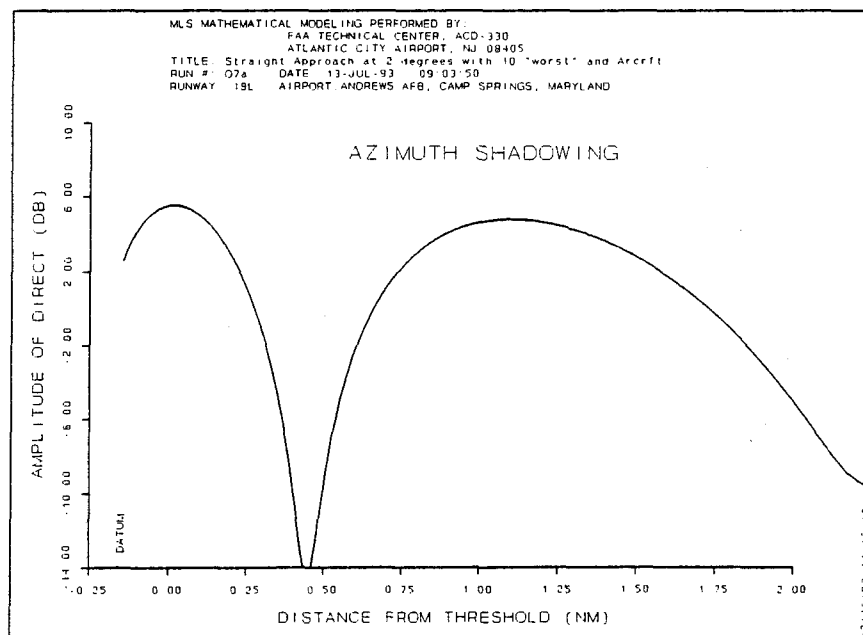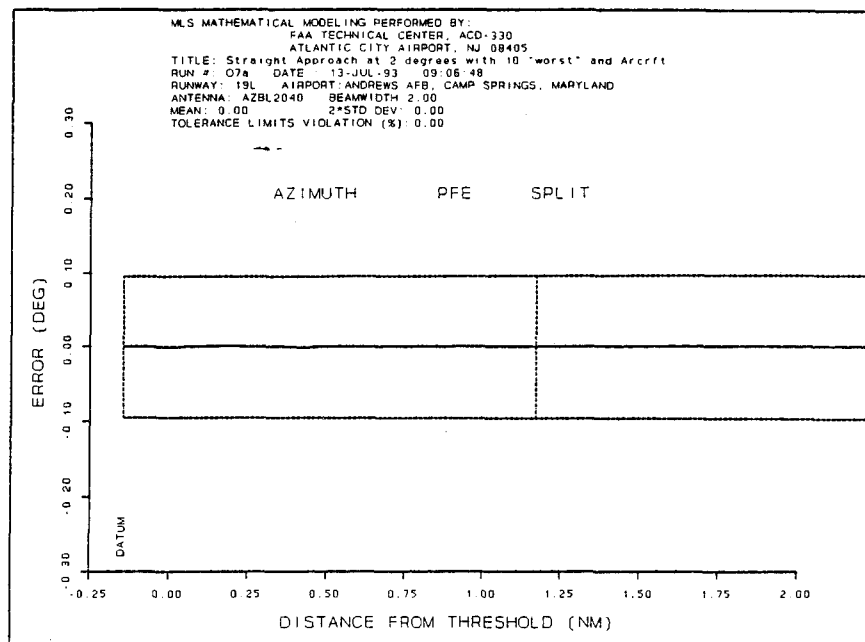PLOT FOR A STRAIGHT APPROACH (2° GPA) FLIGHT PATH.

A-7

MLS MATHEMATICAL MODELING PERFORMED BY:
FAA TECHNICAL CENTER, ACD-330
ATLANTIC CITY AIRPORT, NJ 08405
TITLE: Straight Approach at 2 degrees with 10 "worst" and Arcrft
RUN #: O7a   DATE: 13-JUL-93   09:03:50
RUNWAY: 19L   AIRPORT: ANDREWS AFB, CAMP SPRINGS, MARYLAND

PLOT SYMBOLS

* = BLDG 14
+ = BLDG 6
# = BLDG 15
x = BLDG 4
y = BLDG 13
z = BLDG 3

AZIMUTH SUBSYSTEM

FIGURE A-9.   MLS AZ MULTIPATH SEPARATION ANGLE PLOT
FOR A STRAIGHT APPROACH (2° GPA) FLIGHT PATH.

MLS MATHEMATICAL MODELING PERFORMED BY:
FAA TECHNICAL CENTER, ACD-330
ATLANTIC CITY AIRPORT, NJ 08405
TITLE: Straight Approach at 2 degrees with 10 "worst" and Arcrft
RUN #: O7a   DATE: 13-JUL-93   09:03:50
RUNWAY: 19L   AIRPORT: ANDREWS AFB, CAMP SPRINGS, MARYLAND

AZIMUTH SHADOWING

FIGURE A-10.   MLS AZ COMPOSITE MAGNITUDE PLOT FOR A
STRAIGHT APPROACH (2° GPA) FLIGHT PATH.

A-8

MLS MATHEMATICAL MODELING PERFORMED BY:
FAA TECHNICAL CENTER, ACD-330
ATLANTIC CITY AIRPORT, NJ 08405
TITLE: Straight Approach at 2 degrees with 10 "worst" and Arcrft
RUN #: 07a   DATE : 13-JUL-93   09:06:48
RUNWAY: 19L   AIRPORT: ANDREWS AFB, CAMP SPRINGS, MARYLAND
ANTENNA: AZBL2040   BEAMWIDTH:2.00

AZIMUTH   STATIC   SPLIT
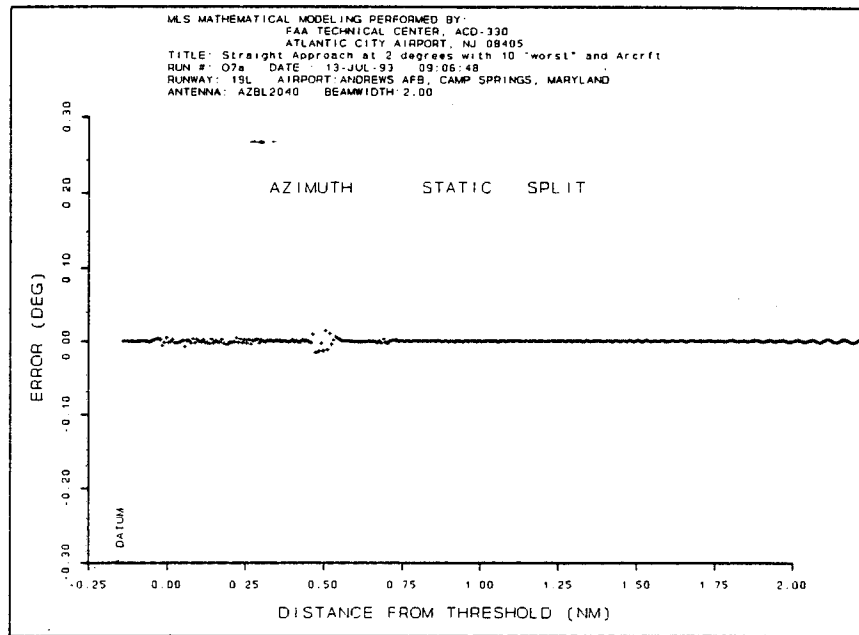
FIGURE A-11.   MLS AZ STATIC ERROR PLOT FOR A STRAIGHT APPROACH (2° GPA) FLIGHT PATH.

MLS MATHEMATICAL MODELING PERFORMED BY:
FAA TECHNICAL CENTER, ACD-330
ATLANTIC CITY AIRPORT, NJ 08405
TITLE: Straight Approach at 2 degrees with 10 "worst" and Arcrft
RUN #: 07a   DATE : 13-JUL-93   09:06:48
RUNWAY: 19L   AIRPORT: ANDREWS AFB, CAMP SPRINGS, MARYLAND
ANTENNA: AZBL2040   BEAMWIDTH 2.00

AZIMUTH   DYNAMIC   SPLIT
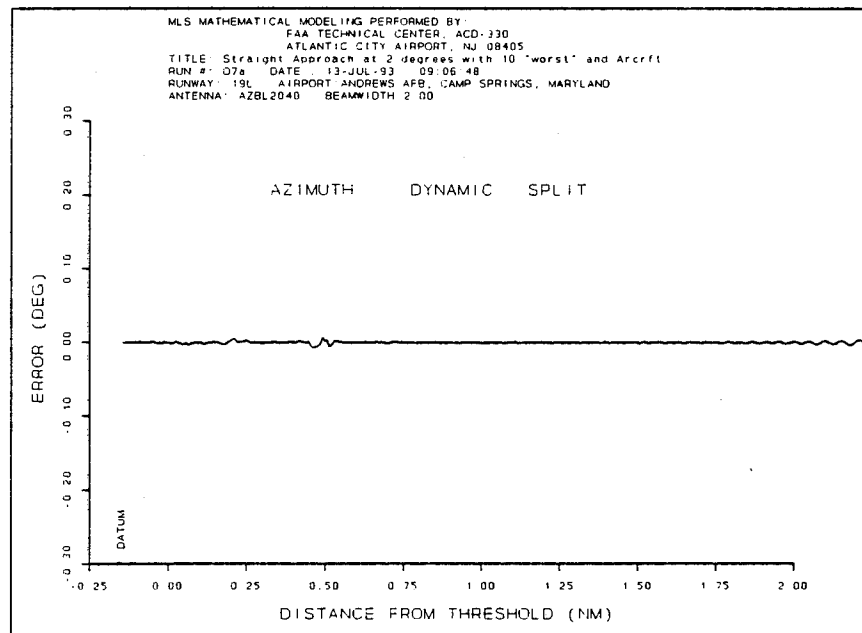
FIGURE A-12.   MLS AZ DYNAMIC ERROR PLOT FOR A STRAIGHT APPROACH (2° GPA) FLIGHT PATH.

A-9

FIGURE A-13.   MLS AZ PATH FOLLOWING ERROR PLOT FOR A
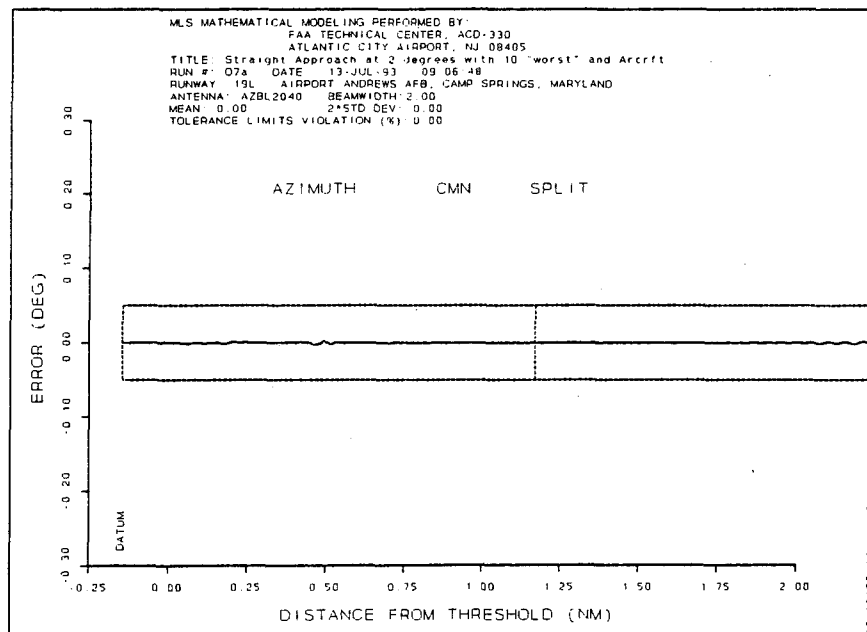   STRAIGHT APPROACH (2° GPA) FLIGHT PATH.

FIGURE A-14.   MLS AZ CONTROL MOTION NOISE PLOT FOR A
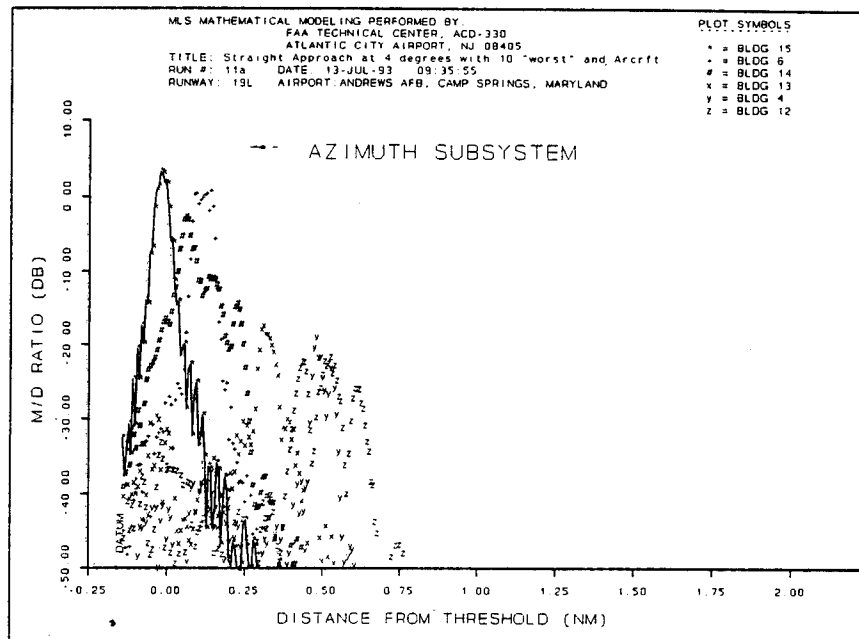   STRAIGHT APPROACH (2° GPA) FLIGHT PATH.

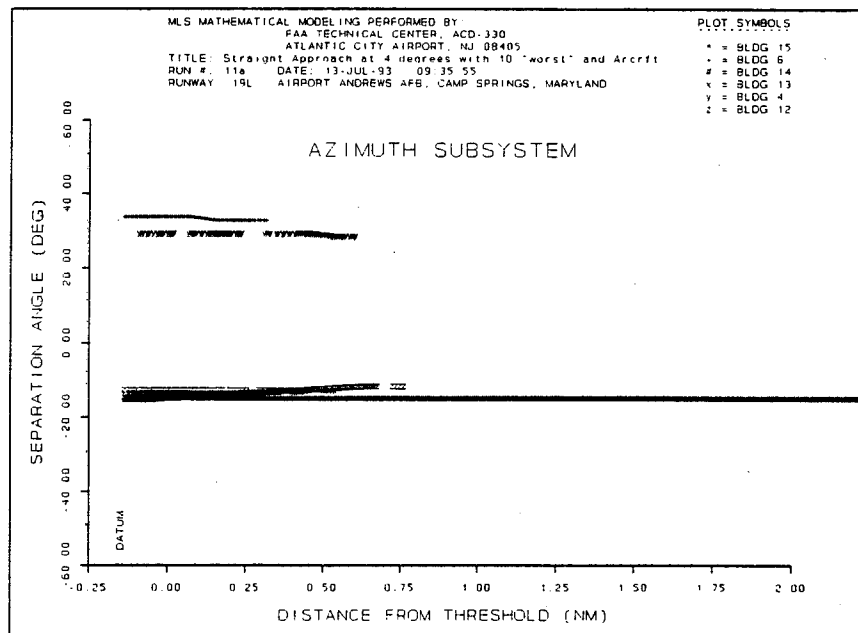**FIGURE A-15.** MLS AZ MULTIPATH RELATIVE MAGNITUDE PLOT FOR A STRAIGHT APPROACH (4° GPA) FLIGHT PATH.

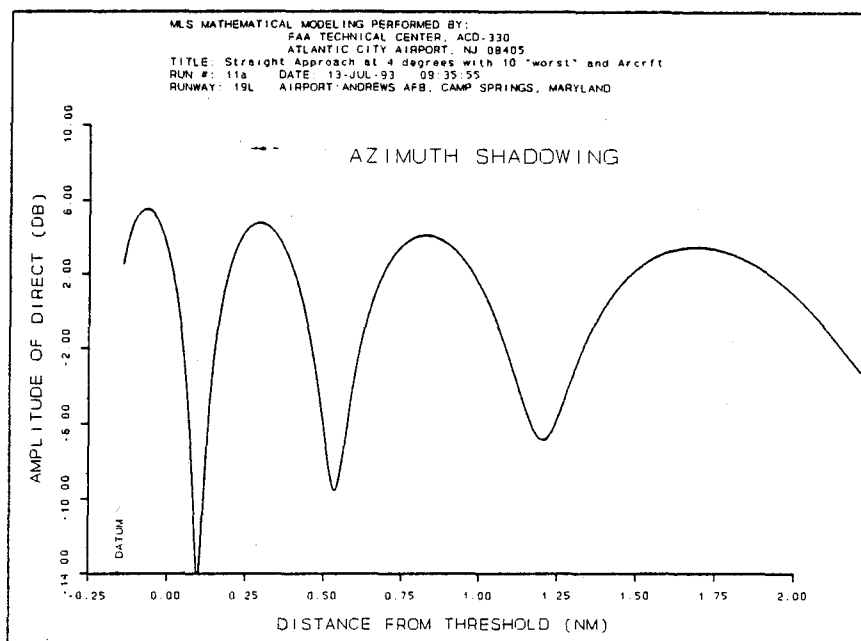**FIGURE A-16.** MLS AZ MULTIPATH SEPARATION ANGLE PLOT FOR A STRAIGHT APPROACH (4° GPA) FLIGHT PATH.

A-11

FIGURE A-17.   MLS AZ COMPOSITE MAGNITUDE PLOT FOR A
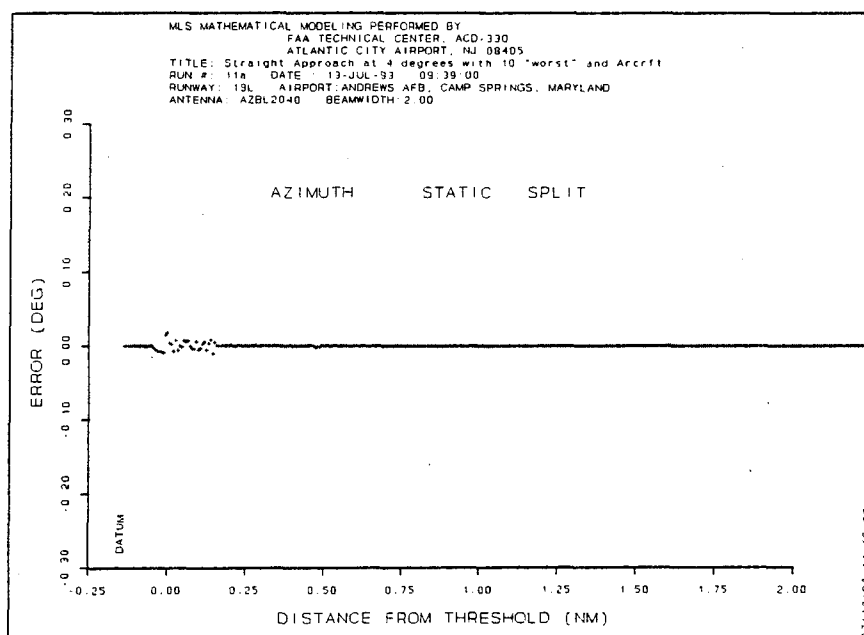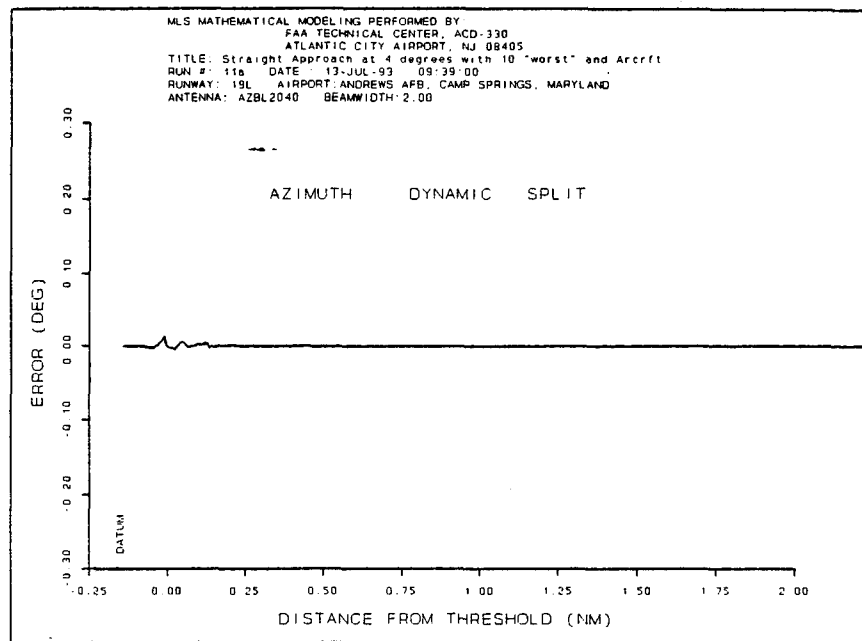STRAIGHT APPROACH (4° GPA) FLIGHT PATH.

FIGURE A-18.   MLS AZ STATIC ERROR PLOT FOR A
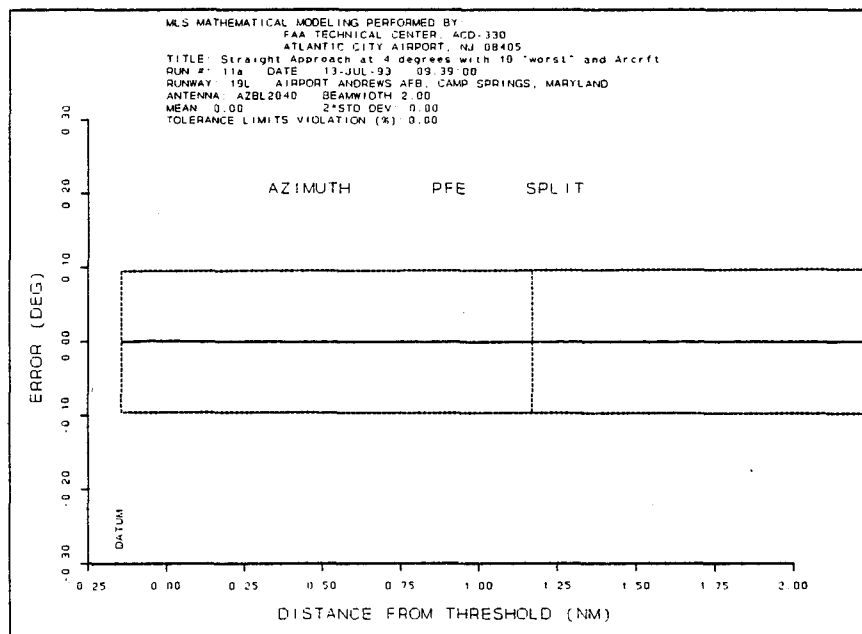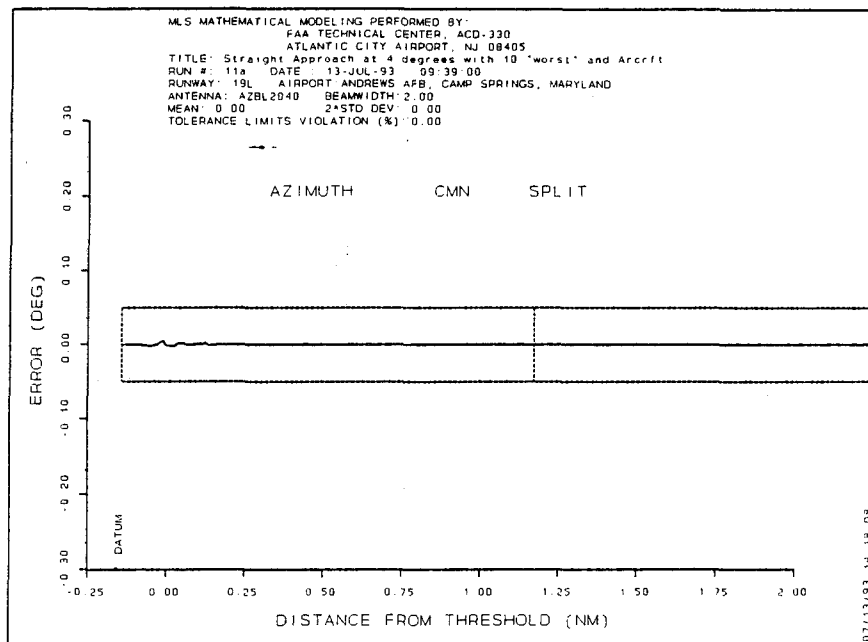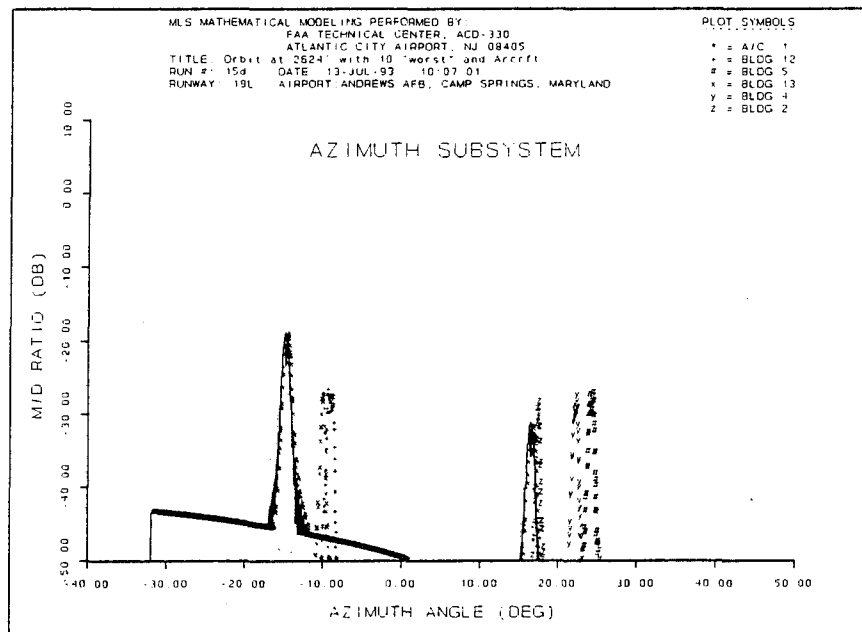STRAIGHT APPROACH (4° GPA) FLIGHT PATH.

MLS MATHEMATICAL MODELING PERFORMED BY
FAA TECHNICAL CENTER, ACD-330
ATLANTIC CITY AIRPORT, NJ 08405
TITLE: Straight Approach at 4 degrees with 10 "worst" and Arcrft
RUN #: 11a   DATE   13-JUL-93   09:39:00
RUNWAY: 19L   AIRPORT: ANDREWS AFB, CAMP SPRINGS, MARYLAND
ANTENNA: AZBL2040   BEAMWIDTH: 2.00

AZIMUTH   DYNAMIC   SPLIT

FIGURE A-19.   MLS AZ DYNAMIC ERROR PLOT FOR A STRAIGHT APPROACH (4° GPA) FLIGHT PATH.

MLS MATHEMATICAL MODELING PERFORMED BY
FAA TECHNICAL CENTER, ACD-330
ATLANTIC CITY AIRPORT, NJ 08405
TITLE: Straight Approach at 4 degrees with 10 "worst" and Arcrft
RUN #: 11a   DATE   13-JUL-93   09:39:00
RUNWAY: 19L   AIRPORT ANDREWS AFB, CAMP SPRINGS, MARYLAND
ANTENNA: AZBL2040   BEAMWIDTH 2.00
MEAN 0.00   2*STD DEV 0.00
TOLERANCE LIMITS VIOLATION (%) 0.00

AZIMUTH   PFE   SPLIT

FIGURE A-20.   MLS AZ PATH FOLLOWING ERROR PLOT FOR A STRAIGHT APPROACH (4° GPA) FLIGHT PATH.

A-13

MLS MATHEMATICAL MODELING PERFORMED BY:
FAA TECHNICAL CENTER, ACD-330
ATLANTIC CITY AIRPORT, NJ 08405
TITLE: Straight Approach at 4 degrees with 10 "worst" and Arcrft
RUN #: 11a   DATE : 13-JUL-93   09:39:00
RUNWAY: 19L   AIRPORT ANDREWS AFB, CAMP SPRINGS, MARYLAND
ANTENNA: AZBL2040   BEAMWIDTH 2.00
MEAN: 0.00   2*STD DEV: 0.00
TOLERANCE LIMITS VIOLATION (%): 0.00

AZIMUTH   CMN   SPLIT

FIGURE A-21.   MLS AZ CONTROL MOTION NOISE PLOT FOR A
STRAIGHT APPROACH (4° GPA) FLIGHT PATH.

MLS MATHEMATICAL MODELING PERFORMED BY:
FAA TECHNICAL CENTER, ACD-330
ATLANTIC CITY AIRPORT, NJ 08405
TITLE: Orbit at 2624' with 10 "worst" and Arcrft
RUN #: 15d   DATE: 13-JUL-93   10:07:01
RUNWAY: 19L   AIRPORT: ANDREWS AFB, CAMP SPRINGS, MARYLAND

PLOT SYMBOLS
* = A/C
+ = BLDG 12
# = BLDG 5
x = BLDG 13
y = BLDG 4
z = BLDG 2

AZIMUTH SUBSYSTEM

FIGURE A-22.   MLS AZ MULTIPATH RELATIVE MAGNITUDE
PLOT FOR AN ORBITAL (2624' ABOVE REFERENCE)
FLIGHT PATH.

A-14
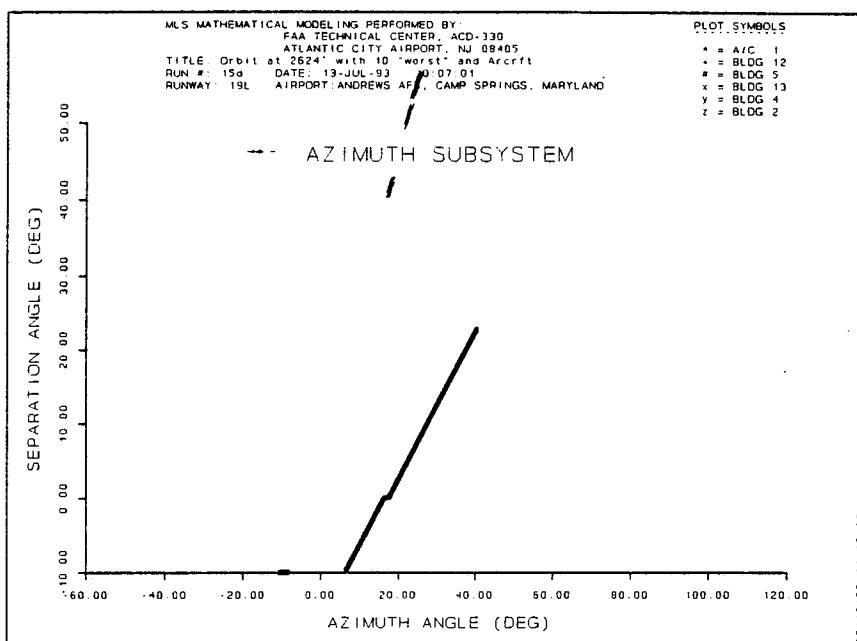
FIGURE A-23. MLS AZ MULTIPATH SEPARATION ANGLE PLOT
FOR AN ORBITAL (2624' ABOVE REFERENCE) FLIGHT PATH.
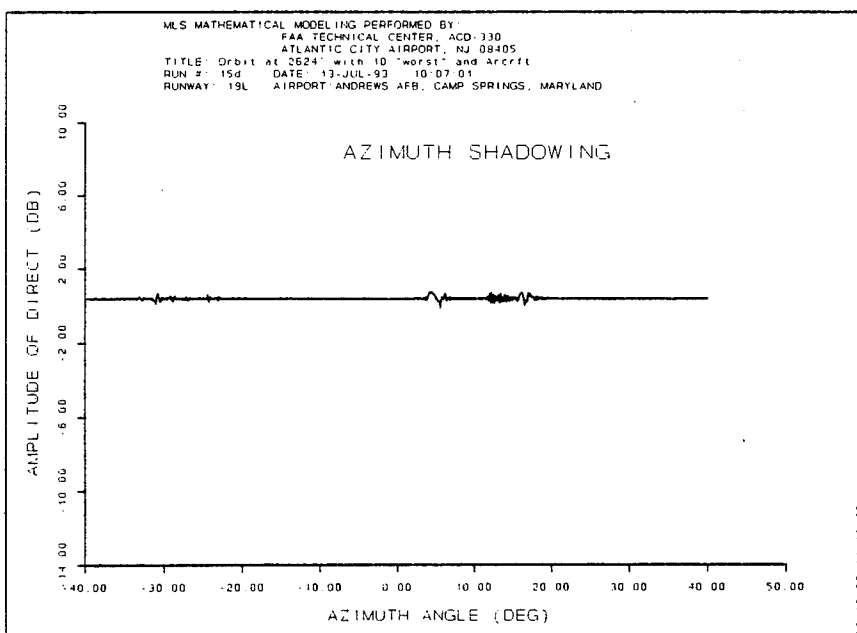
FIGURE A-24. MLS AZ COMPOSITE MAGNITUDE PLOT FOR AN
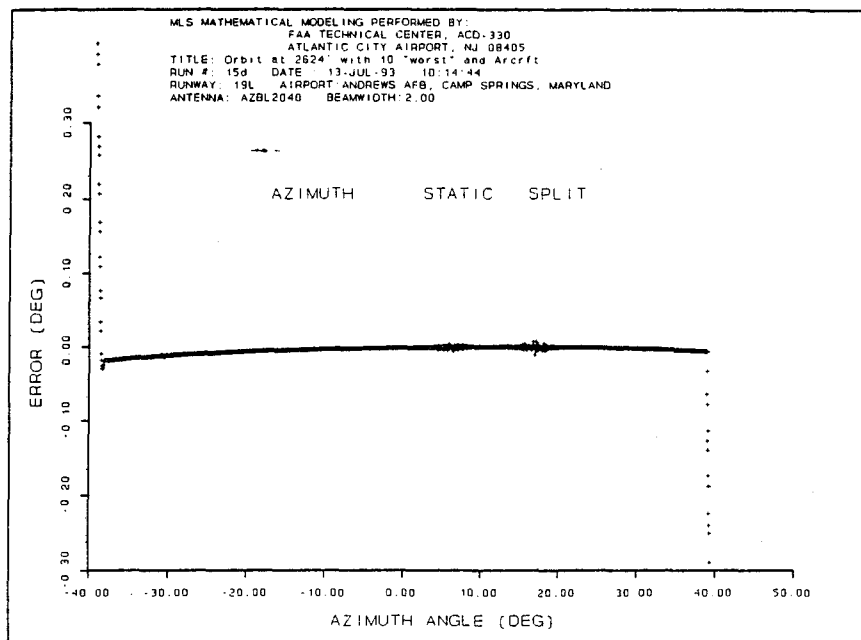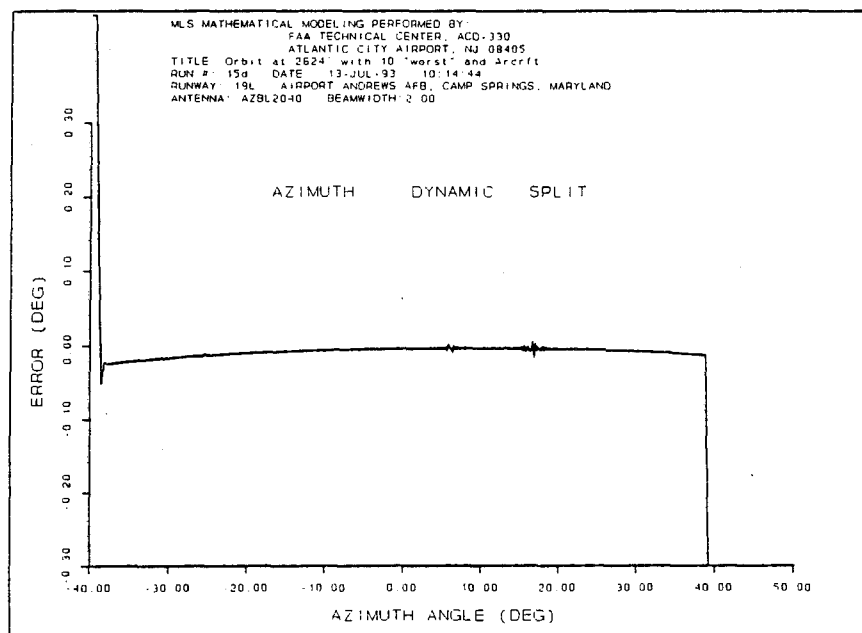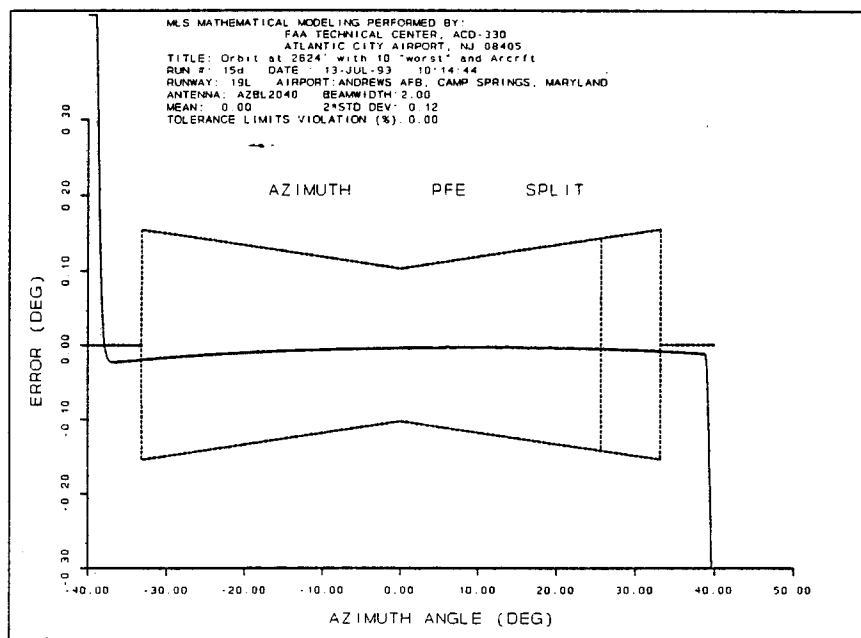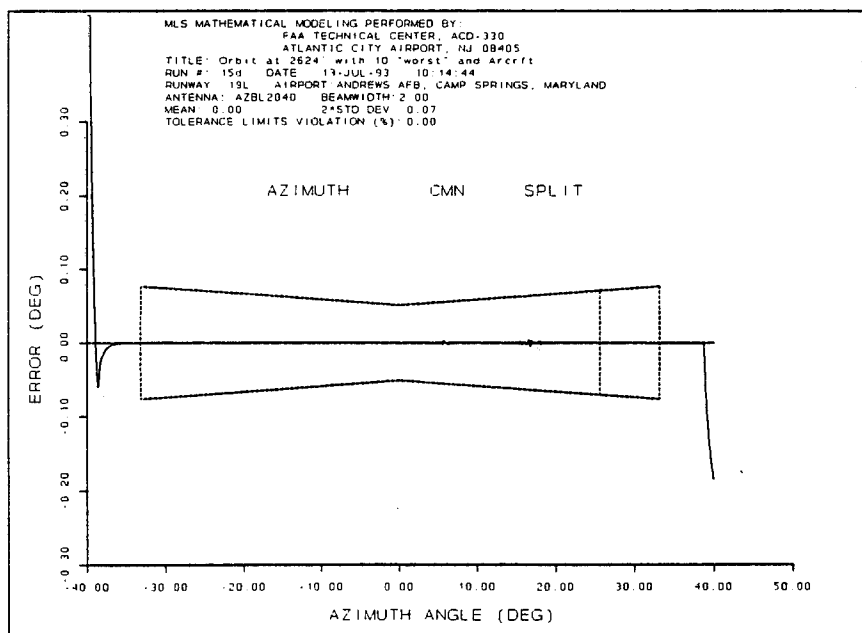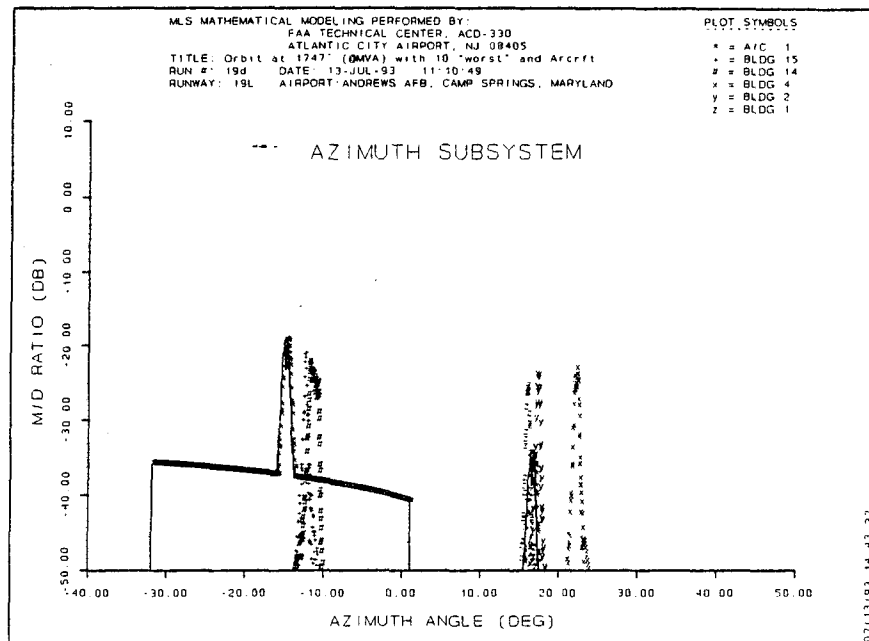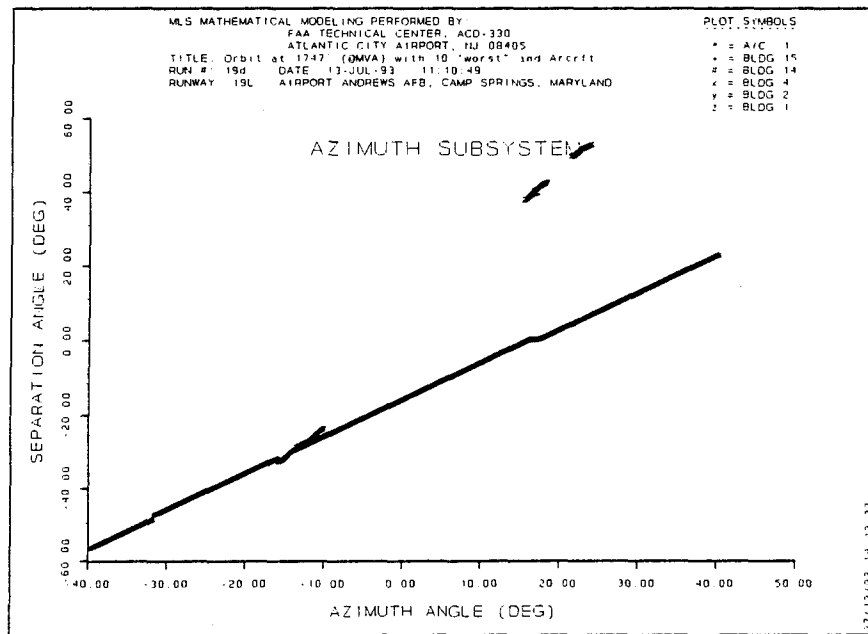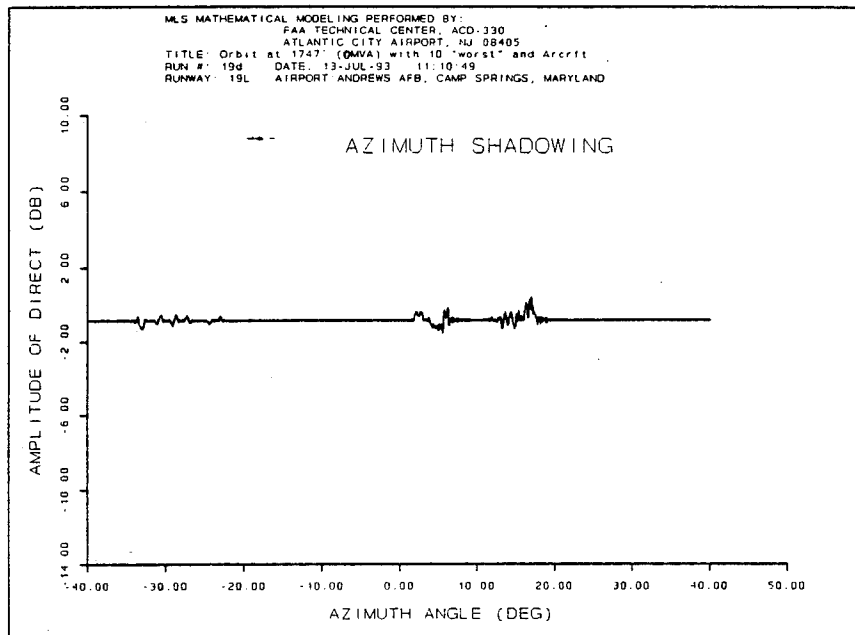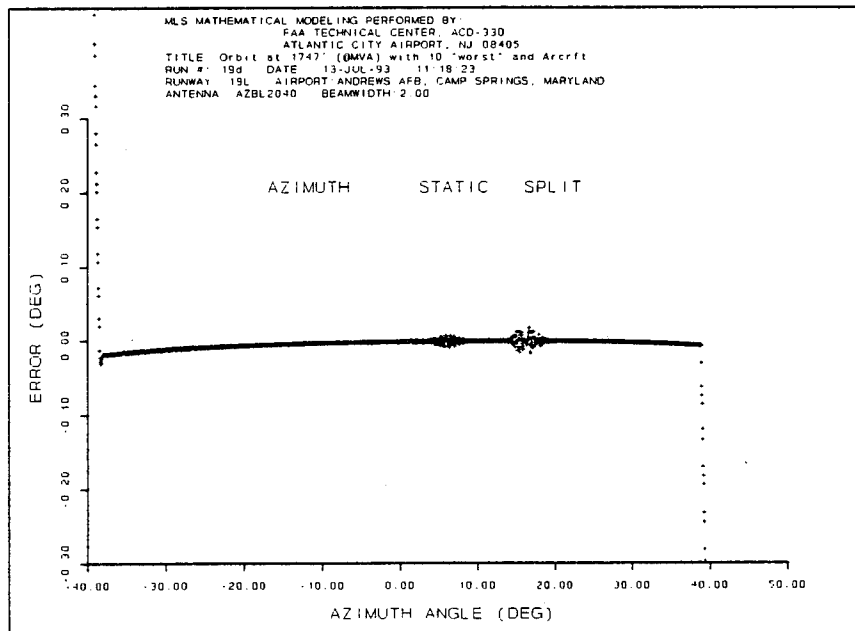ORBITAL (2624' ABOVE REFERENCE) FLIGHT PATH.

A-15

MLS MATHEMATICAL MODELING PERFORMED BY:
FAA TECHNICAL CENTER, ACD-330
ATLANTIC CITY AIRPORT, NJ 08405
TITLE: Orbit at 2624' with 10 "worst" and Arcrft
RUN #: 15d   DATE: 13-JUL-93   10:14:44
RUNWAY: 19L   AIRPORT: ANDREWS AFB, CAMP SPRINGS, MARYLAND
ANTENNA: AZBL2040   BEAMWIDTH: 2.00

AZIMUTH   STATIC   SPLIT

FIGURE A-25. MLS AZ STATIC ERROR PLOT FOR AN ORBITAL (2624′ ABOVE REFERENCE) FLIGHT PATH.

MLS MATHEMATICAL MODELING PERFORMED BY:
FAA TECHNICAL CENTER, ACD-330
ATLANTIC CITY AIRPORT, NJ 08405
TITLE: Orbit at 2624' with 10 "worst" and Arcrft
RUN #: 15d   DATE: 13-JUL-93   10:14:44
RUNWAY: 19L   AIRPORT: ANDREWS AFB, CAMP SPRINGS, MARYLAND
ANTENNA: AZBL2040   BEAMWIDTH: 2.00

AZIMUTH   DYNAMIC   SPLIT

FIGURE A-26. MLS AZ DYNAMIC ERROR PLOT FOR AN ORBITAL (2624′ ABOVE REFERENCE) FLIGHT PATH.
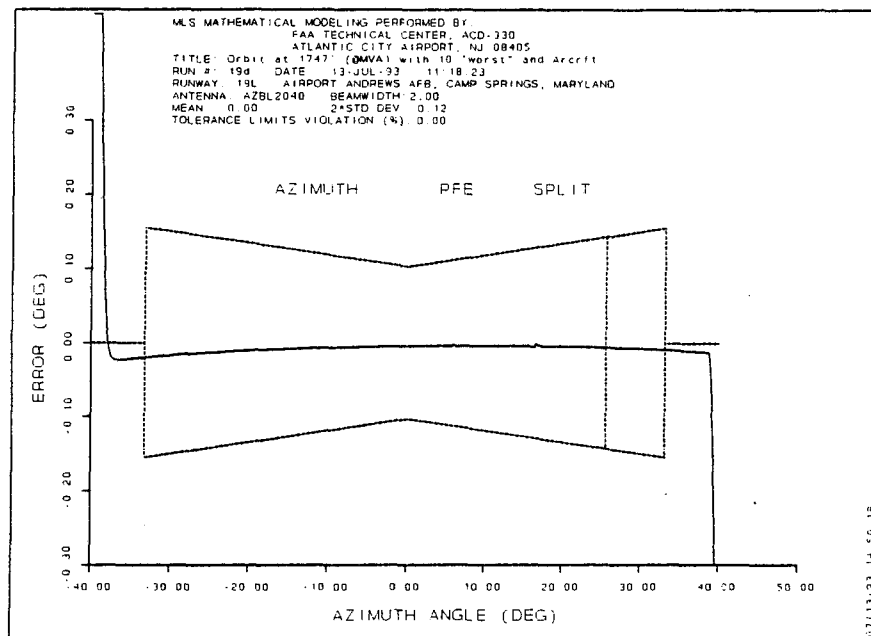
A-16

FIGURE A-27. MLS AZ PATH FOLLOWING ERROR PLOT FOR
AN ORBITAL (2624' ABOVE REFERENCE) FLIGHT PATH.

FIGURE A-28. MLS AZ CONTROL MOTION NOISE PLOT FOR
AN ORBITAL (2624' ABOVE REFERENCE) FLIGHT PATH.

A-17

MLS MATHEMATICAL MODELING PERFORMED BY:
FAA TECHNICAL CENTER, ACD-330
ATLANTIC CITY AIRPORT, NJ 08405
TITLE: Orbit at 1747' (0MVA) with 10 "worst" and Arcrft
RUN #: 19d   DATE: 13-JUL-93   11:10:49
RUNWAY: 19L   AIRPORT:ANDREWS AFB, CAMP SPRINGS, MARYLAND

PLOT SYMBOLS
* = A/C 1
. = BLDG 15
# = BLDG 14
x = BLDG 4
y = BLDG 2
z = BLDG 1

AZIMUTH SUBSYSTEM

FIGURE A-29.   MLS AZ MULTIPATH RELATIVE MAGNITUDE
PLOT FOR AN ORBITAL (1747' ABOVE REFERENCE)
FLIGHT PATH.

MLS MATHEMATICAL MODELING PERFORMED BY
FAA TECHNICAL CENTER, ACD-330
ATLANTIC CITY AIRPORT, NJ 08405
TITLE: Orbit at 1747' (0MVA) with 10 "worst" and Arcrft
RUN #: 19d   DATE: 13-JUL-93   11:10:49
RUNWAY: 19L   AIRPORT ANDREWS AFB, CAMP SPRINGS, MARYLAND

PLOT SYMBOLS
* = A/C 1
. = BLDG 15
# = BLDG 14
x = BLDG 4
y = BLDG 2
z = BLDG 1

AZIMUTH SUBSYSTEM

FIGURE A-30.   MLS AZ MULTIPATH SEPARATION ANGLE PLOT
FOR AN ORBITAL (1747' ABOVE REFERENCE) FLIGHT PATH.

FIGURE A-31. MLS AZ COMPOSITE MAGNITUDE PLOT FOR AN
ORBITAL (1747' ABOVE REFERENCE) FLIGHT PATH.

FIGURE A-32. MLS AZ STATIC ERROR PLOT FOR AN
ORBITAL (1747' ABOVE REFERENCE) FLIGHT PATH.

A-19
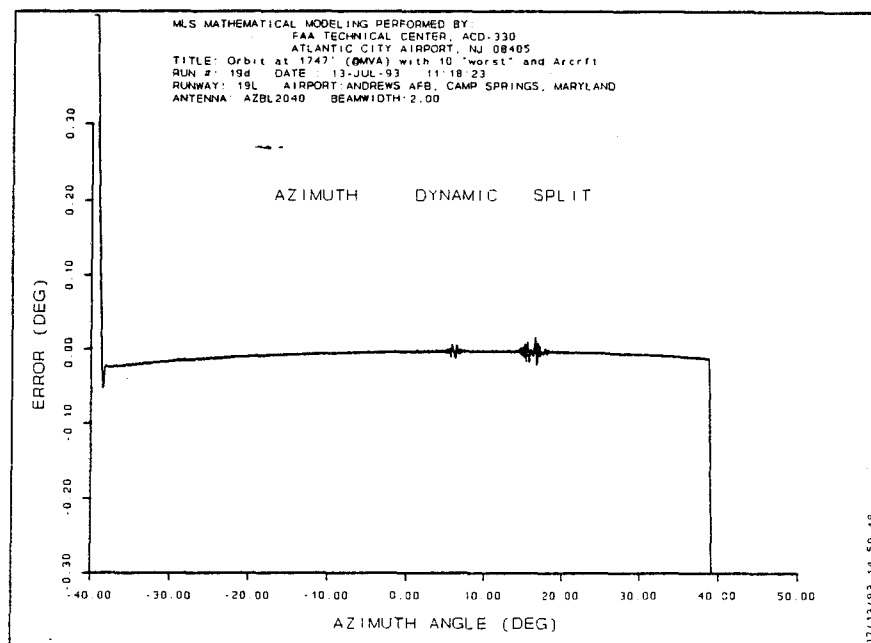
FIGURE A-33. MLS AZ DYNAMIC ERROR PLOT FOR AN ORBITAL (1747' ABOVE REFERENCE) FLIGHT PATH.

FIGURE A-34. MLS AZ PATH FOLLOWING ERROR PLOT FOR AN ORBITAL (1747' ABOVE REFERENCE) FLIGHT PATH.
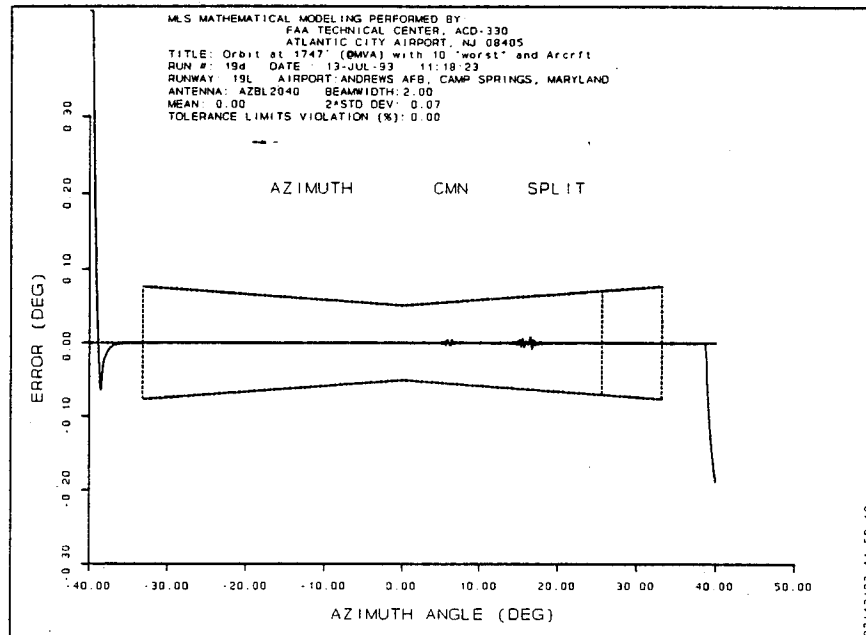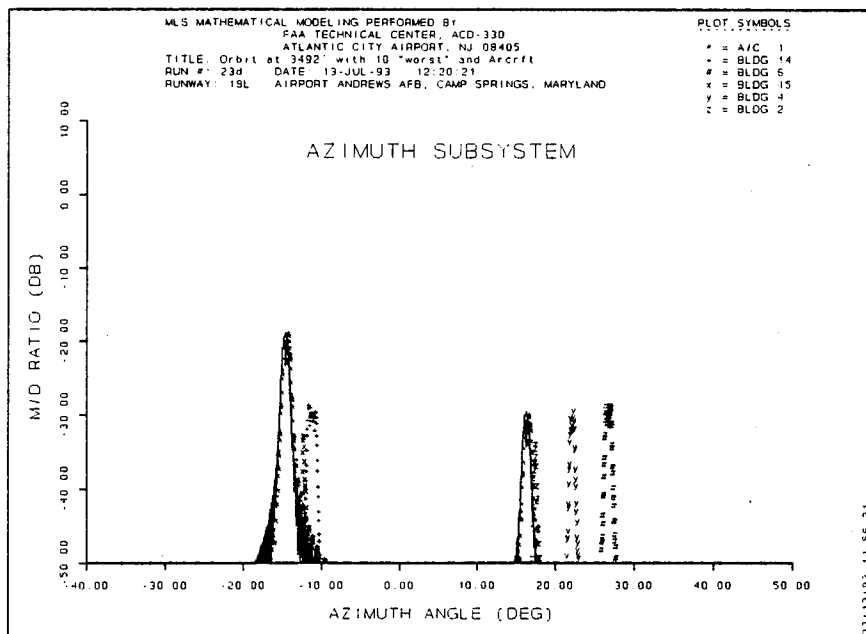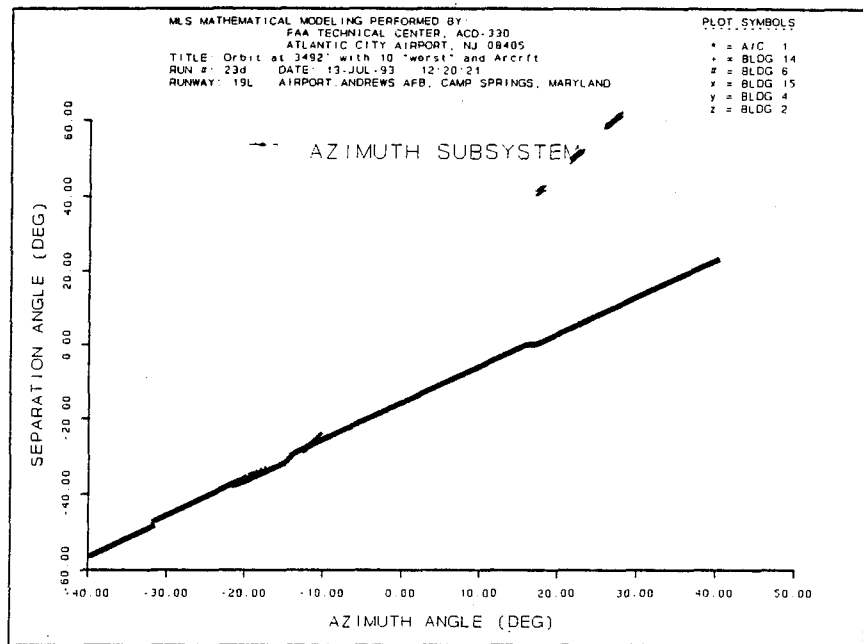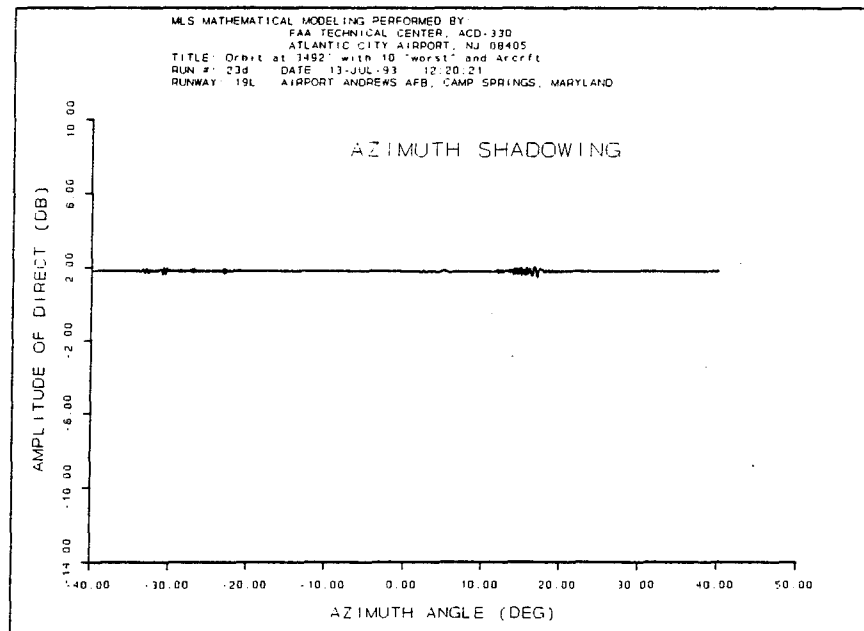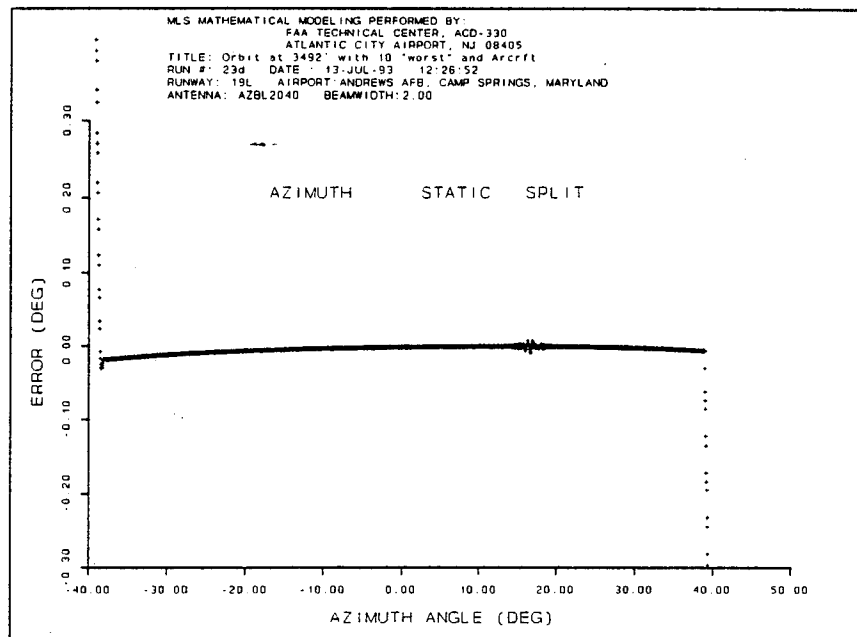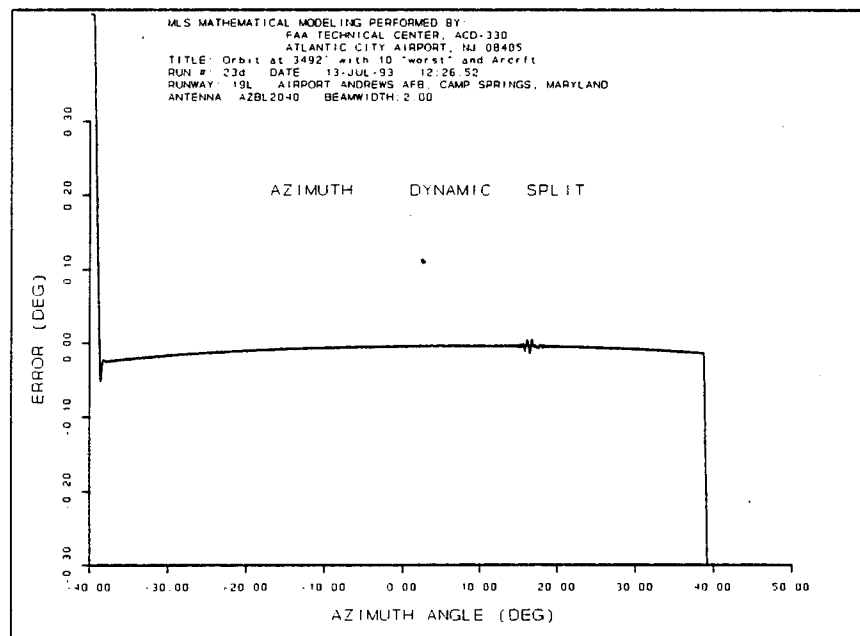
A-20

FIGURE A-35. MLS AZ CONTROL MOTION NOISE PLOT FOR
AN ORBITAL (1747' ABOVE REFERENCE) FLIGHT PATH.

FIGURE A-36. MLS AZ MULTIPATH RELATIVE MAGNITUDE
PLOT FOR AN ORBITAL (3492' ABOVE REFERENCE)
FLIGHT PATH.

A-21

FIGURE A-37. MLS AZ MULTIPATH SEPARATION ANGLE PLOT
FOR AN ORBITAL (3492' ABOVE REFERENCE) FLIGHT PATH.

FIGURE A-38. MLS AZ COMPOSITE MAGNITUDE PLOT FOR AN
ORBITAL (3492' ABOVE REFERENCE) FLIGHT PATH.

A-22

FIGURE A-39. MLS AZ STATIC ERROR PLOT FOR AN ORBITAL (3492' ABOVE REFERENCE) FLIGHT PATH.

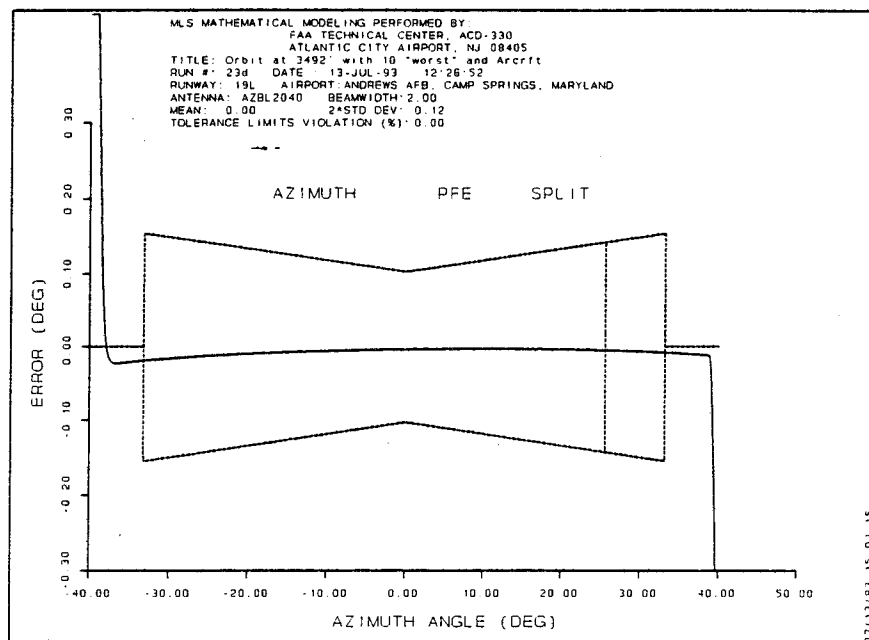FIGURE A-40. MLS AZ DYNAMIC ERROR PLOT FOR AN ORBITAL (3492' ABOVE REFERENCE) FLIGHT PATH.

A-23

FIGURE A-41. MLS AZ PATH FOLLOWING ERROR PLOT FOR
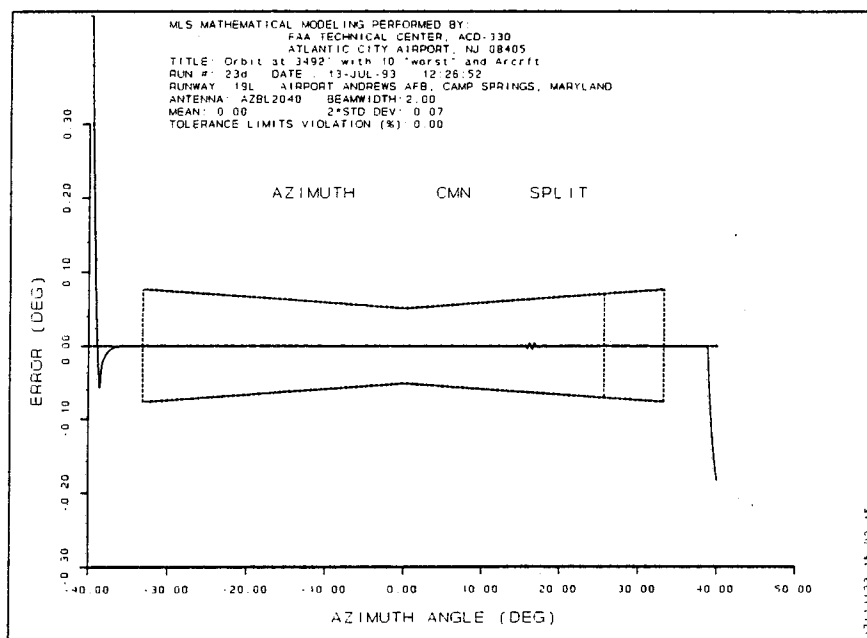AN ORBITAL 3492' ABOVE REFERENCE) FLIGHT PATH.

FIGURE A-42. MLS AZ CONTROL MOTION NOISE PLOT FOR
AN ORBITAL 3492' ABOVE REFERENCE) FLIGHT PATH.

A-24

Appendix B
MLS Elevation Modeling Results
List of Illustrations

Results of modeling effort of the six scenarios with the 10 worst-case contributors of multipath on the guidance provided by the MLS EL are presented in this section.

FIGURE B-1. MLS EL MULTIPATH RELATIVE MAGNITUDE
PLOT FOR A STRAIGHT APPROACH (3° GPA) FLIGHT PATH.

FIGURE B-2. MLS EL MULTIPATH SEPARATION ANGLE
PLOT FOR A STRAIGHT APPROACH (3° GPA) FLIGHT PATH.

MLS MATHEMATICAL MODELING PERFORMED BY:
FAA TECHNICAL CENTER, ACD-330
ATLANTIC CITY AIRPORT, NJ 08405
TITLE: Straight Approach at 3 degrees w/ 10 "worst", arcrft, topo
RUN #: 03a   DATE: 26-JUL-93   16:41:46
RUNWAY: 19L   AIRPORT: ANDREWS AFB, CAMP SPRINGS, MARYLAND

ELEVATION SHADOWING

FIGURE B-3.   MLS EL COMPOSITE MAGNITUDE PLOT FOR A
STRAIGHT APPROACH (3° GPA) FLIGHT PATH.

MLS MATHEMATICAL MODELING PERFORMED BY:
FAA TECHNICAL CENTER, ACD-330
ATLANTIC CITY AIRPORT, NJ 08405
TITLE: Straight Approach at 3 degrees w/ 10 "worst", arcrft, topo
RUN #: 03a   DATE: 26-JUL-93   16:43:50
RUNWAY: 19L   AIRPORT: ANDREWS AFB, CAMP SPRINGS, MARYLAND
ANTENNA: ELB1S   BEAMWIDTH: 1.50

ELEVATION   STATIC   SPLIT
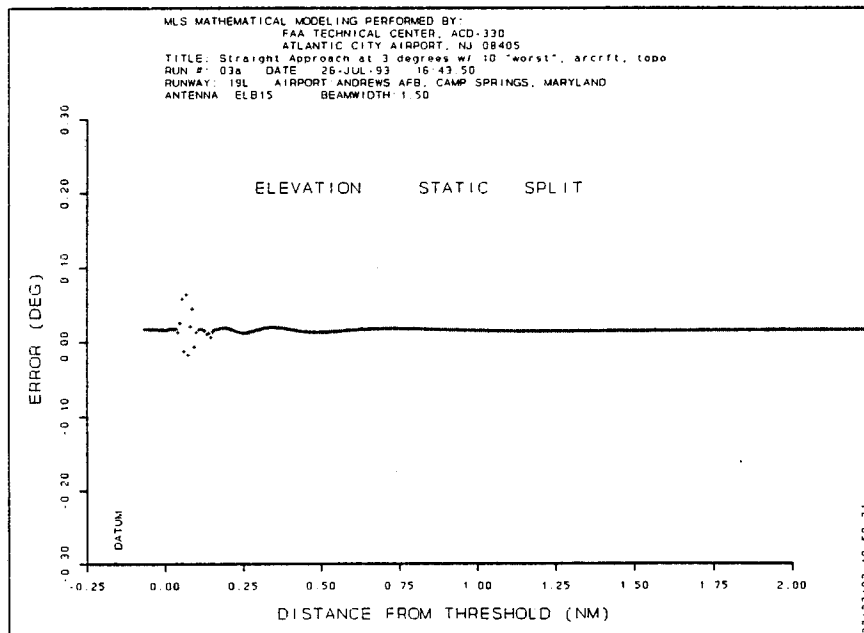
FIGURE B-4.   MLS EL STATIC ERROR PLOT FOR A STRAIGHT
APPROACH (3° GPA) FLIGHT PATH.

B-5
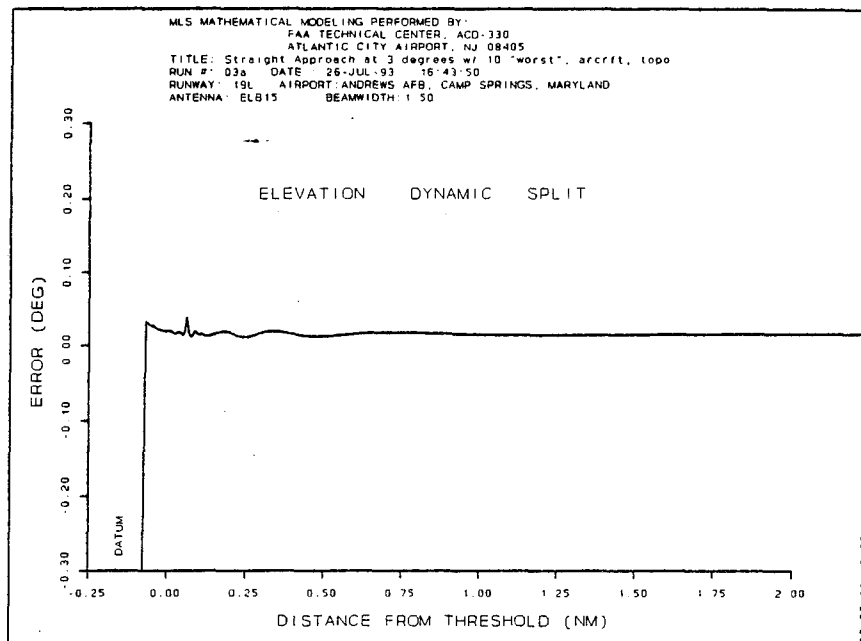
FIGURE B-5. MLS EL DYNAMIC ERROR PLOT FOR A
STRAIGHT APPROACH (3° GPA) FLIGHT PATH.
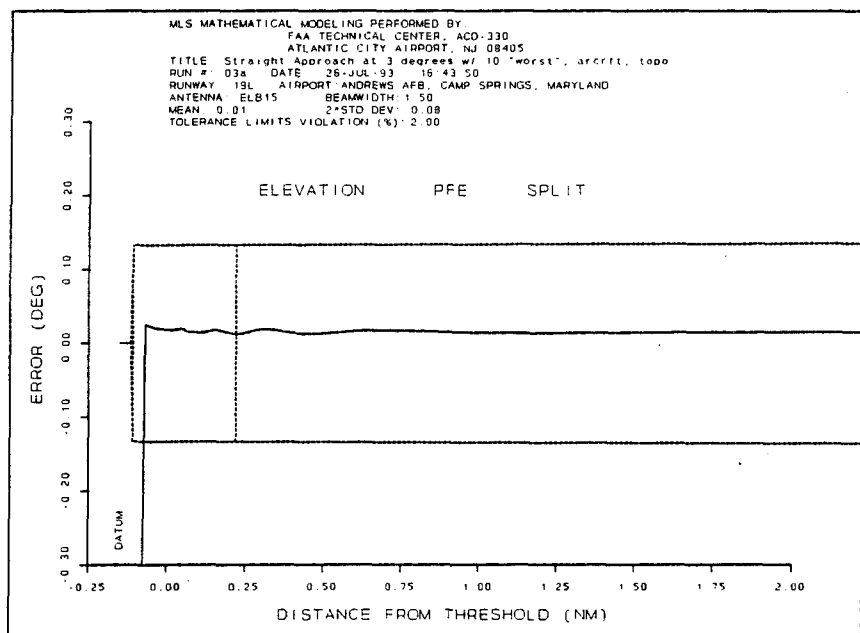
FIGURE B-6. MLS EL PATH FOLLOWING ERROR PLOT FOR A
STRAIGHT APPROACH (3° GPA) FLIGHT PATH.

B-6

MLS MATHEMATICAL MODELING PERFORMED BY:
FAA TECHNICAL CENTER, ACD-330
ATLANTIC CITY AIRPORT, NJ 08405
TITLE: Straight Approach at 3 degrees w/ 10 "worst", arcrft, topo
RUN #: 03a   DATE : 26-JUL-93   16:43:50
RUNWAY: 19L   AIRPORT: ANDREWS AFB, CAMP SPRINGS, MARYLAND
ANTENNA: ELB15   BEAMWIDTH: 1.50
MEAN: 0.00   2*STD DEV: 0.08
TOLERANCE LIMITS VIOLATION (%): 2.00

ELEVATION   CMN   SPLIT

FIGURE B-7.   MLS EL CONTROL MOTION NOISE PLOT FOR A STRAIGHT APPROACH (3° GPA) FLIGHT PATH.

MLS MATHEMATICAL MODELING PERFORMED BY:
FAA TECHNICAL CENTER, ACD-330
ATLANTIC CITY AIRPORT, NJ 08405
TITLE: Straight Approach at 2 degrees with 10 "worst" and Arcrft
RUN #: 07a   DATE: 26-JUL-93   17:06:44
RUNWAY: 19L   AIRPORT: ANDREWS AFB, CAMP SPRINGS, MARYLAND

PLOT SYMBOLS
* = A/C 3
. = BLDG 1
# = BLDG 2
x = BLDG 3
y = BLDG 4
z = A/C 1

ELEVATION SUBSYSTEM

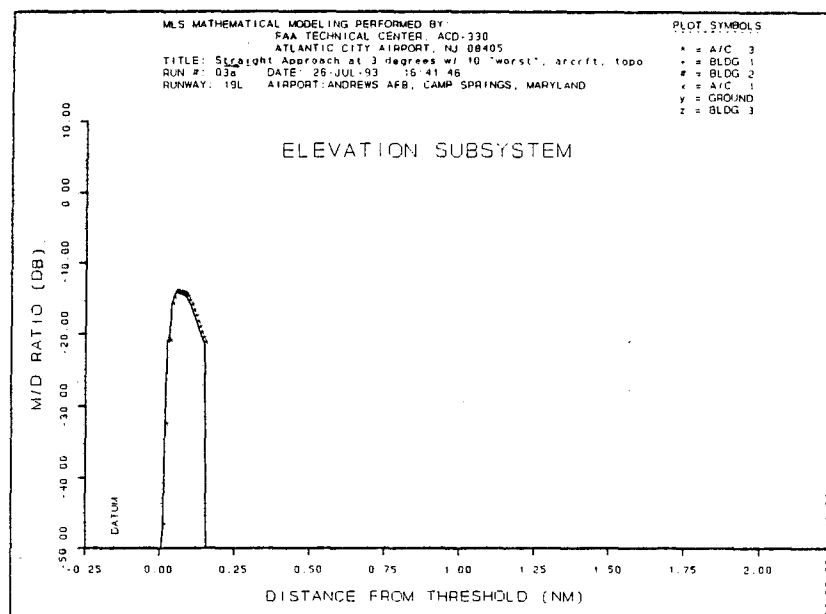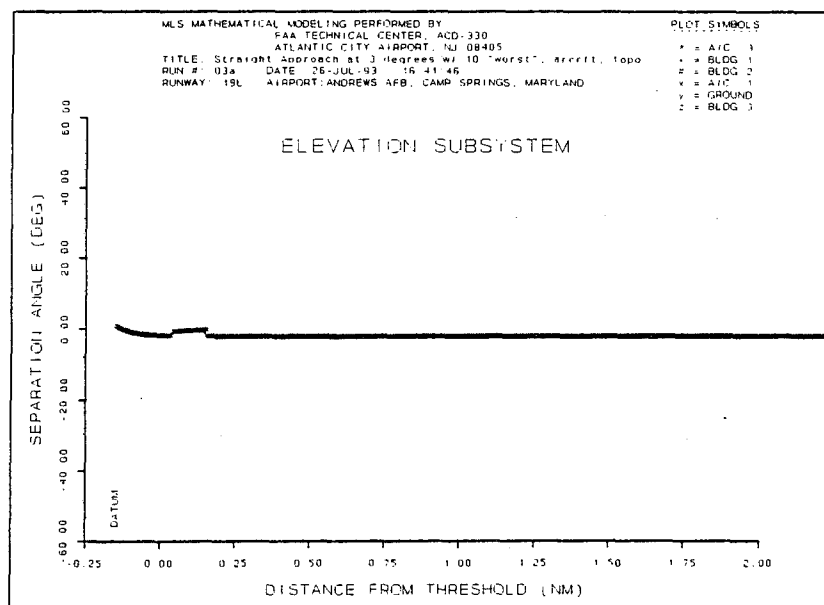**FIGURE B-8.   MLS EL MULTIPATH RELATIVE MAGNITUDE PLOT FOR A STRAIGHT APPROACH (2° GPA) FLIGHT PATH.**

B-7

FIGURE B-9.   MLS EL MULTIPATH SEPARATION ANGLE PLOT
FOR A STRAIGHT APPROACH (2° GPA) FLIGHT PATH.

FIGURE B-10.   MLS EL COMPOSITE MAGNITUDE PLOT FOR A
STRAIGHT APPROACH (2° GPA) FLIGHT PATH.

B-8

MLS MATHEMATICAL MODELING PERFORMED BY:
FAA TECHNICAL CENTER, ACD-330
ATLANTIC CITY AIRPORT, NJ 08405
TITLE: Straight Approach at 2 degrees with 10 "worst" and Arcrft
RUN #: 07a   DATE: 26-JUL-93   17:08:48
RUNWAY: 19L   AIRPORT:ANDREWS AFB, CAMP SPRINGS, MARYLAND
ANTENNA: ELB15   BEAMWIDTH: 1.50

ELEVATION   STATIC   SPLIT

FIGURE B-11.   MLS EL STATIC ERROR PLOT FOR A
STRAIGHT APPROACH (2° GPA) FLIGHT PATH.

MLS MATHEMATICAL MODELING PERFORMED BY:
FAA TECHNICAL CENTER, ACD-330
ATLANTIC CITY AIRPORT, NJ 08405
TITLE: Straight Approach at 2 degrees with 10 "worst" and Arcrft
RUN #: 07a   DATE: 26-JUL-93   17:08:48
RUNWAY: 19L   AIRPORT:ANDREWS AFB, CAMP SPRINGS, MARYLAND
ANTENNA: ELB15   BEAMWIDTH: 1.50

ELEVATION   DYNAMIC   SPLIT

FIGURE B-12.   MLS EL DYNAMIC ERROR PLOT FOR A
STRAIGHT APPROACH (2° GPA) FLIGHT PATH.

B-9

MLS MATHEMATICAL MODELING PERFORMED BY:
              FAA TECHNICAL CENTER, ACD-330
              ATLANTIC CITY AIRPORT, NJ 08405
TITLE: Straight Approach at 2 degrees with 10 "worst" and Arcrft
RUN #: O7a   DATE : 26-JUL-93   17:08:48
RUNWAY: 19L   AIRPORT:ANDREWS AFB, CAMP SPRINGS, MARYLAND
ANTENNA: ELB15   BEAMWIDTH:1.50
MEAN: 0.01   2*STD DEV: 0.08
TOLERANCE LIMITS VIOLATION (%):2.00

ELEVATION   PFE   SPLIT

FIGURE B-13.   MLS EL PATH FOLLOWING ERROR PLOT FOR A
        STRAIGHT APPROACH (2° GPA) FLIGHT PATH.

MLS MATHEMATICAL MODELING PERFORMED BY:
              FAA TECHNICAL CENTER, ACD-330
              ATLANTIC CITY AIRPORT, NJ 08405
TITLE: Straight Approach at 2 degrees with 10 "worst" and Arcrft
RUN #: O7a   DATE   26-JUL-93   17:08:48
RUNWAY: 19L   AIRPORT:ANDREWS AFB, CAMP SPRINGS, MARYLAND
ANTENNA: ELB15   BEAMWIDTH:1.50
MEAN: 0.00   2*STD DEV: 0.08
TOLERANCE LIMITS VIOLATION (%): 2.00

ELEVATION   CMN   SPLIT

FIGURE B-14.   MLS EL CONTROL MOTION NOISE PLOT FOR A
        STRAIGHT APPROACH (2° GPA) FLIGHT PATH.

B-10

FIGURE B-15. MLS EL MULTIPATH RELATIVE MAGNITUDE
PLOT FOR A STRAIGHT APPROACH (4° GPA) FLIGHT PATH.
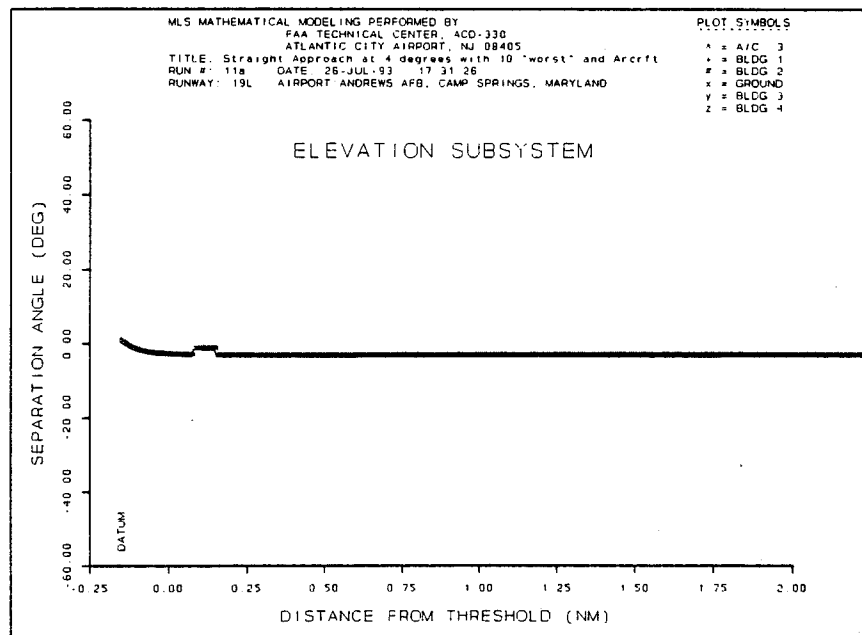
FIGURE B-16. MLS EL MULTIPATH SEPARATION ANGLE PLOT
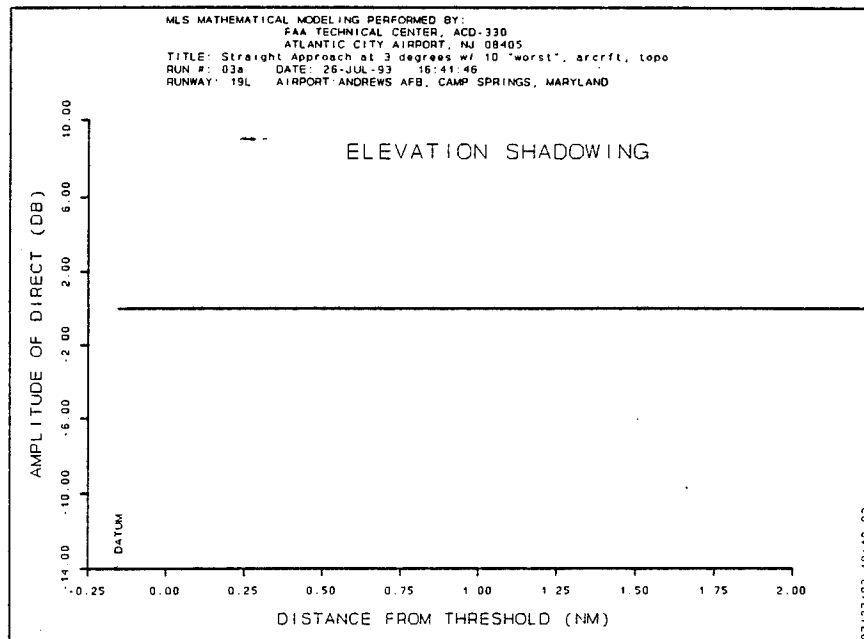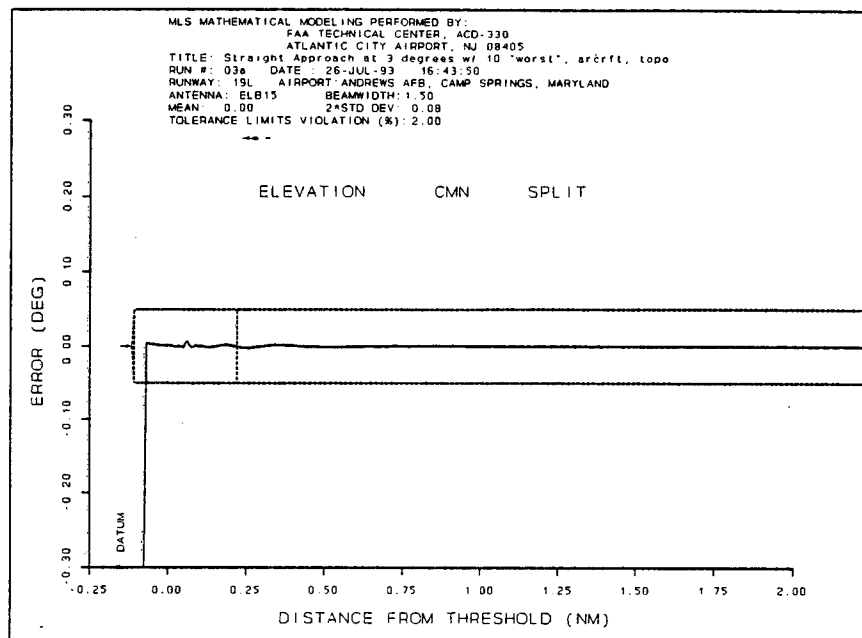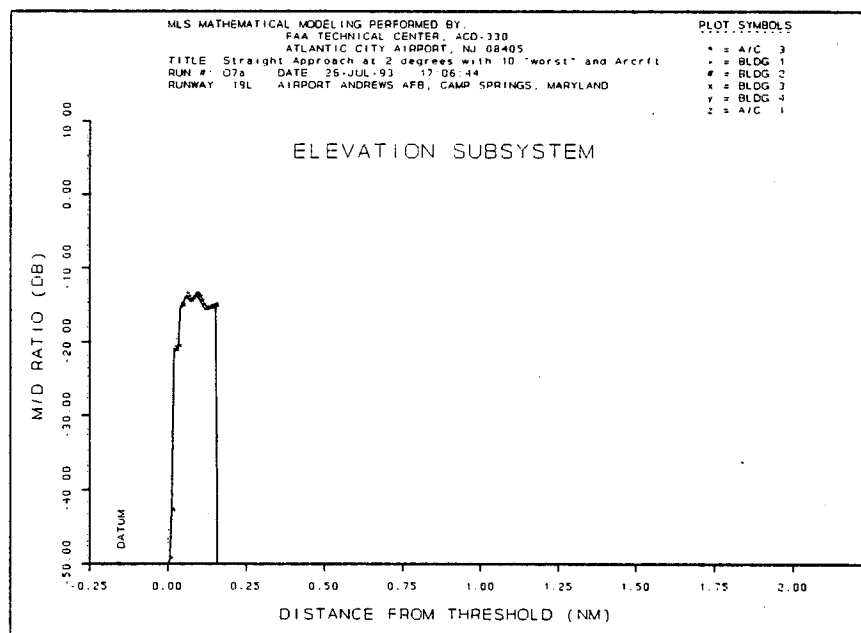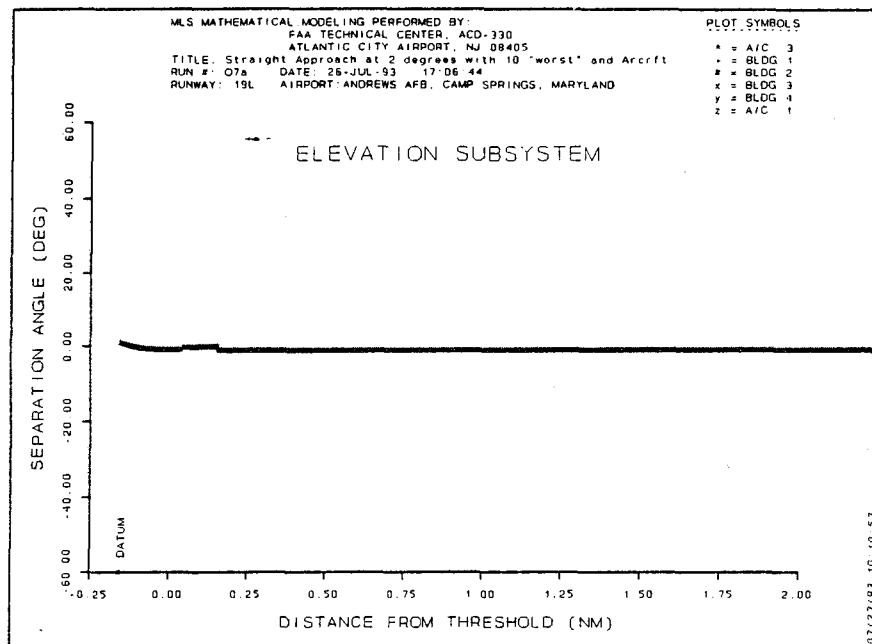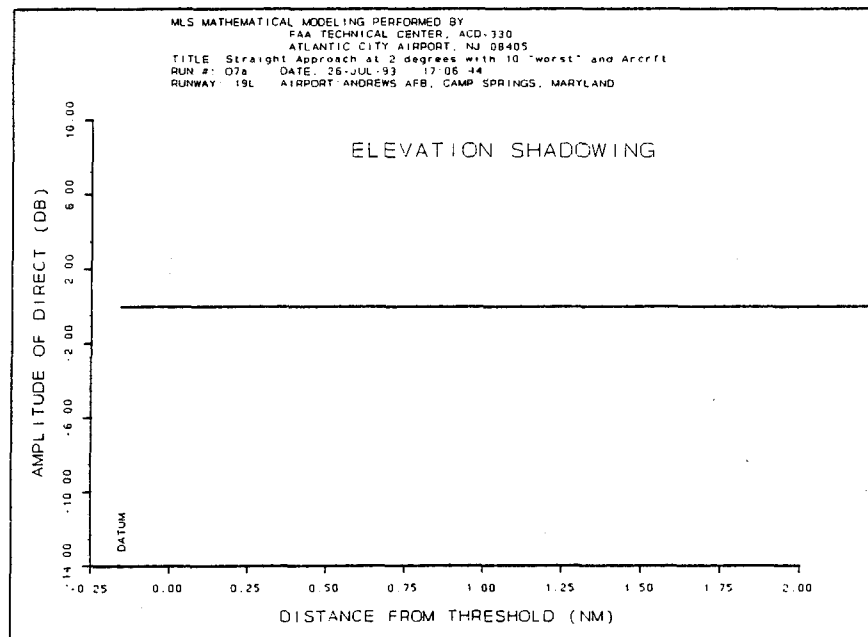FOR A STRAIGHT APPROACH (4° GPA) FLIGHT PATH.

MLS MATHEMATICAL MODELING PERFORMED BY:
                FAA TECHNICAL CENTER, ACD-330
                ATLANTIC CITY AIRPORT, NJ 08405
    TITLE: Straight Approach at 4 degrees with 10 "worst" and Arcrft
    RUN #: 11a   DATE: 26-JUL-93   17:31:26
    RUNWAY: 19L   AIRPORT:ANDREWS AFB, CAMP SPRINGS, MARYLAND

ELEVATION SHADOWING

DISTANCE FROM THRESHOLD (NM)
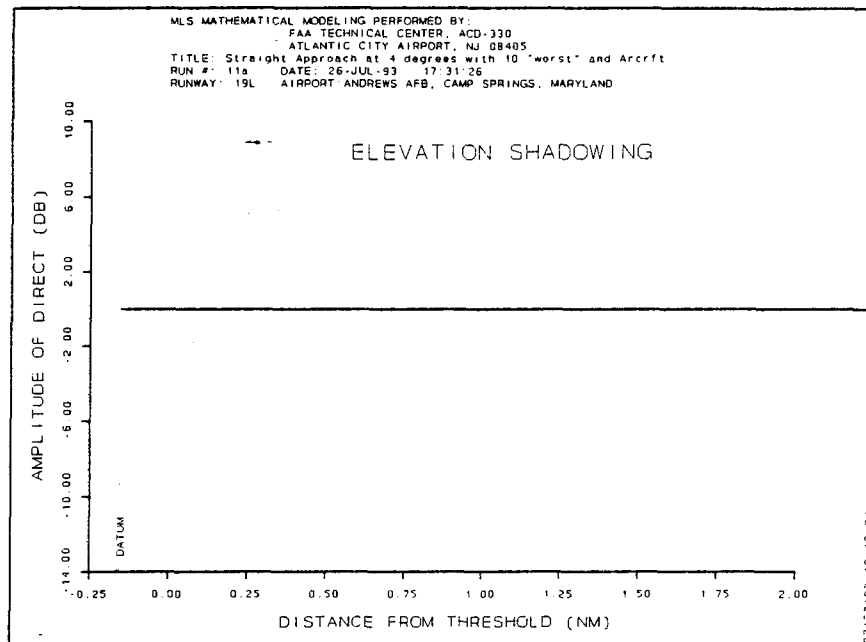
FIGURE B-17. MLS EL COMPOSITE MAGNITUDE PLOT FOR A STRAIGHT APPROACH (4° GPA) FLIGHT PATH.

MLS MATHEMATICAL MODELING PERFORMED BY
                FAA TECHNICAL CENTER, ACD-330
                ATLANTIC CITY AIRPORT, NJ 08405
    TITLE: Straight Approach at 4 degrees with 10 "worst" and Arcrft
    RUN #: 11a   DATE: 26-JUL-93   17:33:30
    RUNWAY: 19L   AIRPORT ANDREWS AFB, CAMP SPRINGS, MARYLAND
    ANTENNA: ELB15   BEAMWIDTH:1.50

ELEVATION   STATIC   SPLIT
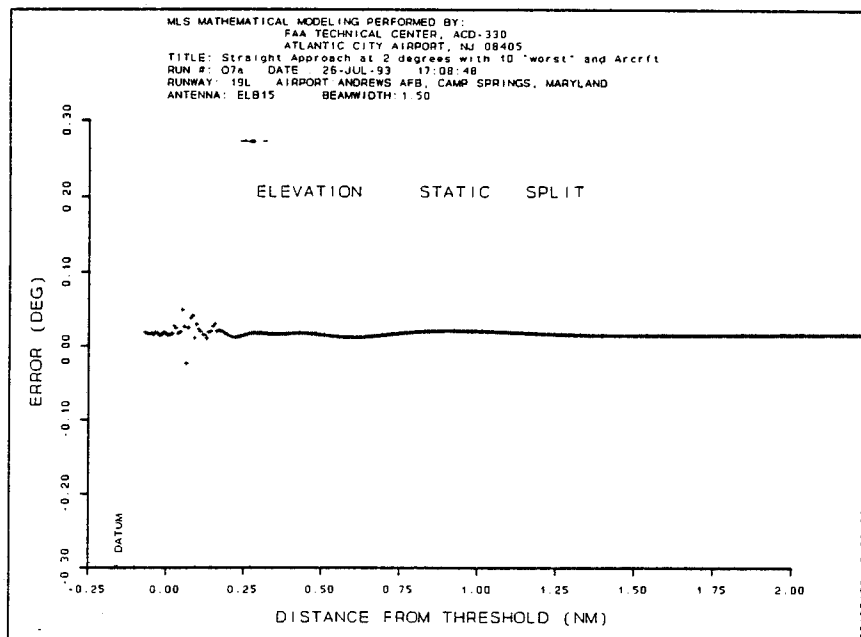
DISTANCE FROM THRESHOLD (NM)
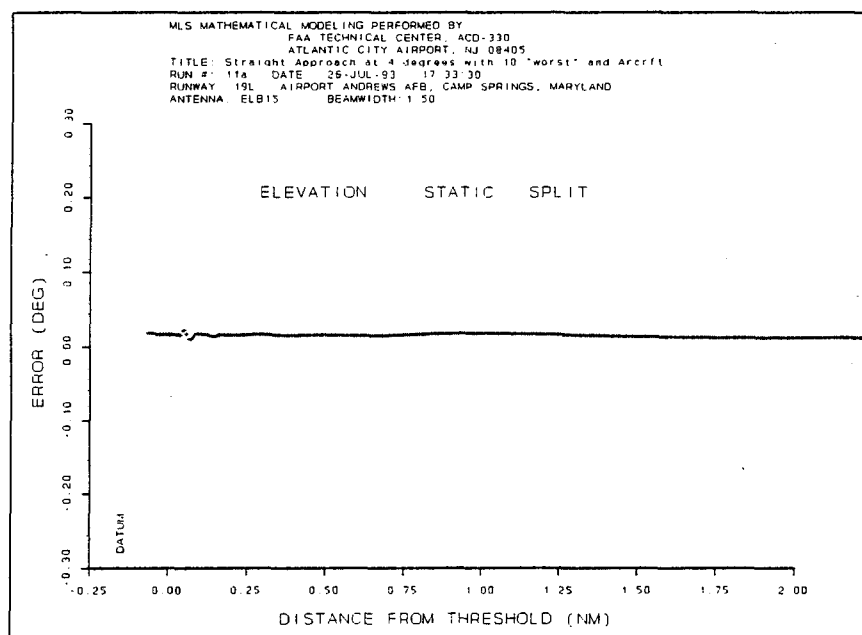
FIGURE B-18. MLS EL STATIC ERROR PLOT FOR A STRAIGHT APPROACH (4° GPA) FLIGHT PATH.
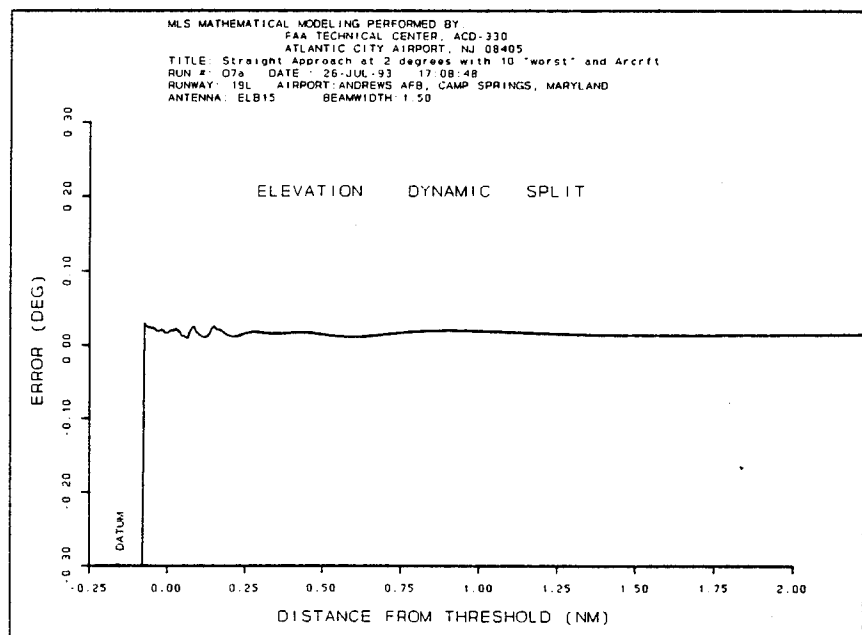
B-12
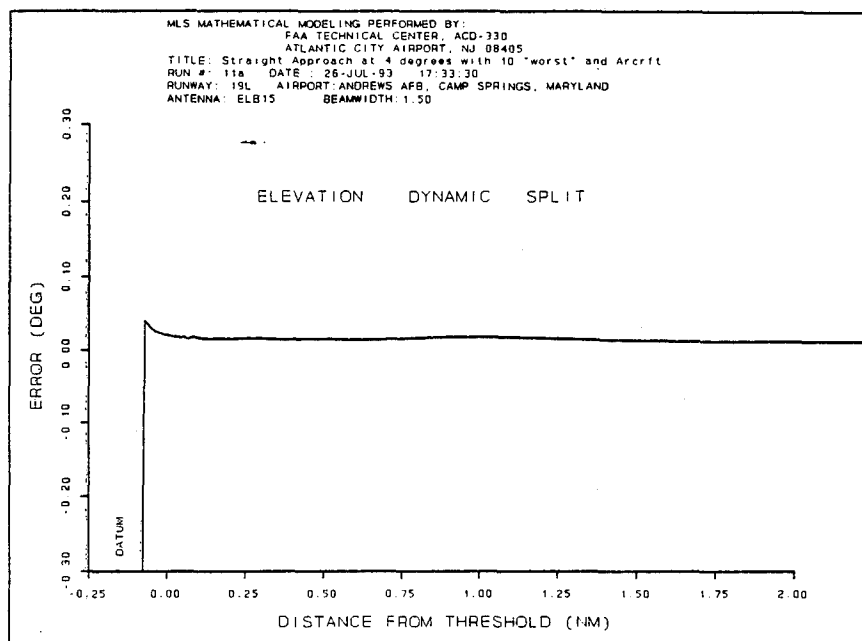
FIGURE B-19. MLS EL DYNAMIC ERROR PLOT FOR A
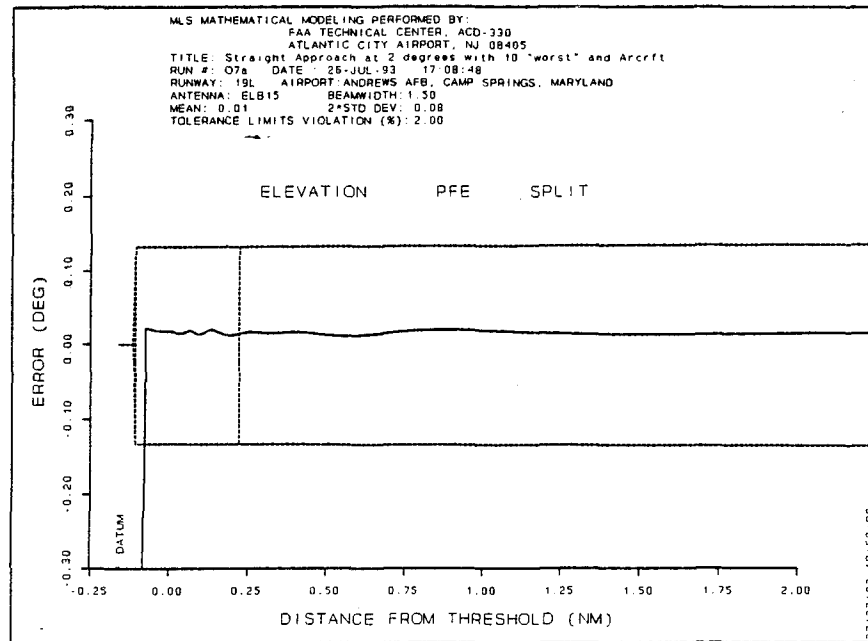STRAIGHT APPROACH (4° GPA) FLIGHT PATH.
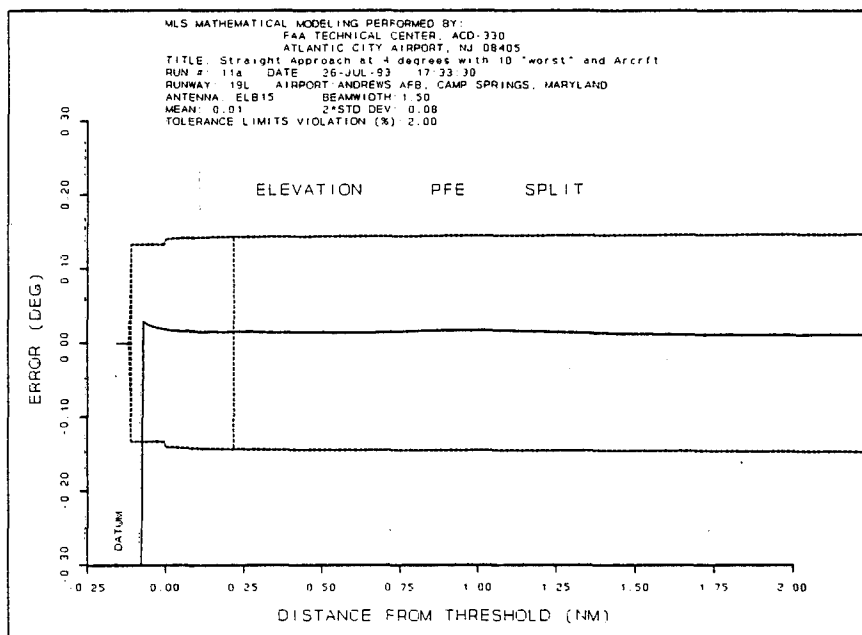
FIGURE B-20. MLS EL PATH FOLLOWING ERROR PLOT FOR A
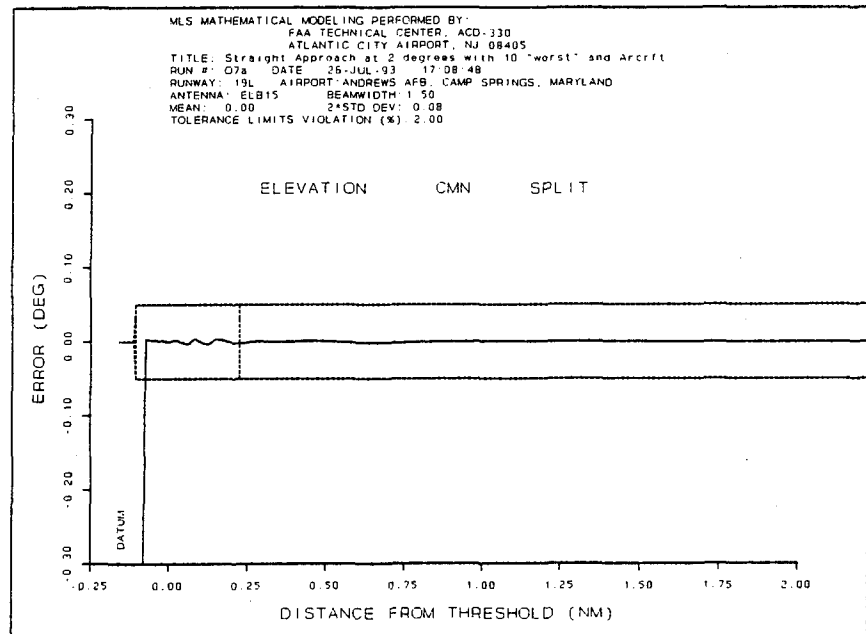STRAIGHT APPROACH (4° GPA) FLIGHT PATH.
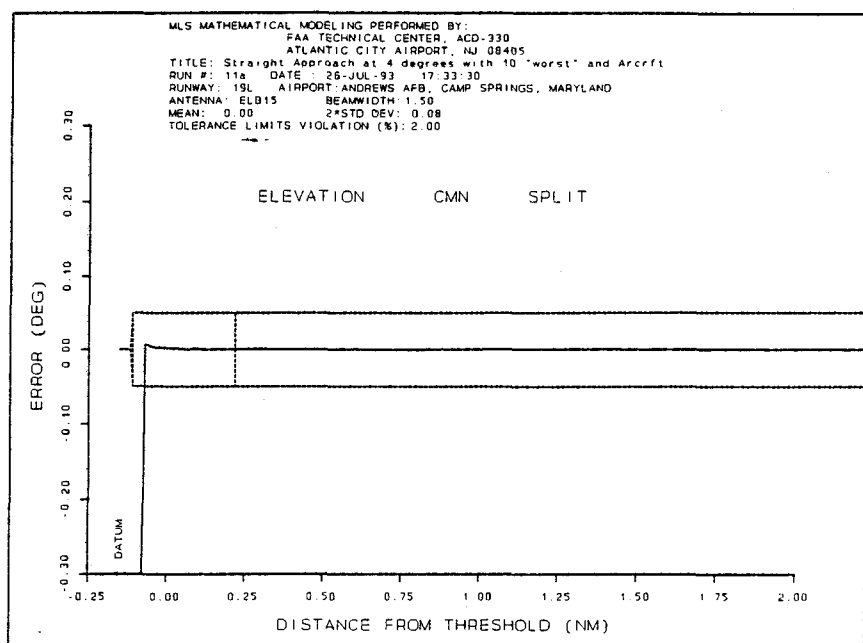
FIGURE B-21. MLS EL CONTROL MOTION NOISE PLOT FOR A
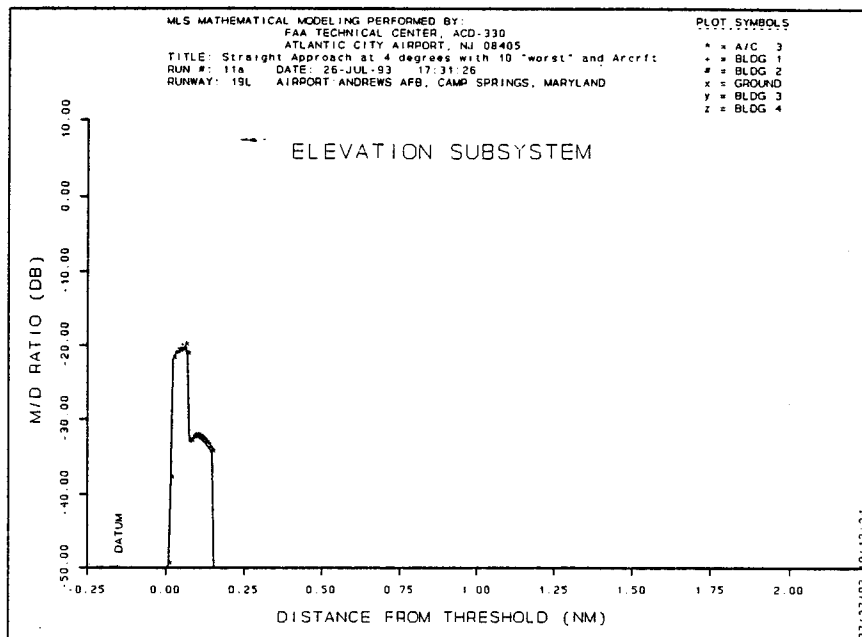STRAIGHT APPROACH (4° GPA) FLIGHT PATH.

FIGURE B-22. MLS EL MULTIPATH RELATIVE MAGNITUDE
PLOT FOR AN ORBITAL (2624' ABOVE REFERENCE)
FLIGHT PATH.

ELEVATION SUBSYSTEM
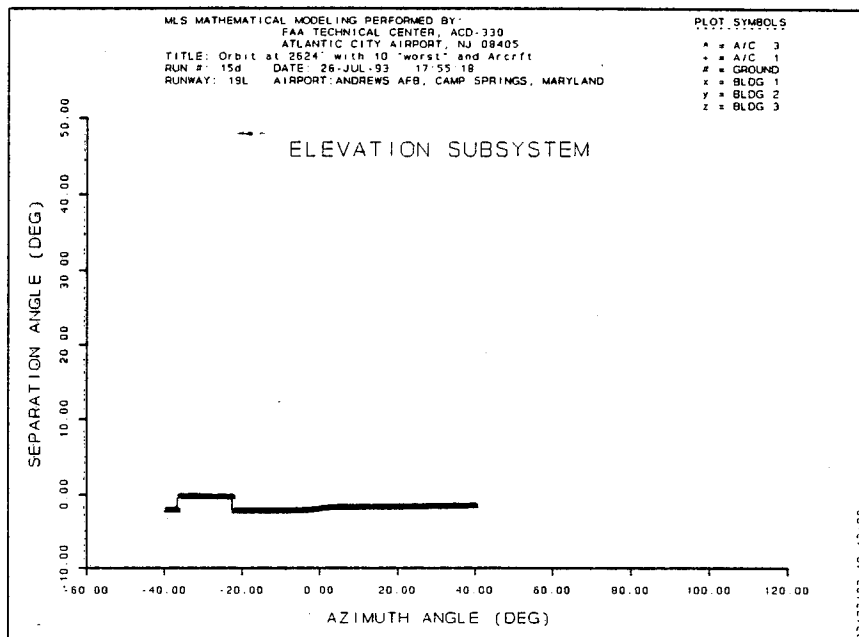
FIGURE B-23. MLS EL MULTIPATH SEPARATION ANGLE PLOT
FOR AN ORBITAL (2624' ABOVE REFERENCE) FLIGHT PATH.

ELEVATION SHADOWING

FIGURE B-24. MLS EL COMPOSITE MAGNITUDE PLOT FOR AN
ORBITAL (2624' ABOVE REFERENCE) FLIGHT PATH.

MLS MATHEMATICAL MODELING PERFORMED BY:
FAA TECHNICAL CENTER, ACD-330
ATLANTIC CITY AIRPORT, NJ 08405
TITLE: Orbit at 2624' with 10 'worst' and Arcrft
RUN #: 15d   DATE : 26-JUL-93   18:00:24
RUNWAY: 19L   AIRPORT:ANDREWS AFB, CAMP SPRINGS, MARYLAND
ANTENNA: ELB15   BEAMWIDTH:1.50

ELEVATION   STATIC   SPLIT
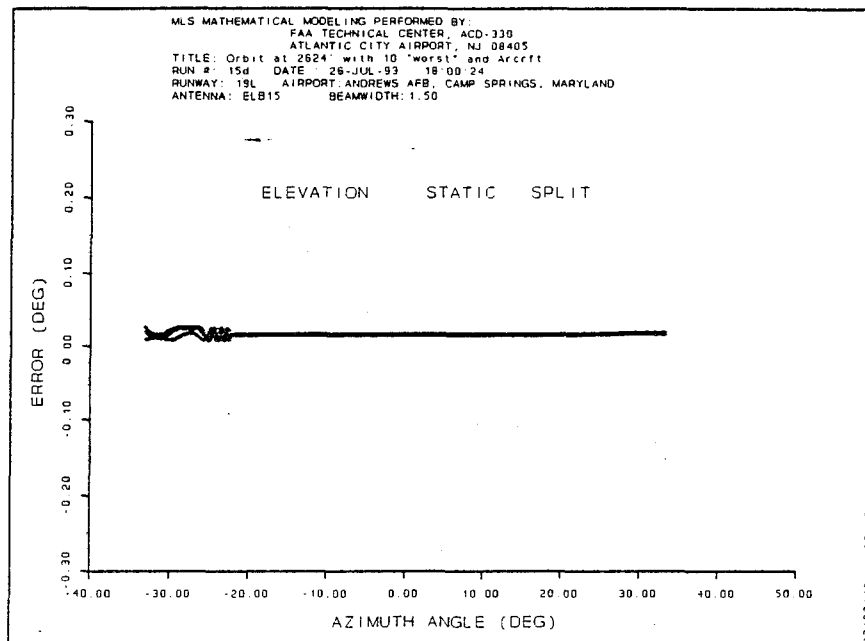
FIGURE B-25. MLS EL STATIC ERROR PLOT FOR AN ORBITAL (2624' ABOVE REFERENCE) FLIGHT PATH.

MLS MATHEMATICAL MODELING PERFORMED BY:
FAA TECHNICAL CENTER, ACD-330
ATLANTIC CITY AIRPORT, NJ 08405
TITLE: Orbit at 2624' with 10 'worst' and Arcrft
RUN #: 15d   DATE : 26-JUL-93   18:00:24
RUNWAY: 19L   AIRPORT:ANDREWS AFB, CAMP SPRINGS, MARYLAND
ANTENNA: ELB15   BEAMWIDTH:1.50

ELEVATION   DYNAMIC   SPLIT
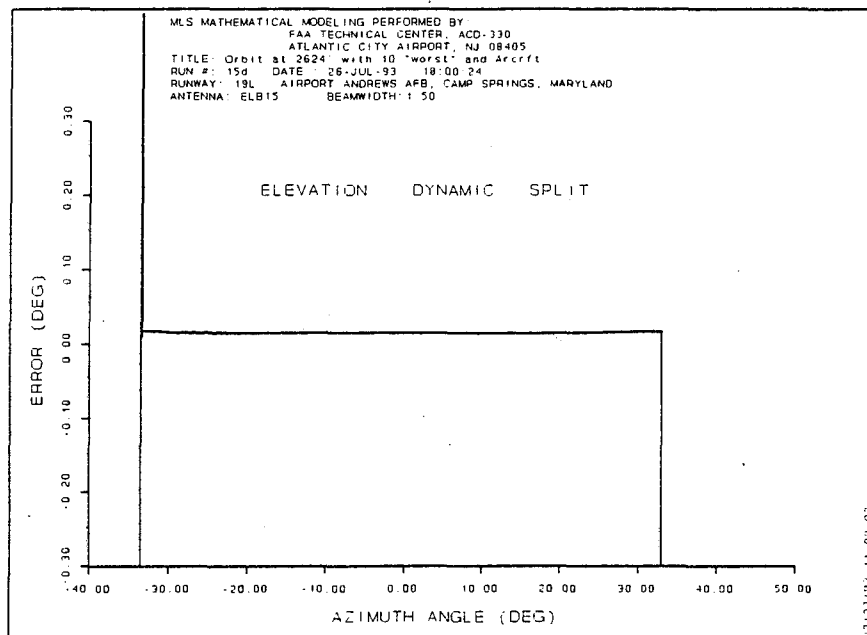
FIGURE B-26. MLS EL DYNAMIC ERROR PLOT FOR AN ORBITAL (2624' ABOVE REFERENCE) FLIGHT PATH.

B-16

MLS MATHEMATICAL MODELING PERFORMED BY:
FAA TECHNICAL CENTER, ACD-330
ATLANTIC CITY AIRPORT, NJ 08405
TITLE: Orbit at 2624' with 10 "worst" and Arcrft
RUN #: 15d   DATE : 26-JUL-93   18:00:24
RUNWAY: 19L   AIRPORT:ANDREWS AFB, CAMP SPRINGS, MARYLAND
ANTENNA: ELB15   BEAMWIDTH:1.50
MEAN: -0.04   2*STD DEV: 0.24
TOLERANCE LIMITS VIOLATION (%): 2.00

ELEVATION   PFE   SPLIT

ERROR (DEG)

AZIMUTH ANGLE (DEG)
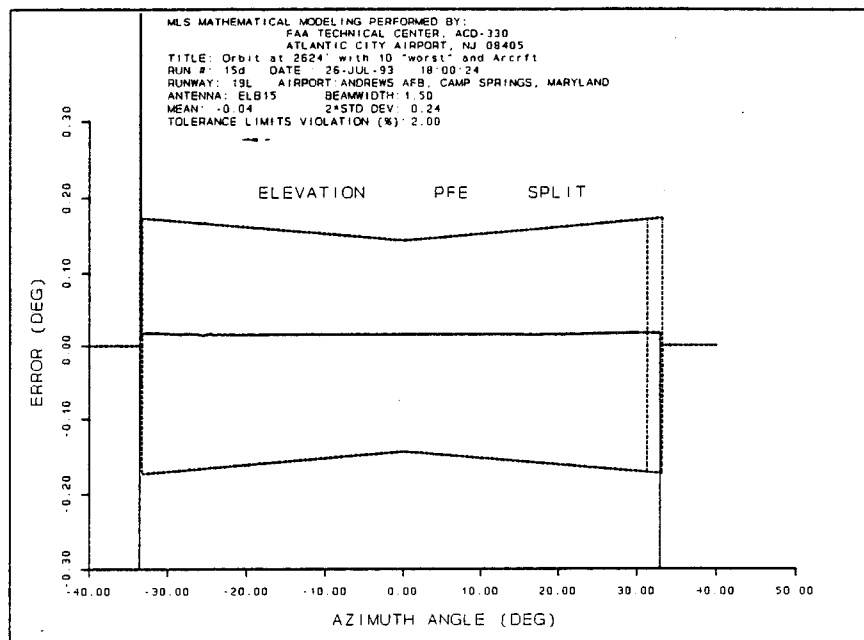
FIGURE B-27. MLS EL PATH FOLLOWING ERROR PLOT FOR AN ORBITAL (2624' ABOVE REFERENCE) FLIGHT PATH.

MLS MATHEMATICAL MODELING PERFORMED BY:
FAA TECHNICAL CENTER, ACD-330
ATLANTIC CITY AIRPORT, NJ 08405
TITLE: Orbit at 2624' with 10 "worst" and Arcrft
RUN #: 15d   DATE : 26-JUL-93   18:00:24
RUNWAY: 19L   AIRPORT:ANDREWS AFB, CAMP SPRINGS, MARYLAND
ANTENNA: ELB15   BEAMWIDTH:1.50
MEAN: -0.05   2*STD DEV: 0.23
TOLERANCE LIMITS VIOLATION (%): 2.00

ELEVATION   CMN   SPLIT

ERROR (DEG)

AZIMUTH ANGLE (DEG)

FIGURE B-28. MLS EL CONTROL MOTION NOISE PLOT FOR AN ORBITAL (2624' ABOVE REFERENCE) FLIGHT PATH.
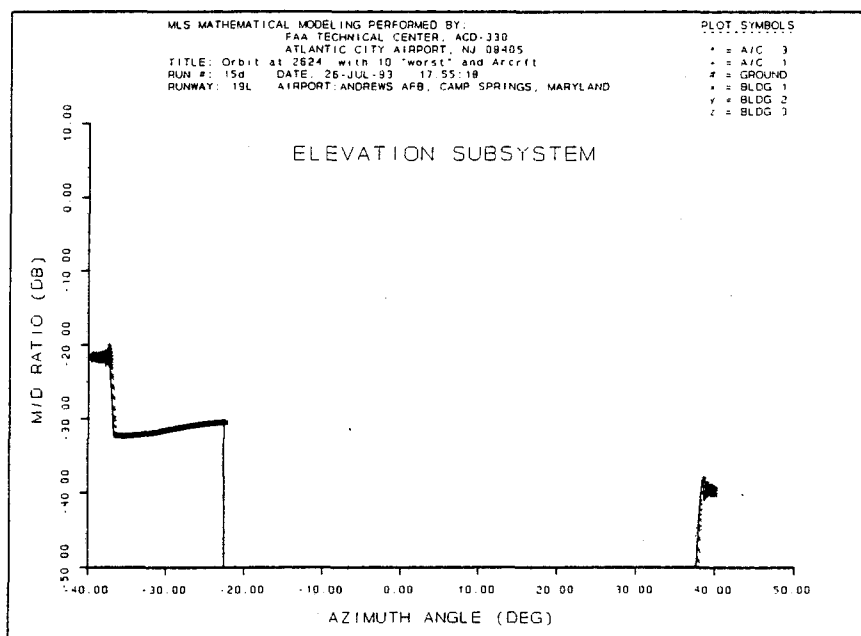
B-17

FIGURE B-29. MLS EL MULTIPATH RELATIVE MAGNITUDE
PLOT FOR AN ORBITAL (1747' ABOVE REFERENCE)
FLIGHT PATH.
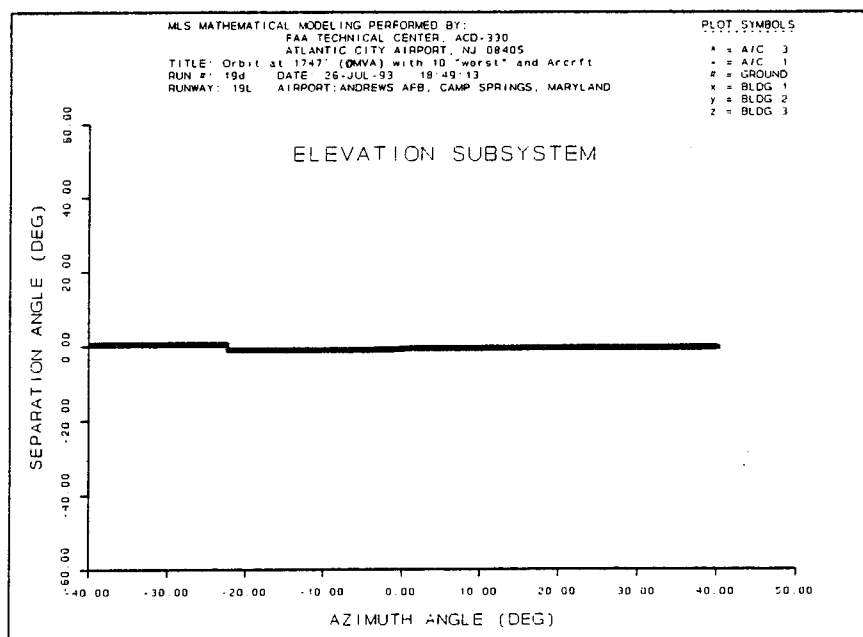
FIGURE B-30. MLS EL MULTIPATH SEPARATION ANGLE PLOT
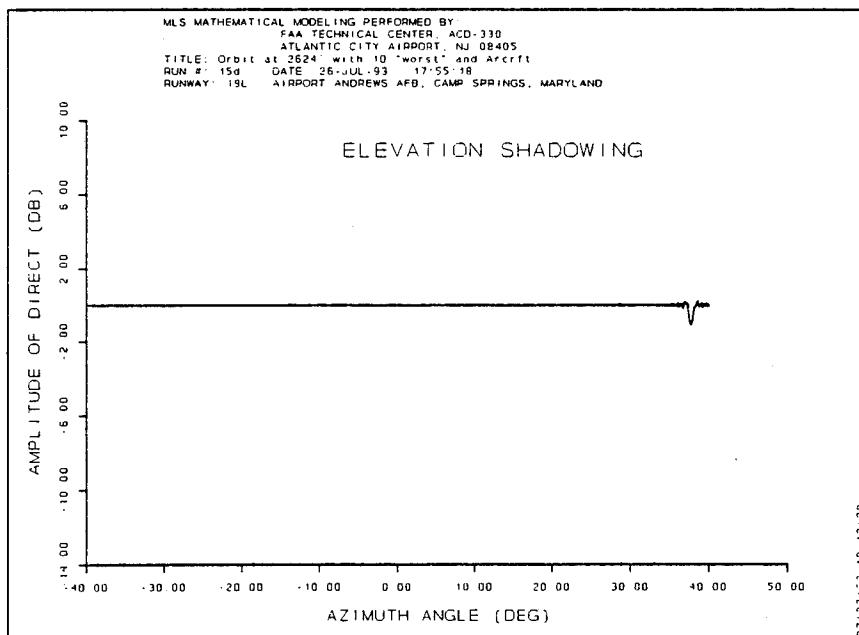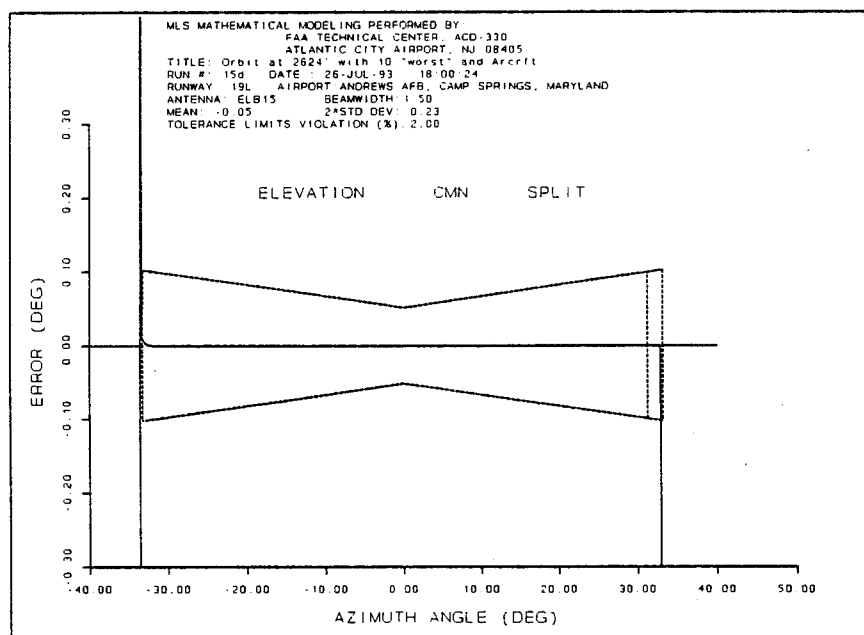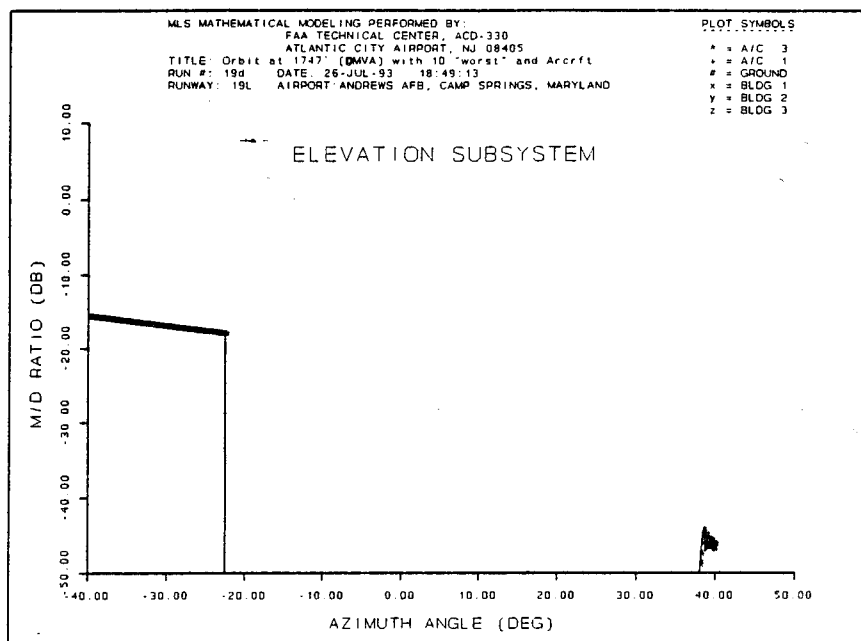FOR AN ORBITAL (1747' ABOVE REFERENCE) FLIGHT PATH.

MLS MATHEMATICAL MODELING PERFORMED BY:
FAA TECHNICAL CENTER, ACD-330
ATLANTIC CITY AIRPORT, NJ 08405
TITLE: Orbit at 1747' (OMVA) with 10 "worst" and Arcrft
RUN #: 19d   DATE: 26-JUL-93   18:49:13
RUNWAY: 19L   AIRPORT:ANDREWS AFB, CAMP SPRINGS, MARYLAND

ELEVATION SHADOWING
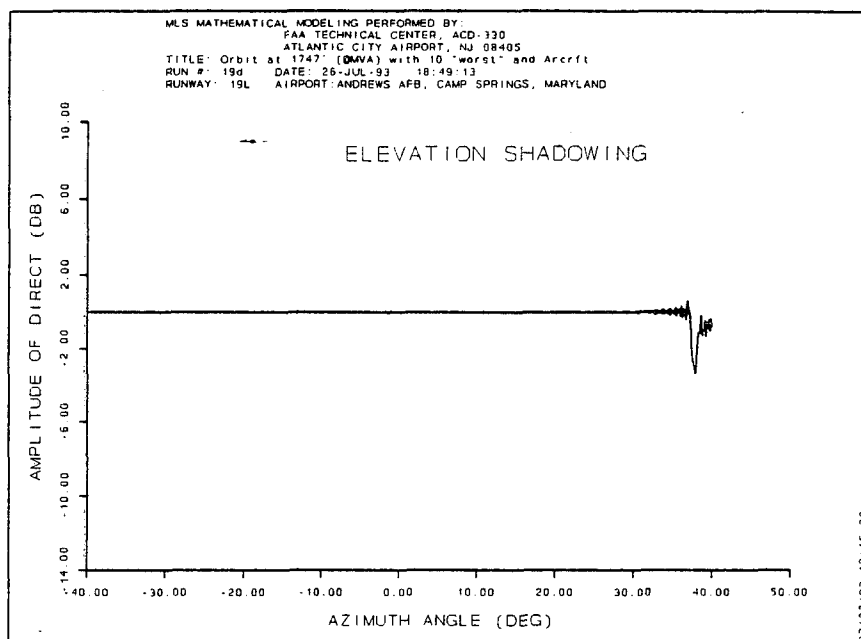
FIGURE B-31. MLS EL COMPOSITE MAGNITUDE PLOT FOR AN
ORBITAL (1747' ABOVE REFERENCE) FLIGHT PATH.

MLS MATHEMATICAL MODELING PERFORMED BY:
FAA TECHNICAL CENTER, ACD-330
ATLANTIC CITY AIRPORT, NJ 08405
TITLE: Orbit at 1747' (OMVA) with 10 "worst" and Arcrft
RUN #: 19d   DATE : 26-JUL-93   18:54:27
RUNWAY: 19L   AIRPORT:ANDREWS AFB, CAMP SPRINGS, MARYLAND
ANTENNA: ELB15   BEAMWIDTH: 1.50

ELEVATION   STATIC   SPLIT
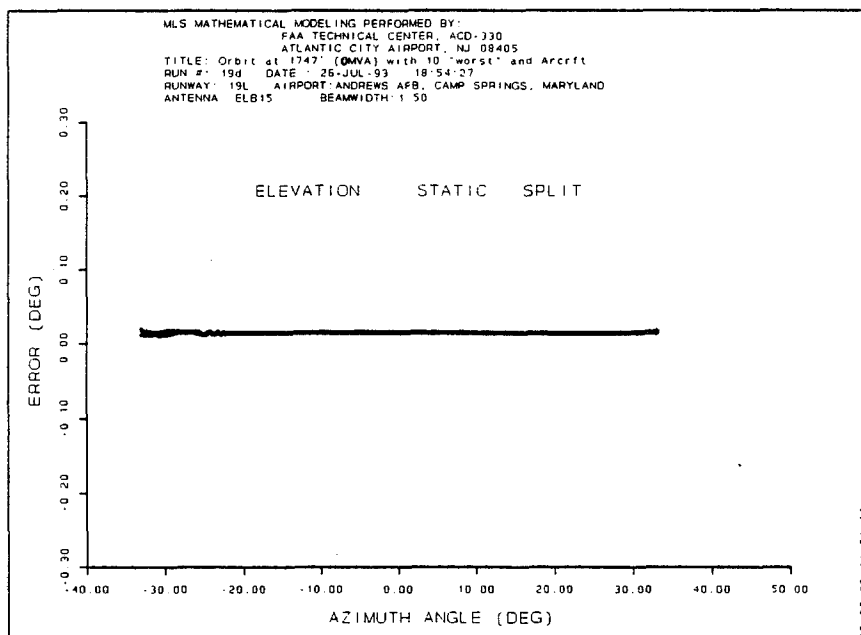
FIGURE B-32. MLS EL STATIC ERROR PLOT FOR AN
ORBITAL (1747' ABOVE REFERENCE) FLIGHT PATH.

B-19

MLS MATHEMATICAL MODELING PERFORMED BY:
                    FAA TECHNICAL CENTER, ACD-330
                    ATLANTIC CITY AIRPORT, NJ 08405
TITLE: Orbit at 1747' (OMVA) with 10 "worst" and Arcrft
RUN #: 19d   DATE : 26-JUL-93   18:54:27
RUNWAY: 19L   AIRPORT:ANDREWS AFB, CAMP SPRINGS, MARYLAND
ANTENNA: EL815   BEAMWIDTH:1.50

ELEVATION   DYNAMIC   SPLIT

ERROR (DEG)

AZIMUTH ANGLE (DEG)
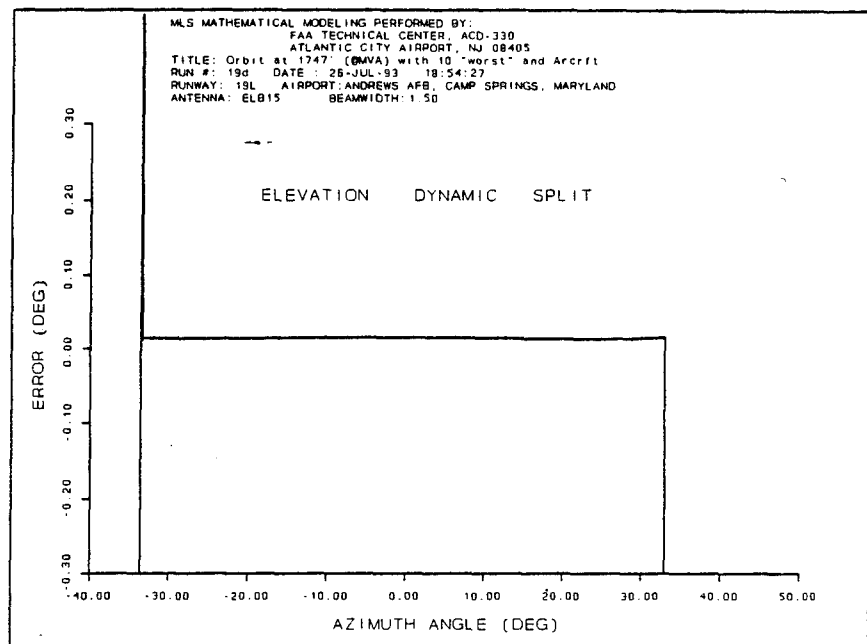
FIGURE B-33.   MLS EL DYNAMIC ERROR PLOT FOR AN ORBITAL (1747' ABOVE REFERENCE) FLIGHT PATH.

MLS MATHEMATICAL MODELING PERFORMED BY:
                    FAA TECHNICAL CENTER, ACD-330
                    ATLANTIC CITY AIRPORT, NJ 08405
TITLE: Orbit at 1747' (OMVA) with 10 "worst" and Arcrft
RUN #: 19d   DATE : 26-JUL-93   18:54:27
RUNWAY: 19L   AIRPORT:ANDREWS AFB, CAMP SPRINGS, MARYLAND
ANTENNA: EL815   BEAMWIDTH:1.50
MEAN: -0.04   2*STD DEV: 0.24
TOLERANCE LIMITS VIOLATION (%): 2.00

ELEVATION   PFE   SPLIT

ERROR (DEG)

AZIMUTH ANGLE (DEG)
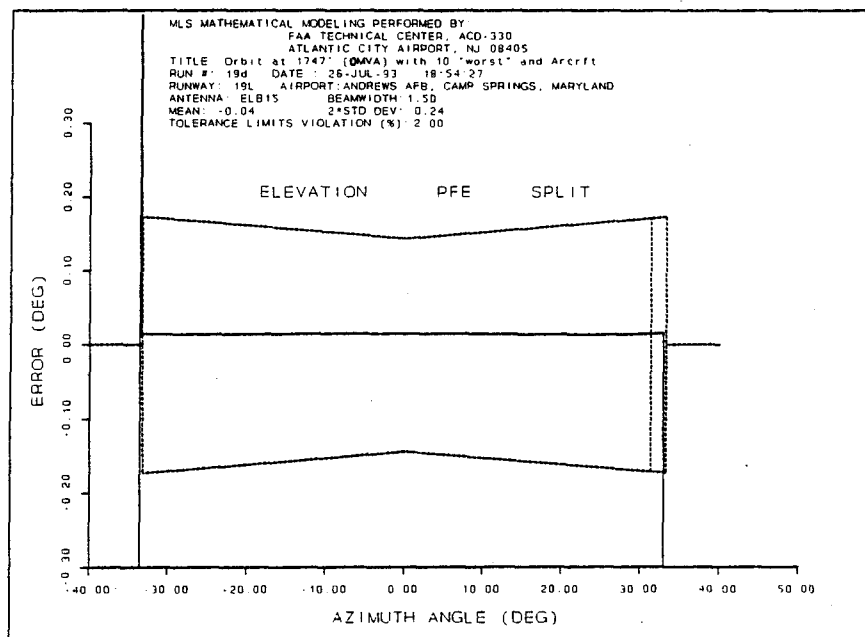
FIGURE B-34.   MLS EL PATH FOLLOWING ERROR PLOT FOR AN ORBITAL (1747' ABOVE REFERENCE) FLIGHT PATH.

B-20

MLS MATHEMATICAL MODELING PERFORMED BY:
FAA TECHNICAL CENTER, ACD-330
ATLANTIC CITY AIRPORT, NJ 08405
TITLE: Orbit at 1747' (OMVA) with 10 'worst' and Arcrft
RUN #: 19d   DATE : 26-JUL-93   18:54:27
RUNWAY: 19L   AIRPORT:ANDREWS AFB, CAMP SPRINGS, MARYLAND
ANTENNA: ELB15   BEAMWIDTH:1.50
MEAN: -0.05   2*STD DEV: 0.23
TOLERANCE LIMITS VIOLATION (%): 2.00

ELEVATION   CMN   SPLIT

FIGURE B-35. MLS EL CONTROL MOTION NOISE PLOT FOR
AN ORBITAL (1747' ABOVE REFERENCE) FLIGHT PATH.

MLS MATHEMATICAL MODELING PERFORMED BY:
FAA TECHNICAL CENTER, ACD-330
ATLANTIC CITY AIRPORT, NJ 08405
TITLE: Orbit at 3492' with 10 'worst' and Arcrft
RUN #: 23d   DATE: 27-JUL-93   08:37:40
RUNWAY: 19L   AIRPORT:ANDREWS AFB, CAMP SPRINGS, MARYLAND

PLOT SYMBOLS
* = A/C 3
. = GROUND
# = BLDG 1
x = BLDG 2
y = BLDG 3
z = BLDG 4

ELEVATION SUBSYSTEM

FIGURE B-36. MLS EL MULTIPATH RELATIVE MAGNITUDE
PLOT FOR AN ORBITAL (3492' ABOVE REFERENCE) FLIGHT
PATH.

B-21

ELEVATION SUBSYSTEM
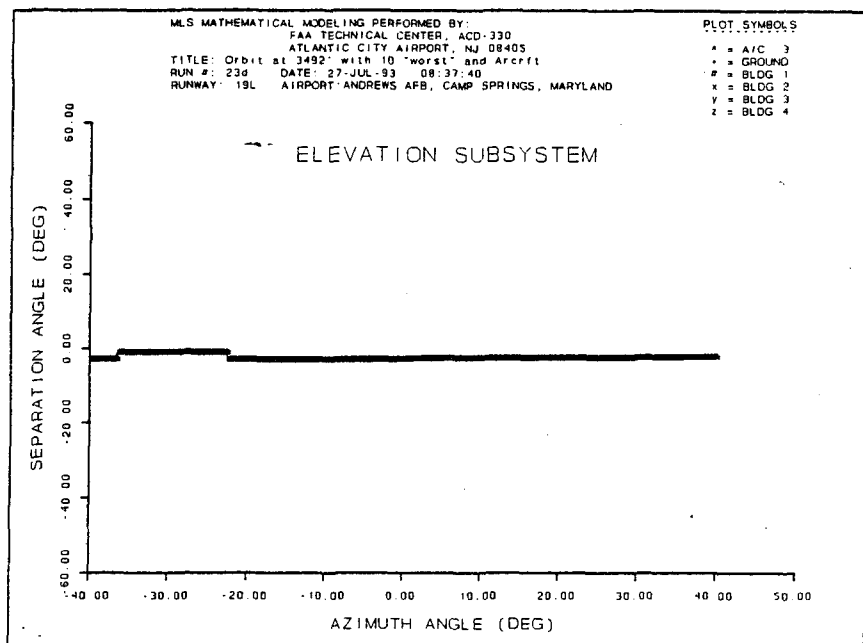
FIGURE B-37. MLS EL MULTIPATH SEPARATION ANGLE PLOT FOR AN ORBITAL (3492′ ABOVE REFERENCE) FLIGHT PATH.

ELEVATION SHADOWING

FIGURE B-38. MLS EL COMPOSITE MAGNITUDE PLOT FOR AN ORBITAL (3492′ ABOVE REFERENCE) FLIGHT PATH.

B-22

FIGURE B-39. MLS EL STATIC ERROR PLOT FOR AN
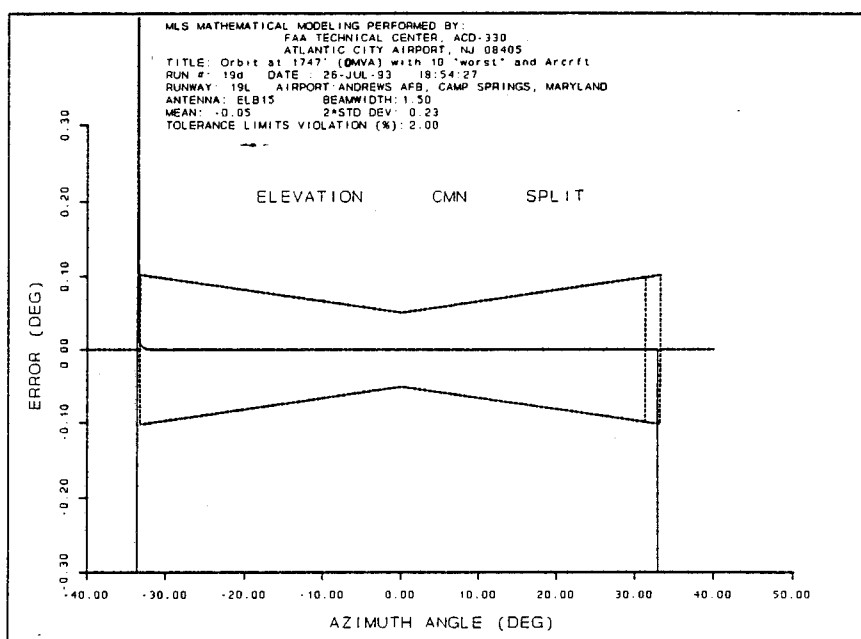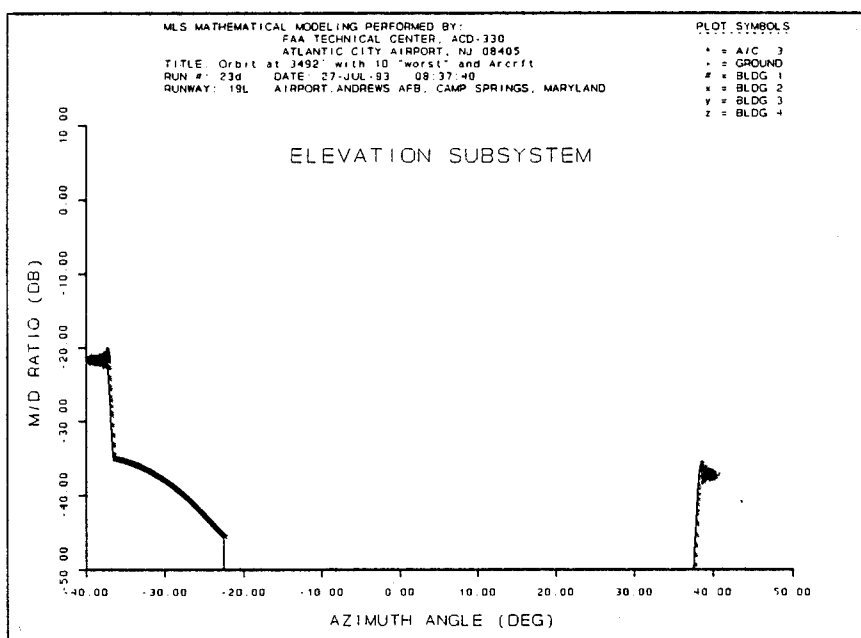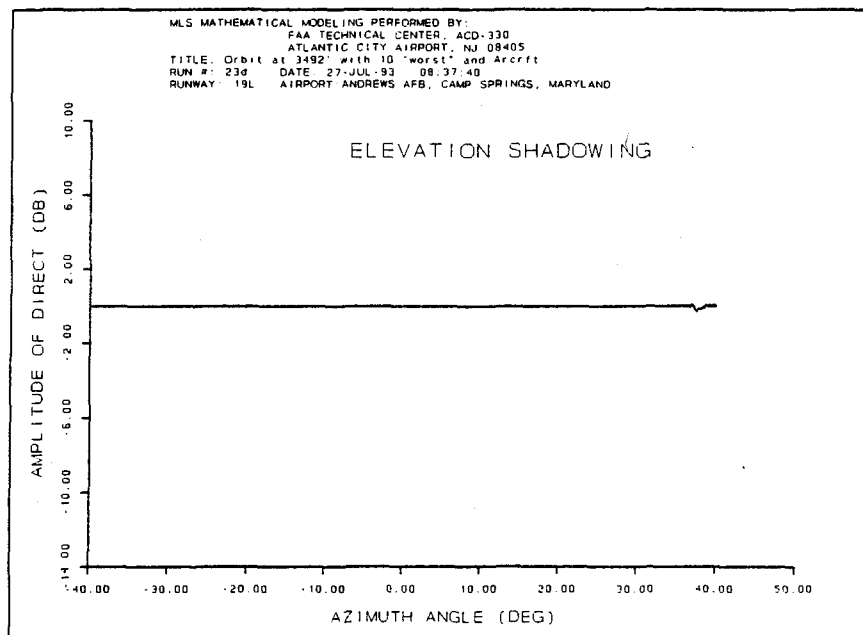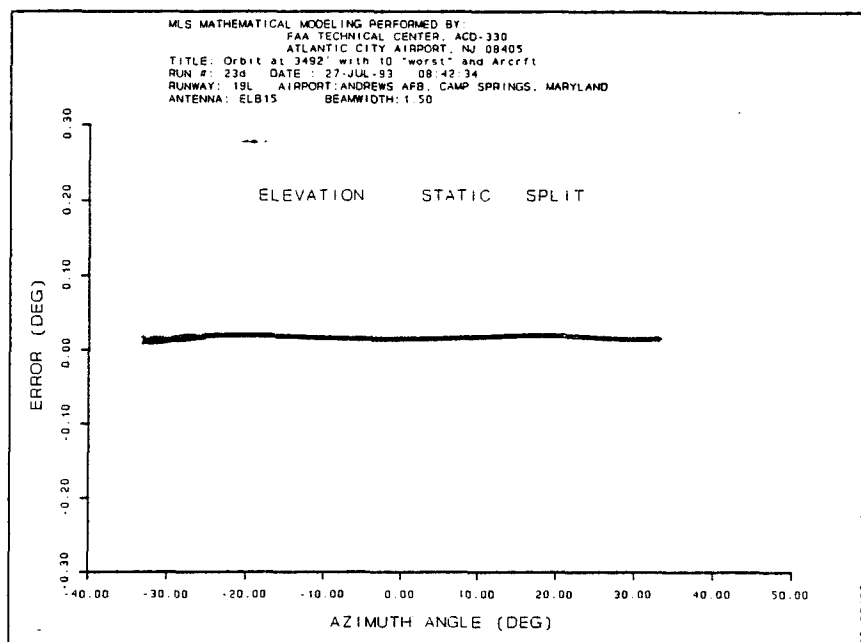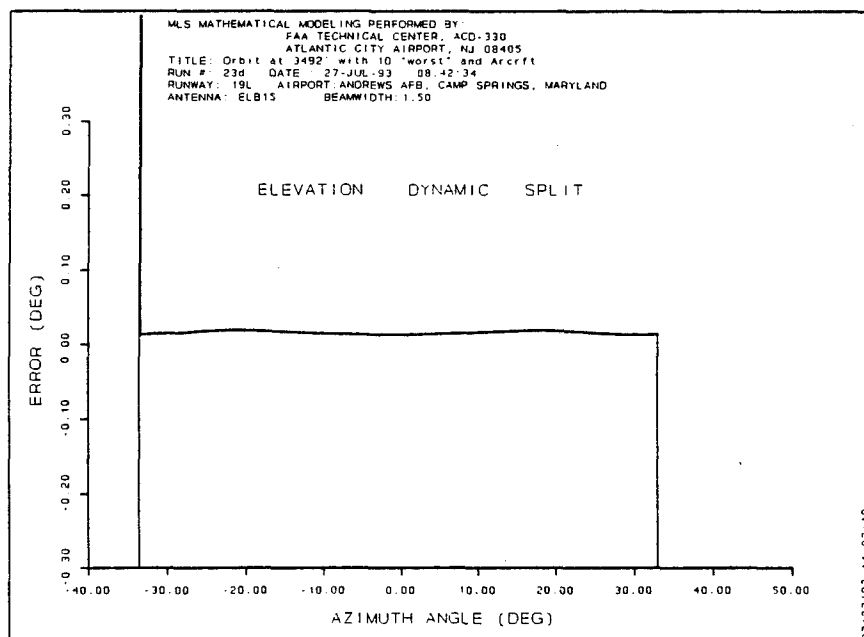ORBITAL (3492′ ABOVE REFERENCE) FLIGHT PATH.

FIGURE B-40. MLS EL DYNAMIC ERROR PLOT FOR AN
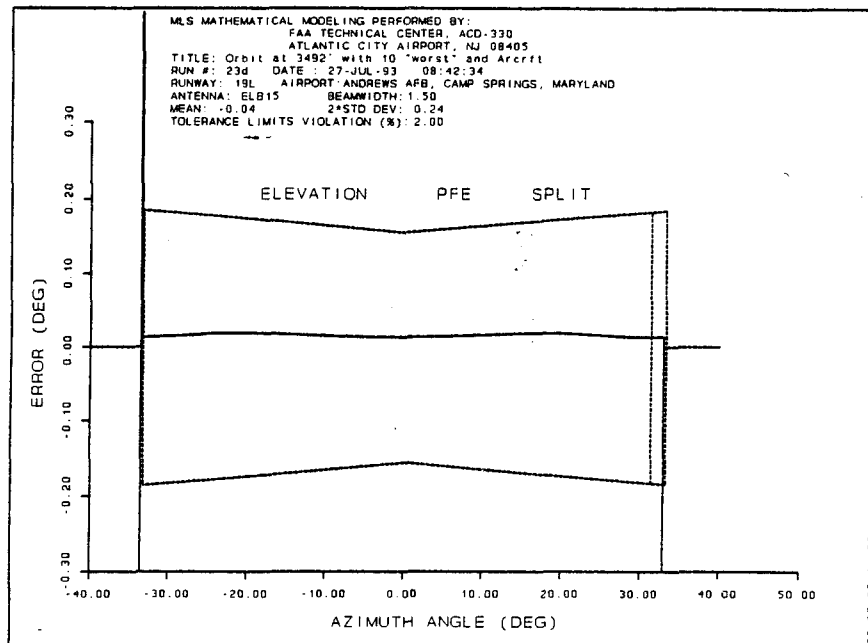ORBITAL (3492′ ABOVE REFERENCE) FLIGHT PATH.

FIGURE B-41.   MLS EL PATH FOLLOWING ERROR PLOT FOR
AN ORBITAL (3492' ABOVE REFERENCE) FLIGHT PATH.
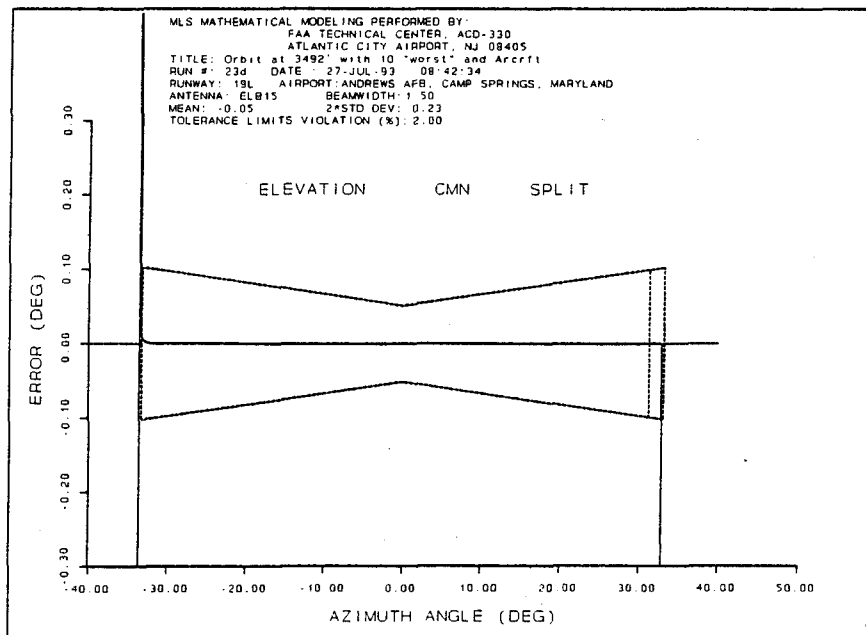

FIGURE B-42..   MLS EL CONTROL MOTION NOISE PLOT FOR
AN ORBITAL (3492' ABOVE REFERENCE) FLIGHT PATH.

Appendix C
DME/P Modeling Results
List of Illustrations

Results of modeling effort of the six scenarios with the 10 worst-case contributors of multipath on the guidance provided by the DME/P are presented in this section.
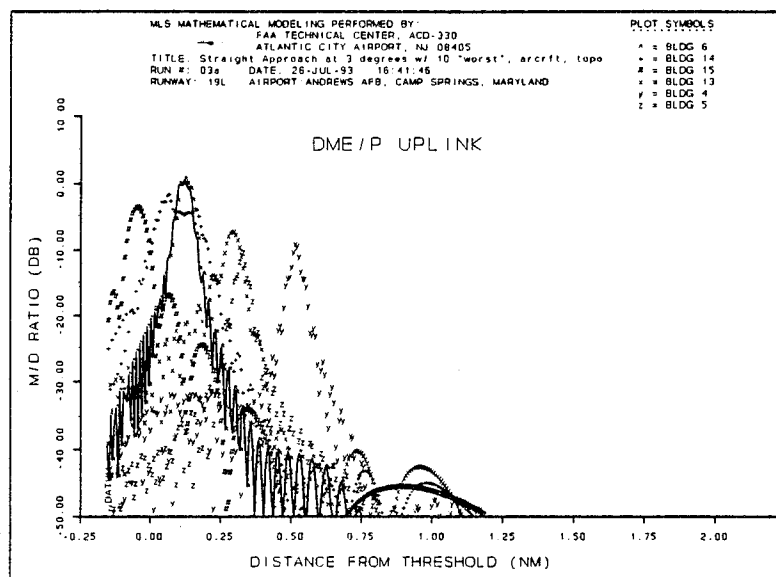
FIGURE C-1. DME/P UPLINK MULTIPATH RELATIVE MAGNITUDE
PLOT FOR A STRAIGHT APPROACH (3° GPA) FLIGHT PATH.
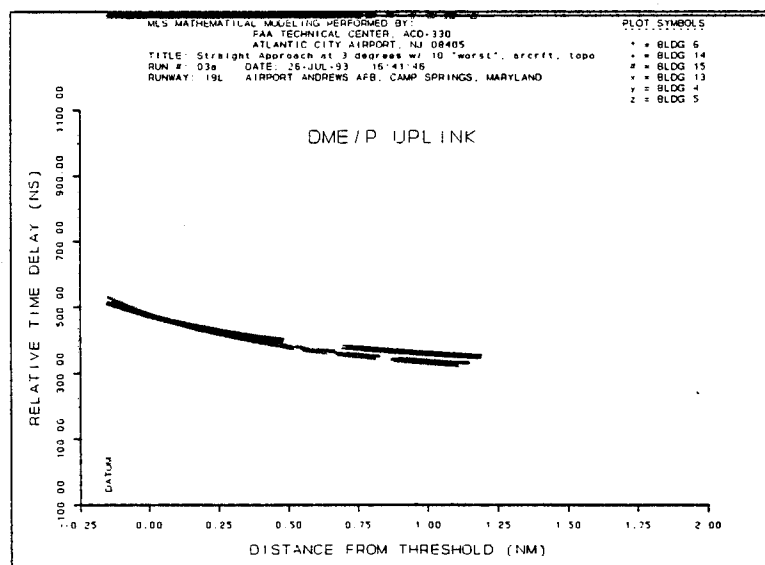
FIGURE C-2. DME/P UPLINK RELATIVE TIME DELAY PLOT FOR
A STRAIGHT APPROACH (3° GPA) FLIGHT PATH.

C-5

FIGURE C-3. DME/P DOWNLINK MULTIPATH RELATIVE
MAGNITUDE PLOT FOR A STRAIGHT APPROACH (3° GPA)
FLIGHT PATH.
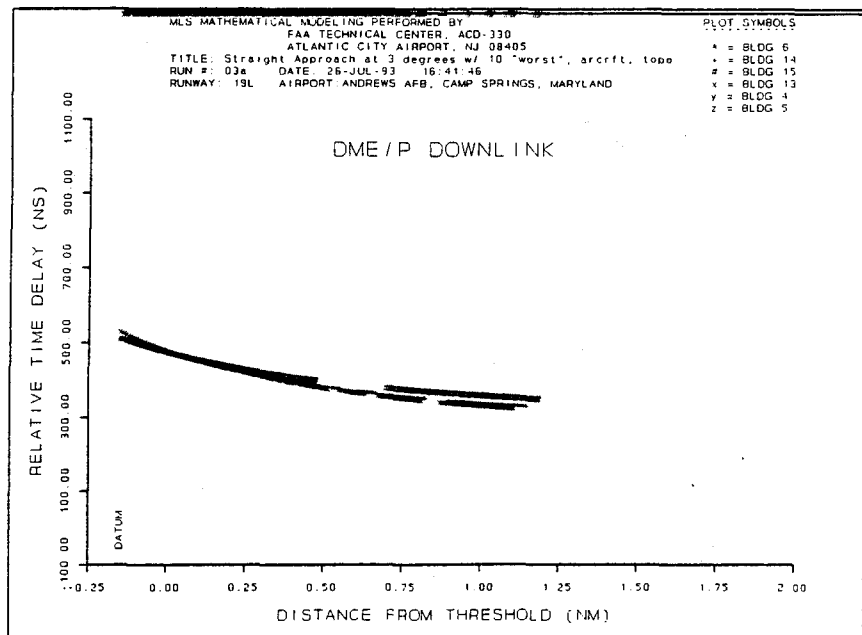
FIGURE C-4. DME/P DOWNLINK RELATIVE TIME DELAY PLOT
FOR A STRAIGHT APPROACH (3° GPA) FLIGHT PATH.

FIGURE C-5. DME/P UPLINK COMPOSITE MAGNITUDE PLOT FOR A STRAIGHT APPROACH (3° GPA) FLIGHT PATH.
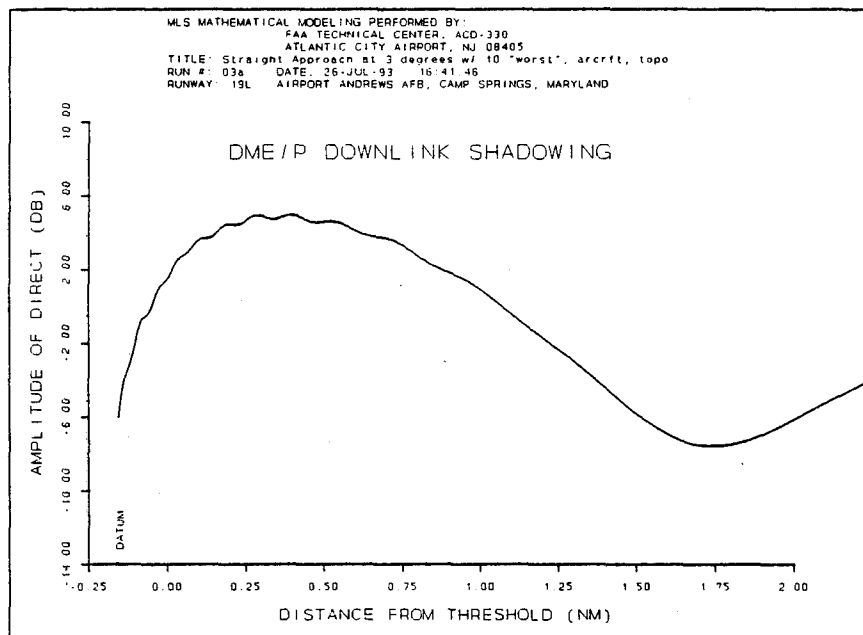
FIGURE C-6. DME/P DOWNLINK COMPOSITE MAGNITUDE PLOT FOR A STRAIGHT APPROACH (3° GPA) FLIGHT PATH.
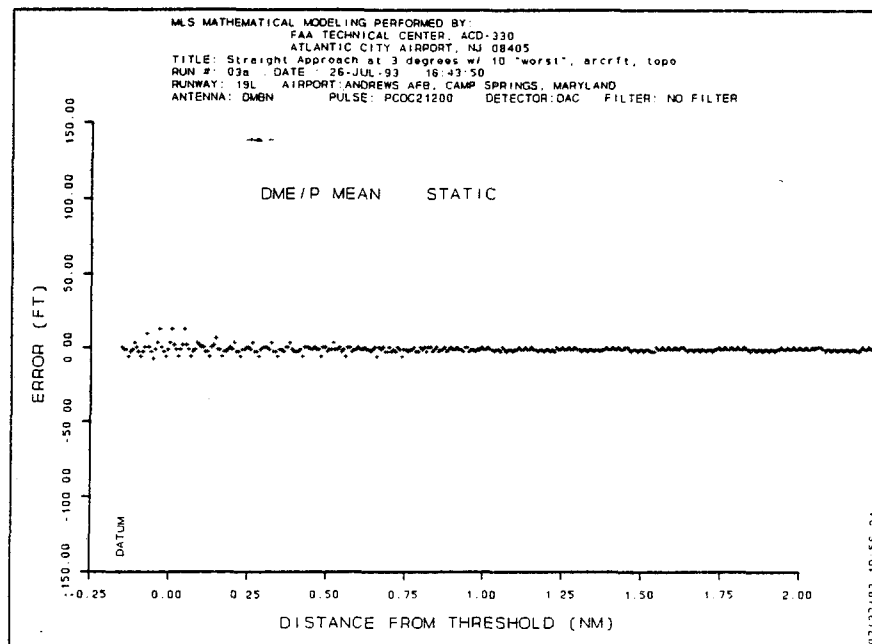
FIGURE C-7. DME/P STATIC ERROR PLOT FOR A STRAIGHT
APPROACH (3° GPA) FLIGHT PATH.
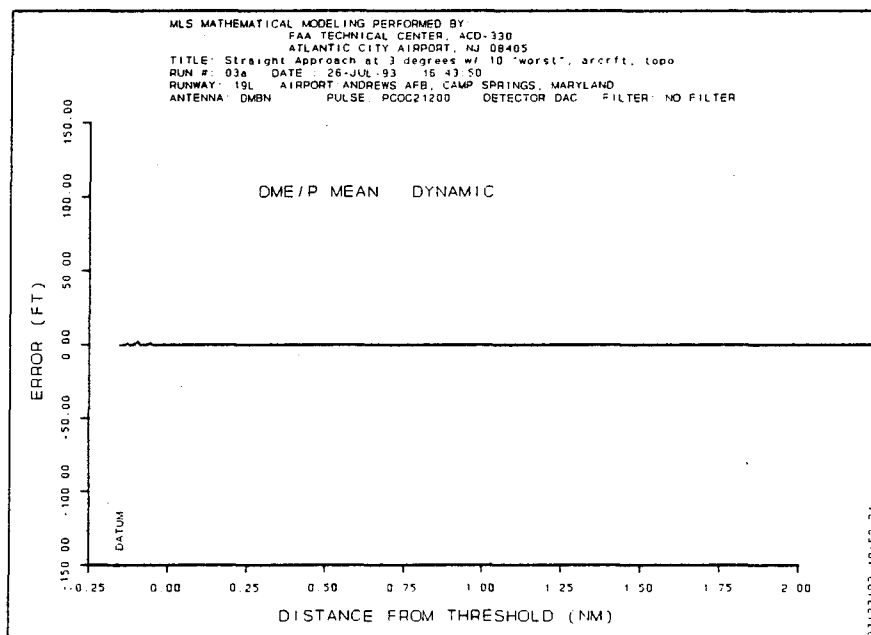
FIGURE C-8. DME/P DYNAMIC ERROR PLOT FOR A STRAIGHT
APPROACH (3° GPA) FLIGHT PATH.

C-8

MLS MATHEMATICAL MODELING PERFORMED BY:
FAA TECHNICAL CENTER, ACD-330
ATLANTIC CITY AIRPORT, NJ 08405
TITLE: Straight Approach at 3 degrees w/ 10 "worst", arcrft, topo
RUN #: 03a   DATE 26-JUL-93   16:43:50
RUNWAY: 19L   AIRPORT:ANDREWS AFB, CAMP SPRINGS, MARYLAND
ANTENNA: DMBN   PULSE: PCOC21200   DETECTOR:DAC   FILTER: NO FILTER
MEAN: 0.01   2*STD DEV: 0.22
TOLERANCE LIMITS VIOLATION (%): 0.00

DME/P MEAN   PFE
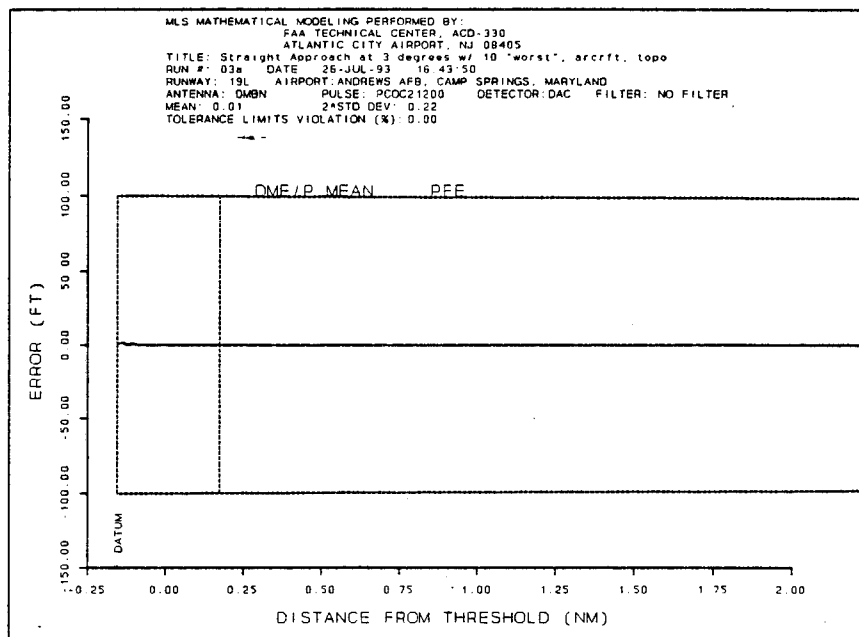
FIGURE C-9.   DME/P PATH FOLLOWING ERROR PLOT FOR A STRAIGHT APPROACH (3° GPA) FLIGHT PATH.

MLS MATHEMATICAL MODELING PERFORMED BY:
FAA TECHNICAL CENTER, ACD-330
ATLANTIC CITY AIRPORT, NJ 08405
TITLE: Straight Approach at 3 degrees w/ 10 "worst", arcrft, topo
RUN # 03a   DATE 26-JUL-93   16:43:50
RUNWAY: 19L   AIRPORT:ANDREWS AFB, CAMP SPRINGS, MARYLAND
ANTENNA DMBN   PULSE PCOC21200   DETECTOR:DAC   FILTER: NO FILTER
MEAN: 0.00   2*STD DEV: 0.10
TOLERANCE LIMITS VIOLATION (%): 0.00

DME/P MEAN   CMN
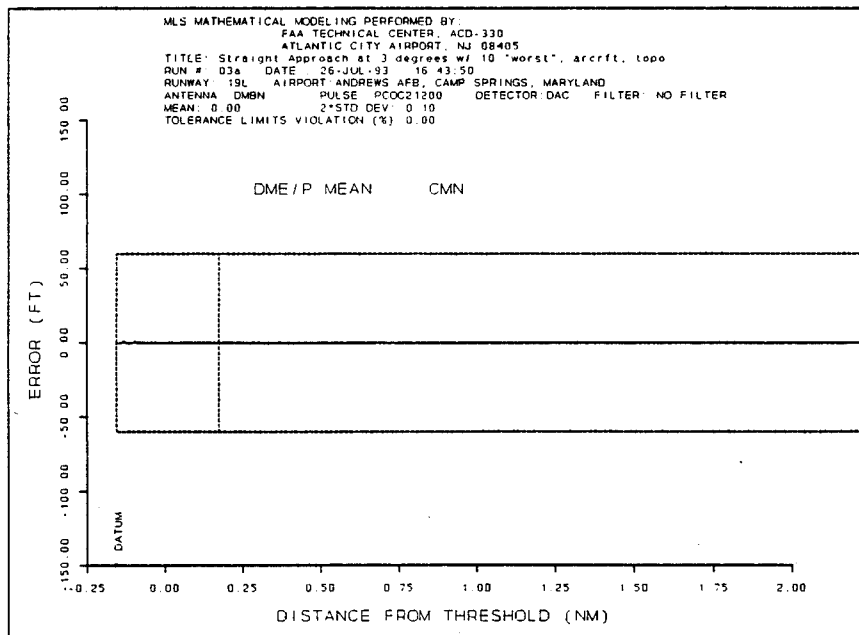
FIGURE C-10.   DME/P CONTROL MOTION NOISE PLOT FOR A STRAIGHT APPROACH (3° GPA) FLIGHT PATH.

C-9
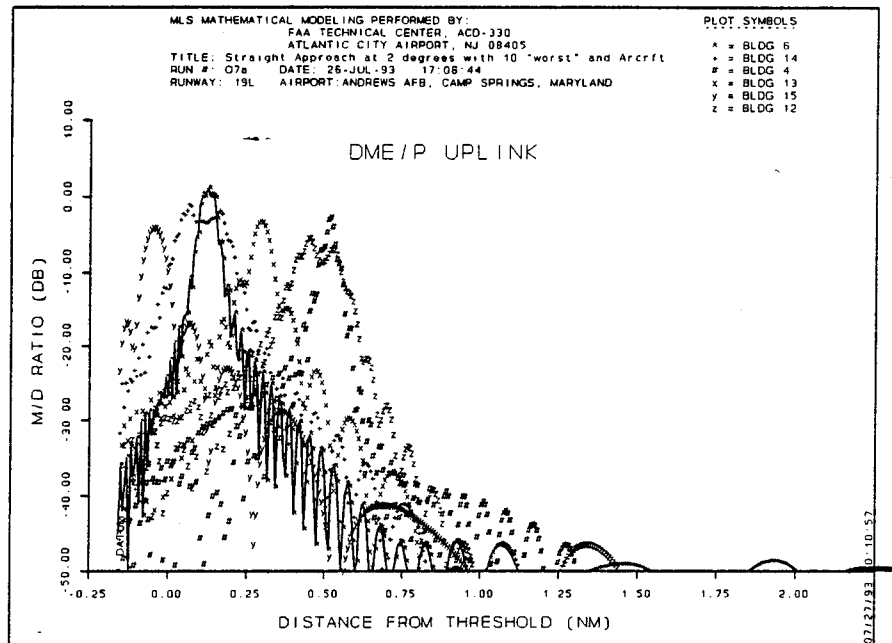
FIGURE C-11. DME/P UPLINK MULTIPATH RELATIVE
MAGNITUDE PLOT FOR A STRAIGHT APPROACH (2° GPA)
FLIGHT PATH.
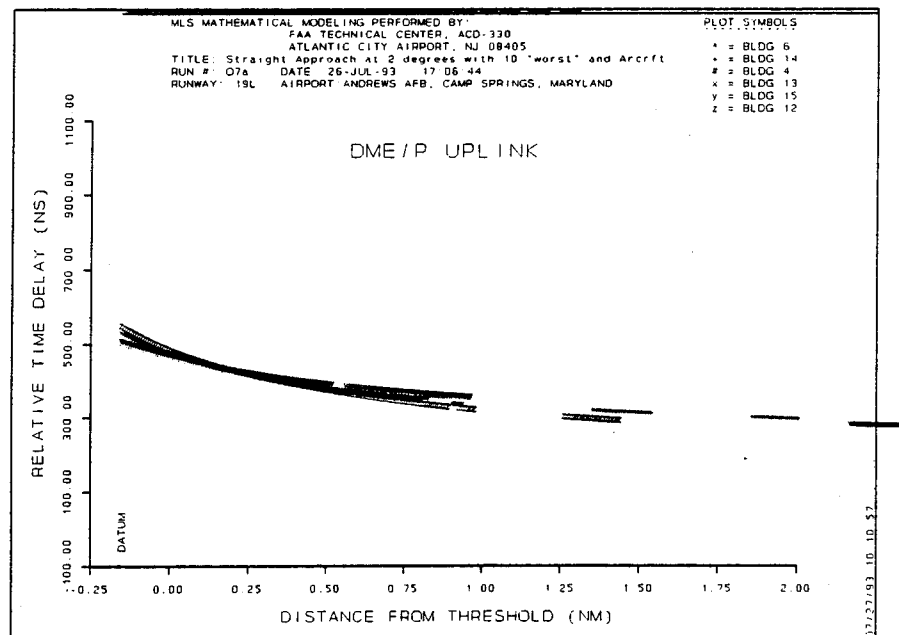
FIGURE C-12. DME/P UPLINK RELATIVE TIME DELAY PLOT
FOR A STRAIGHT APPROACH (2° GPA) FLIGHT PATH.

C-10
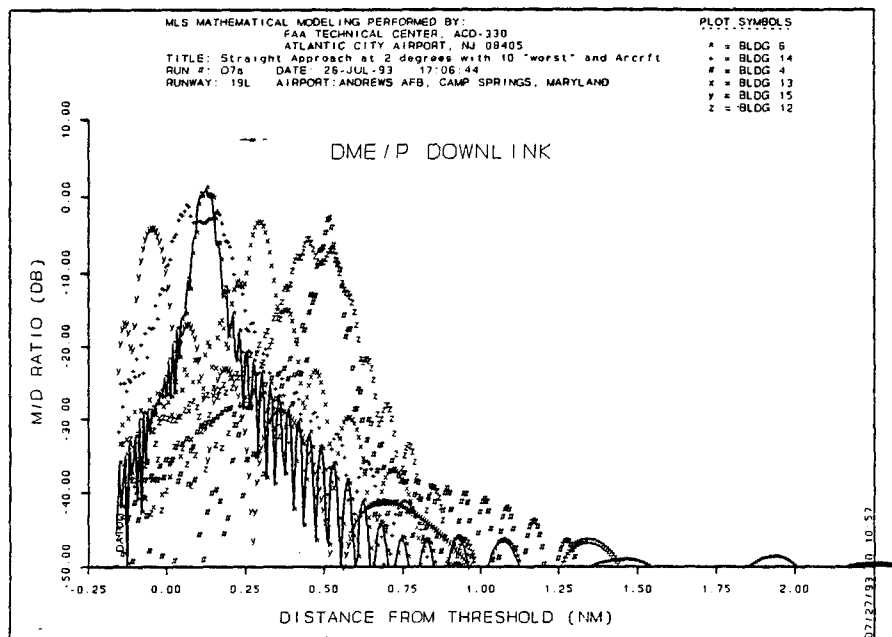
FIGURE C-13. DME/P DOWNLINK MULTIPATH RELATIVE
MAGNITUDE PLOT FOR A STRAIGHT APPROACH (2° GPA)
FLIGHT PATH.
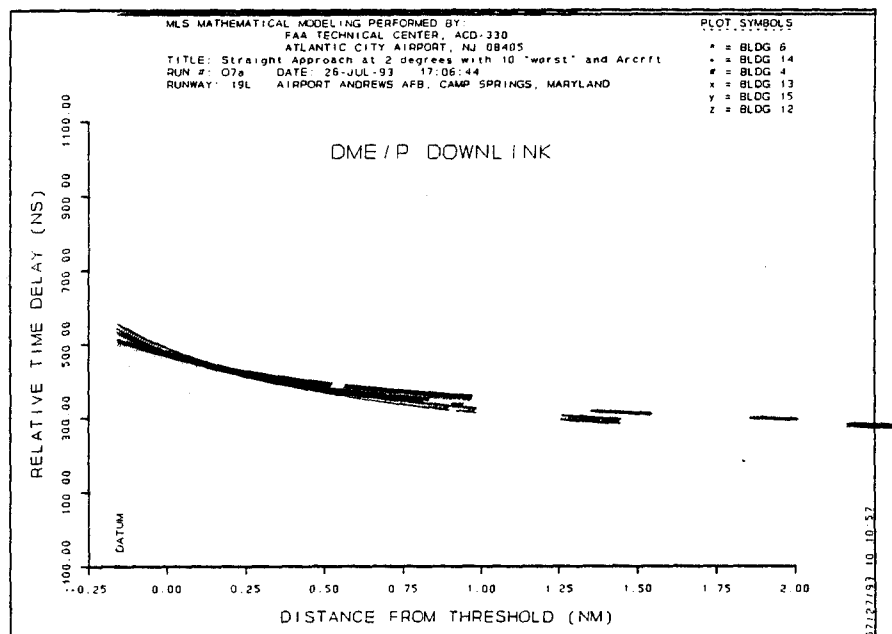
FIGURE C-14. DME/P DOWNLINK RELATIVE TIME DELAY
PLOT FOR A STRAIGHT APPROACH (2° GPA) FLIGHT PATH.

MLS MATHEMATICAL MODELING PERFORMED BY:
FAA TECHNICAL CENTER, ACD-330
ATLANTIC CITY AIRPORT, NJ 08405
TITLE: Straight Approach at 2 degrees with 10 "worst" and Arcrft
RUN #: 07a   DATE: 26-JUL-93   17:06:44
RUNWAY: 19L   AIRPORT:ANDREWS AFB, CAMP SPRINGS, MARYLAND

DME/P UPLINK SHADOWING
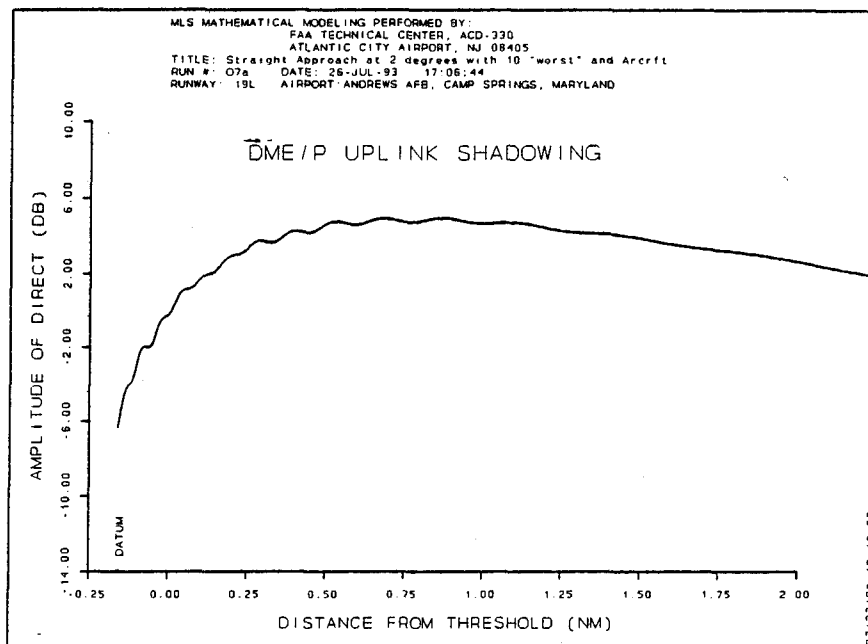
FIGURE C-15. DME/P UPLINK COMPOSITE MAGNITUDE PLOT FOR A STRAIGHT APPROACH (2° GPA) FLIGHT PATH.

MLS MATHEMATICAL MODELING PERFORMED BY:
FAA TECHNICAL CENTER, ACD-330
ATLANTIC CITY AIRPORT, NJ 08405
TITLE: Straight Approach at 2 degrees with 10 "worst" and Arcrft
RUN #: 07a   DATE: 26-JUL-93   17:06:44
RUNWAY: 19L   AIRPORT:ANDREWS AFB, CAMP SPRINGS, MARYLAND

DME/P DOWNLINK SHADOWING
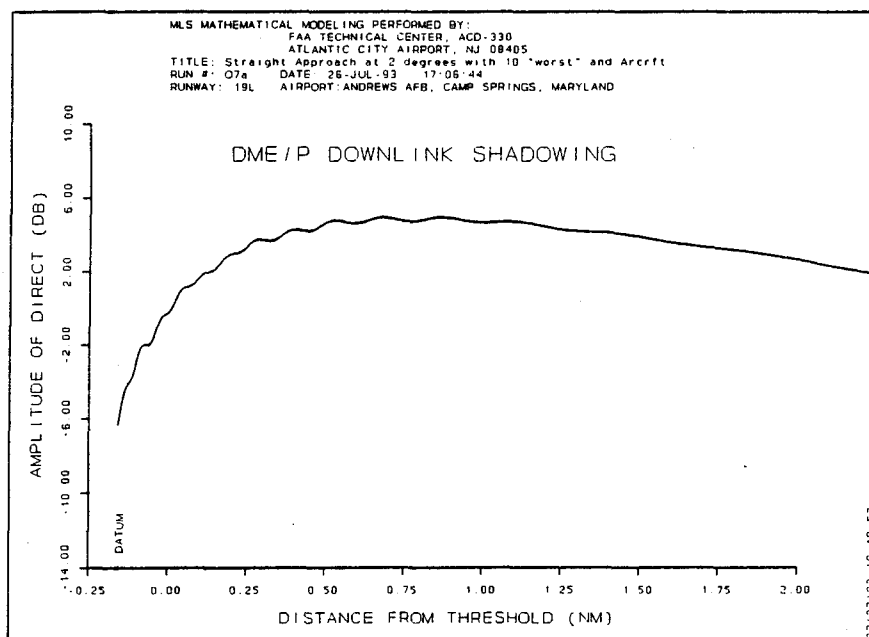
FIGURE C-16. DME/P DOWNLINK COMPOSITE MAGNITUDE PLOT FOR A STRAIGHT APPROACH (2° GPA) FLIGHT PATH.
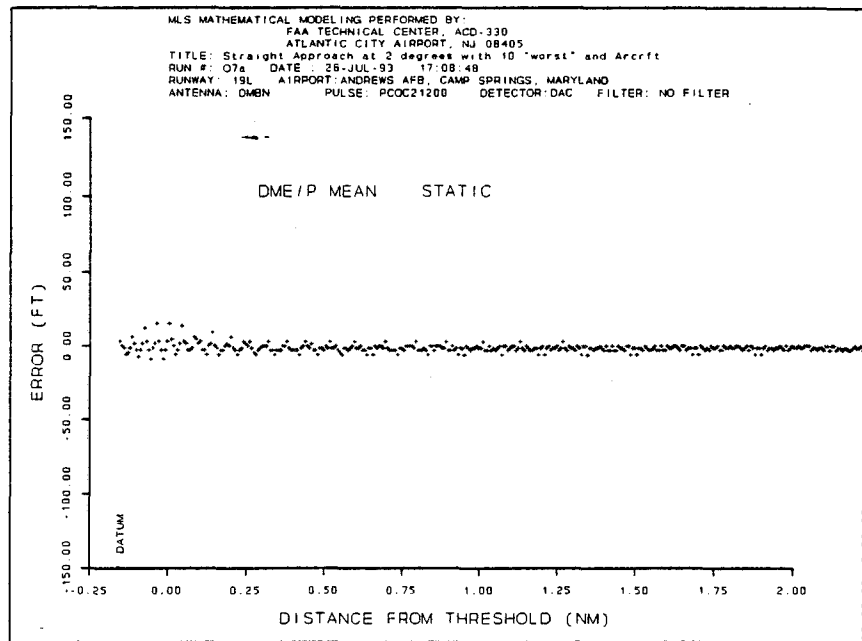
FIGURE C-17.   DME/P STATIC ERROR PLOT FOR A STRAIGHT
APPROACH (2° GPA) FLIGHT PATH.
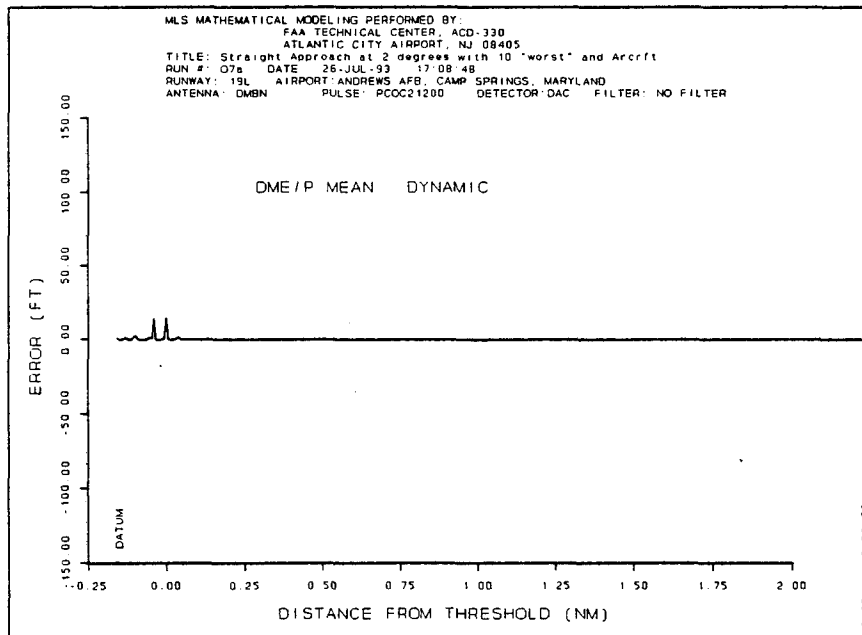
FIGURE C-18.   DME/P DYNAMIC ERROR PLOT FOR A
STRAIGHT APPROACH (2° GPA) FLIGHT PATH.

C-13
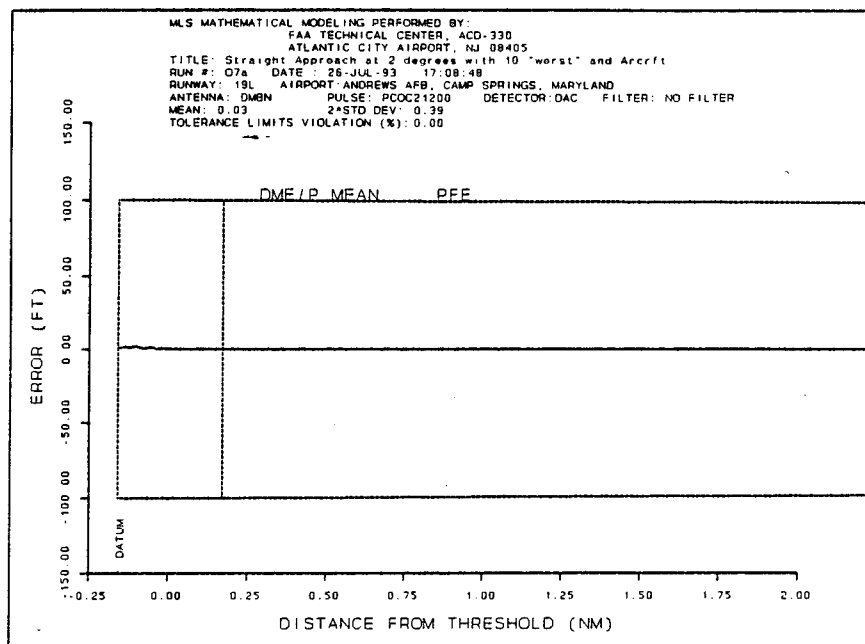
FIGURE C-19. DME/P PATH FOLLOWING ERROR PLOT FOR A
STRAIGHT APPROACH (2° GPA) FLIGHT PATH.
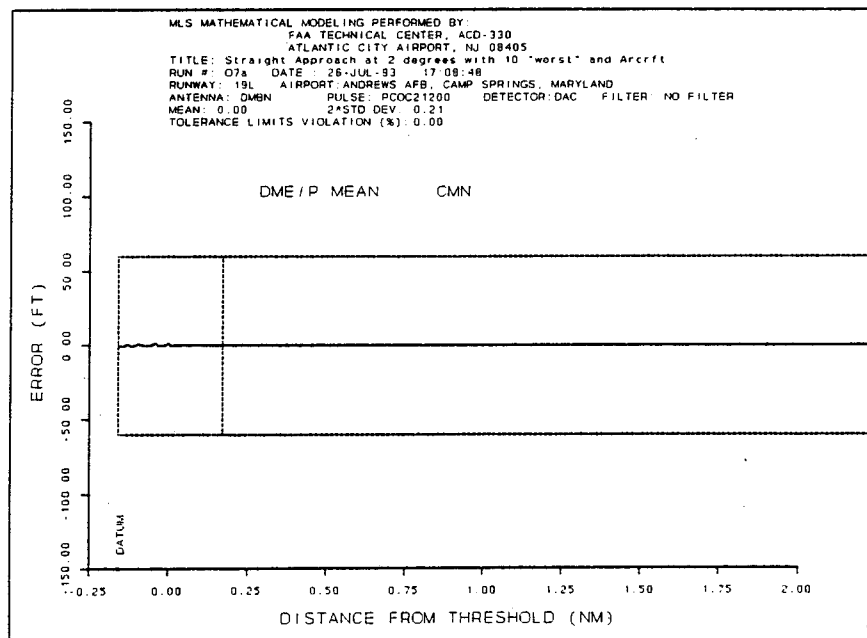
FIGURE C-20. DME/P CONTROL MOTION NOISE PLOT FOR A
STRAIGHT APPROACH (2° GPA) FLIGHT PATH.

C-14
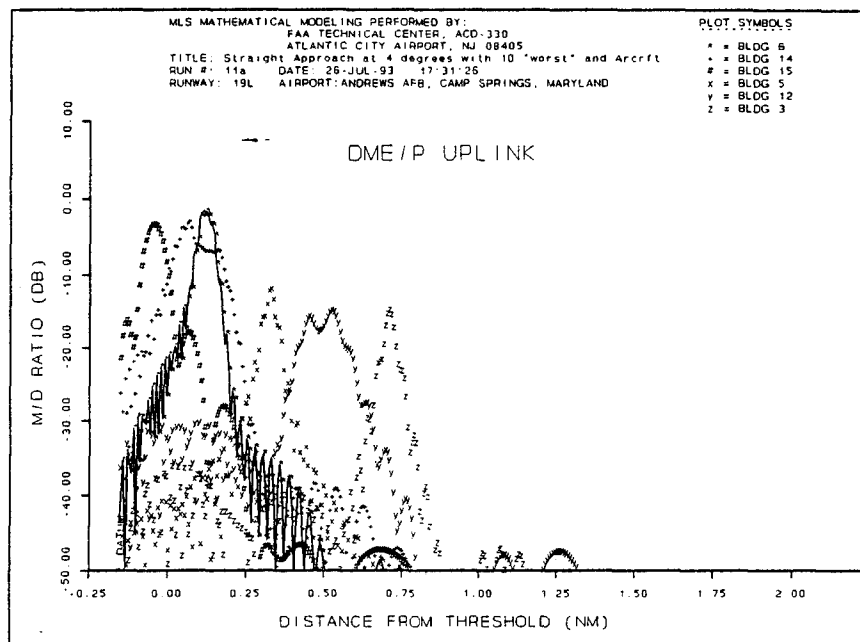
FIGURE C-21. DME/P UPLINK MULTIPATH RELATIVE
MAGNITUDE PLOT FOR A STRAIGHT APPROACH (4° GPA)
FLIGHT PATH.
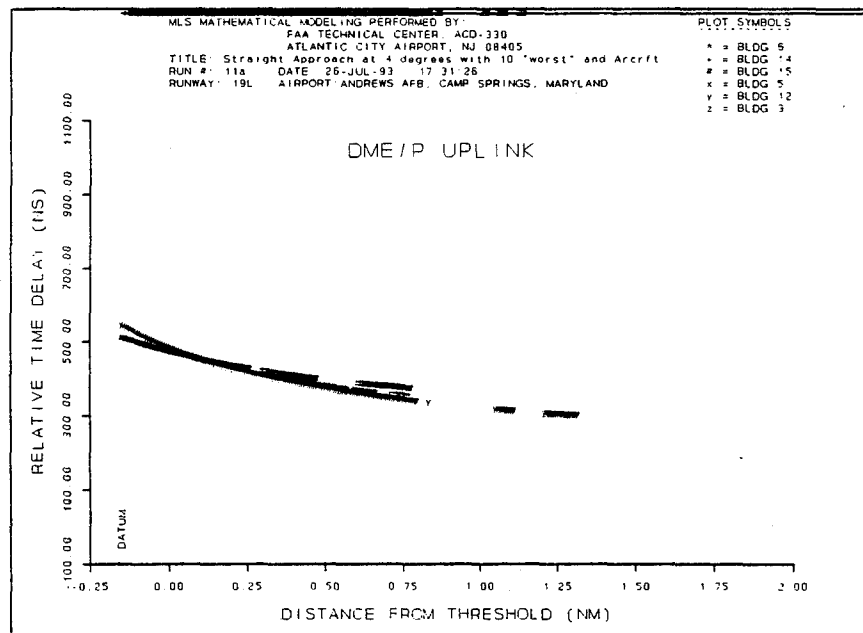
FIGURE C-22. DME/P UPLINK RELATIVE TIME DELAY PLOT
OR A STRAIGHT APPROACH (4° GPA) FLIGHT PATH.
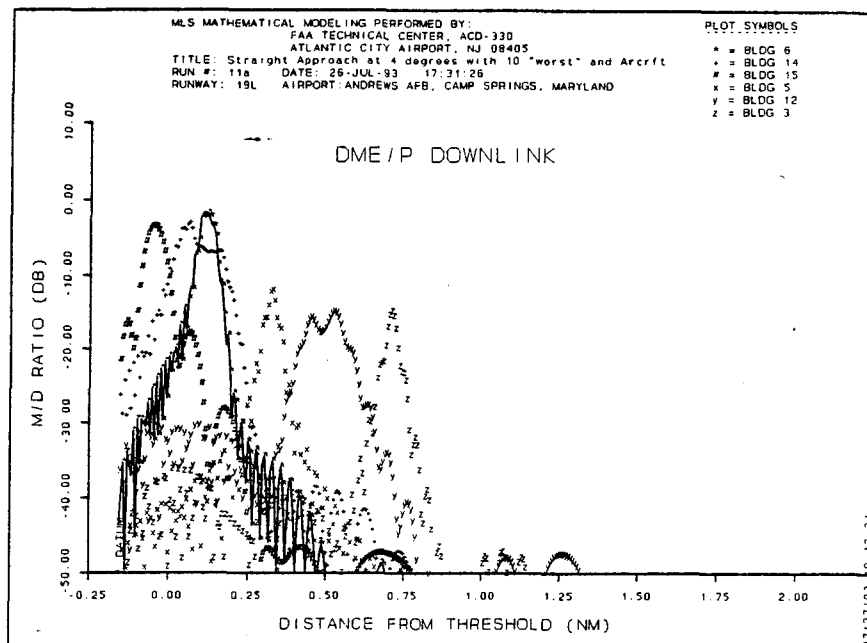
FIGURE C-23. DME/P DOWNLINK MULTIPATH RELATIVE
MAGNITUDE PLOT FOR A STRAIGHT APPROACH (4° GPA)
FLIGHT PATH.
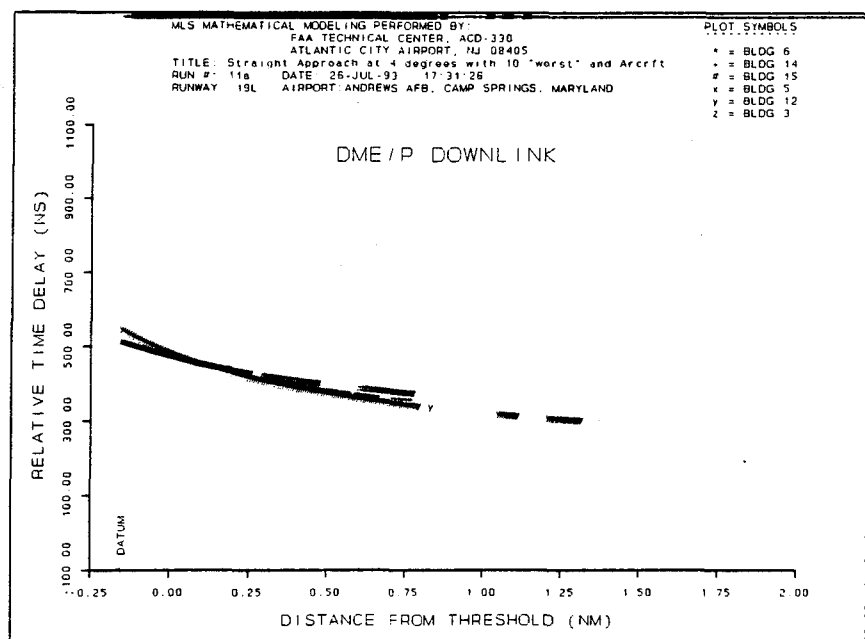
FIGURE C-24. DME/P DOWNLINK RELATIVE TIME DELAY
PLOT FOR A STRAIGHT APPROACH (4° GPA) FLIGHT PATH.

MLS MATHEMATICAL MODELING PERFORMED BY:
FAA TECHNICAL CENTER, ACD-330
ATLANTIC CITY AIRPORT, NJ 08405
TITLE: Straight Approach at 4 degrees with 10 "worst" and Arcrft
RUN #: 11a   DATE: 26-JUL-93   17:31:26
RUNWAY: 19L   AIRPORT:ANDREWS AFB, CAMP SPRINGS, MARYLAND

DME/P UPLINK SHADOWING

AMPLITUDE OF DIRECT (DB)

DISTANCE FROM THRESHOLD (NM)
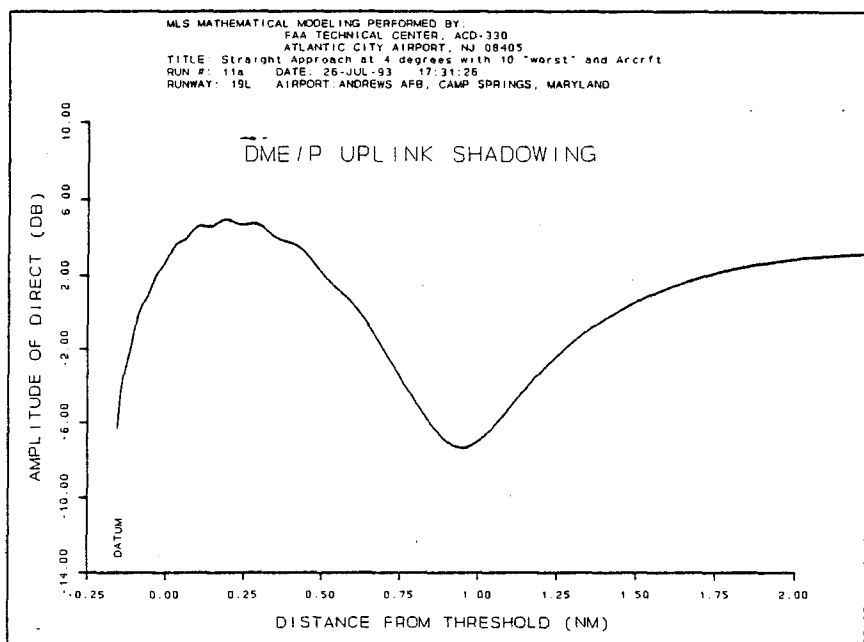
FIGURE C-25.   DME/P UPLINK COMPOSITE MAGNITUDE PLOT
FOR A STRAIGHT APPROACH (4° GPA) FLIGHT PATH.

MLS MATHEMATICAL MODELING PERFORMED BY:
FAA TECHNICAL CENTER, ACD-330
ATLANTIC CITY AIRPORT, NJ 08405
TITLE: Straight Approach at 4 degrees with 10 "worst" and Arcrft
RUN #: 11a   DATE: 26-JUL-93   17:31:26
RUNWAY: 19L   AIRPORT:ANDREWS AFB, CAMP SPRINGS, MARYLAND

DME/P DOWNLINK SHADOWING

AMPLITUDE OF DIRECT (DB)

DISTANCE FROM THRESHOLD (NM)
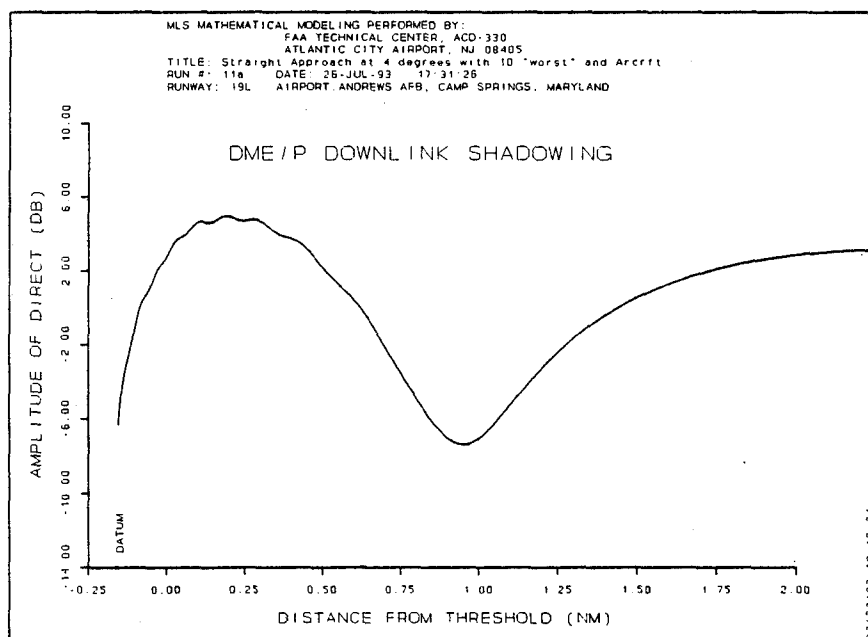
FIGURE C-26.   DME/P DOWNLINK COMPOSITE MAGNITUDE
PLOT FOR A STRAIGHT APPROACH (4° GPA) FLIGHT PATH.

C-17
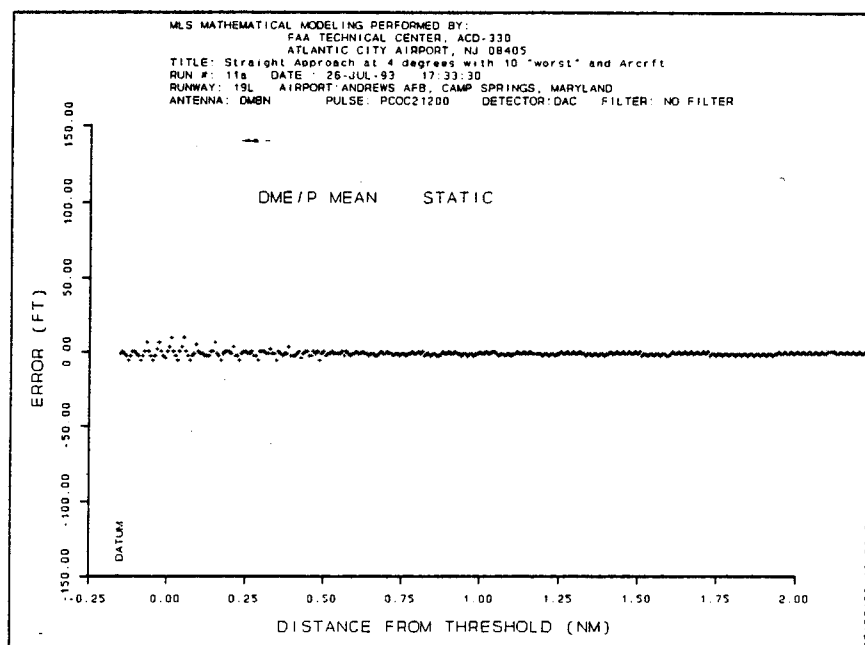
FIGURE C-27. DME/P STATIC ERROR PLOT FOR A STRAIGHT
APPROACH (4° GPA) FLIGHT PATH.
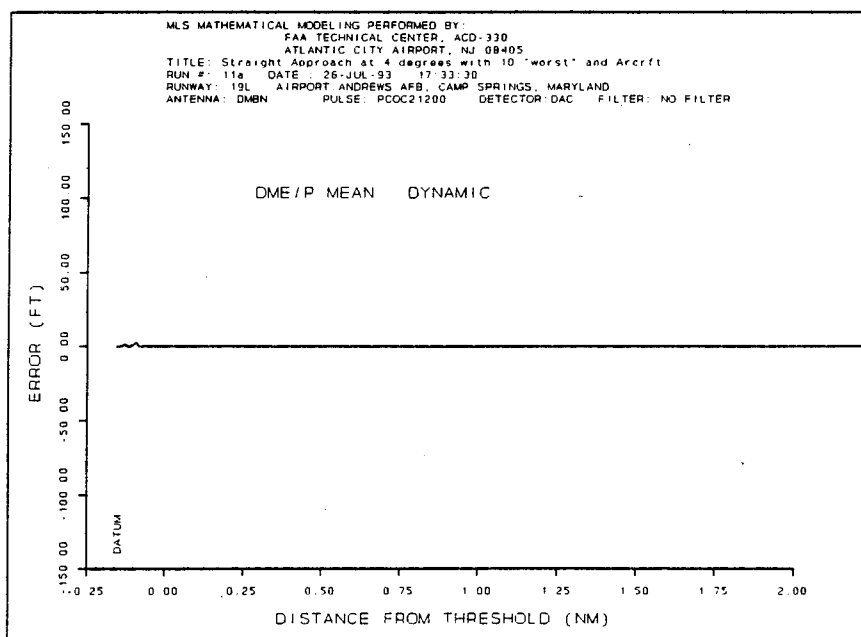
FIGURE C-28. DME/P DYNAMIC ERROR PLOT FOR A
STRAIGHT APPROACH (4° GPA) FLIGHT PATH.

C-18
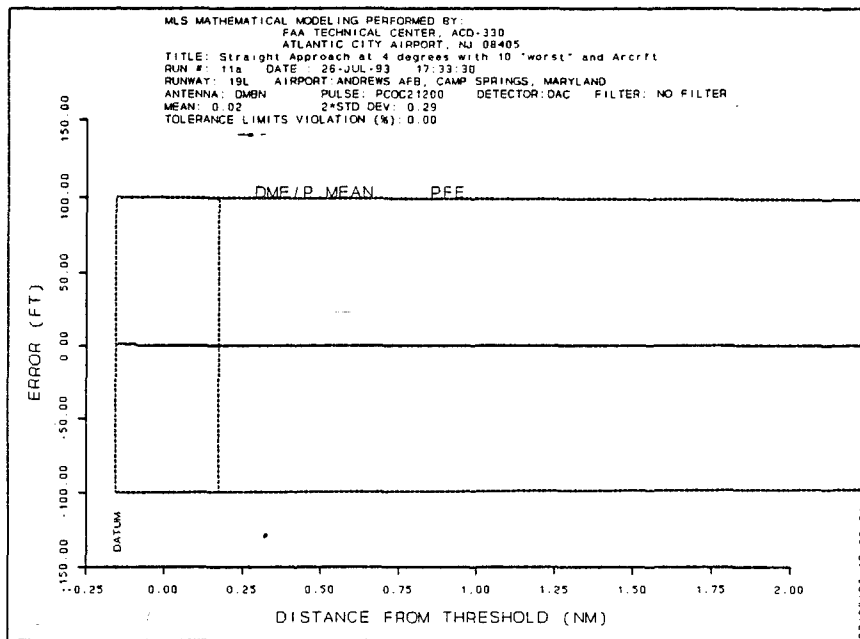
FIGURE C-29. DME/P PATH FOLLOWING ERROR PLOT FOR A
STRAIGHT APPROACH (4° GPA) FLIGHT PATH.
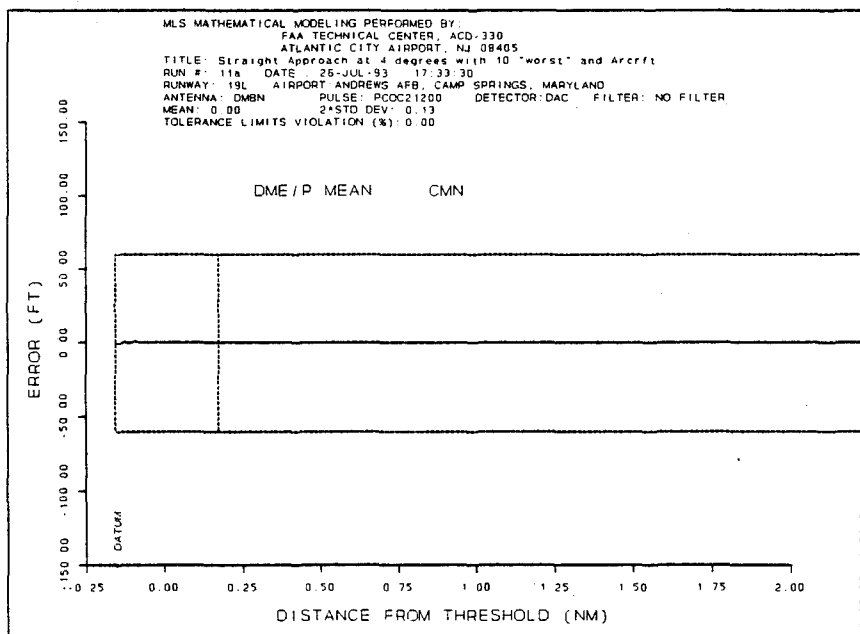
FIGURE C-30. DME/P CONTROL MOTION NOISE PLOT FOR A
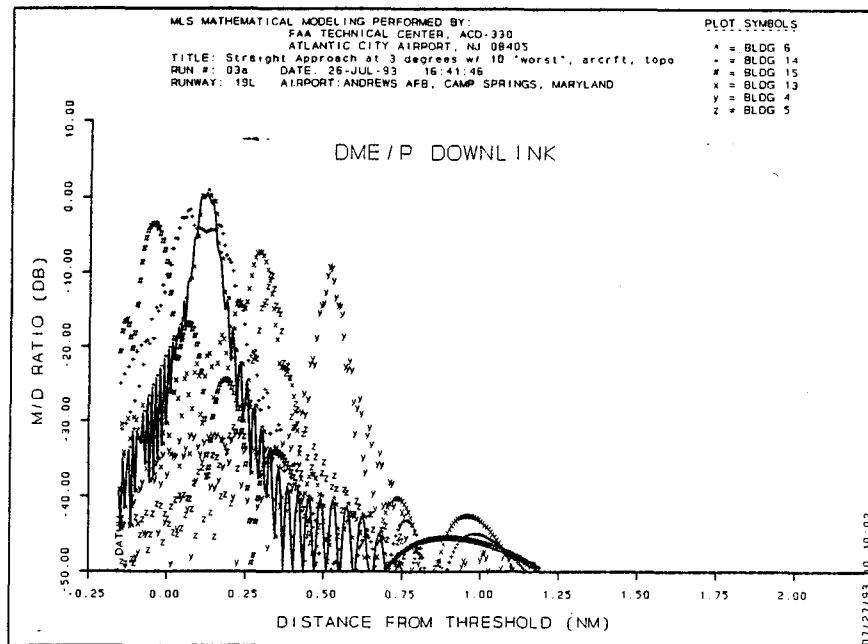STRAIGHT APPROACH (4° GPA) FLIGHT PATH.

C-19
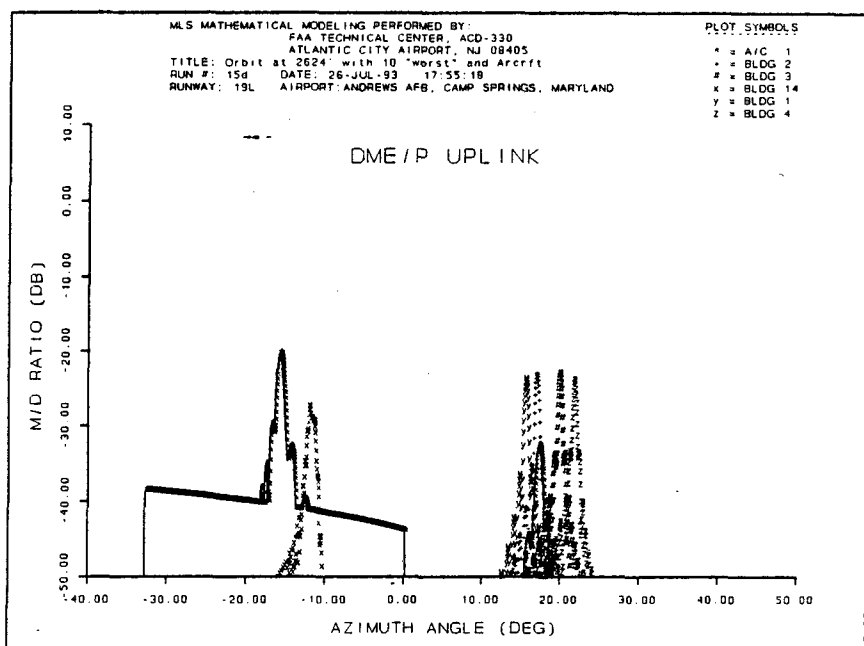
**FIGURE C-31.** DME/P UPLINK MULTIPATH RELATIVE MAGNITUDE PLOT FOR AN ORBITAL (2624' ABOVE REF.) FLIGHT PATH.
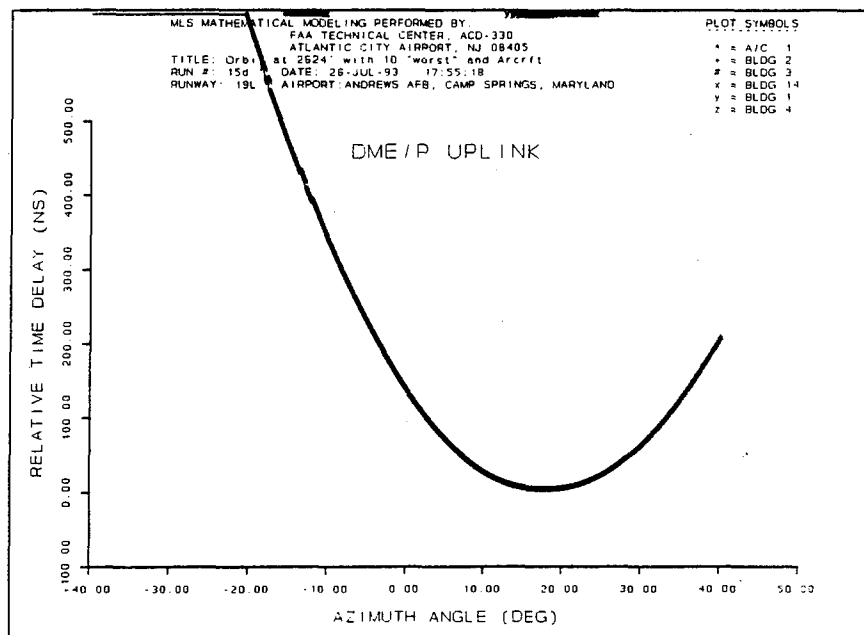
FIGURE C-32. DME/P UPLINK RELATIVE TIME DELAY PLOT FOR AN ORBITAL (2624' ABOVE REF.) FLIGHT PATH.
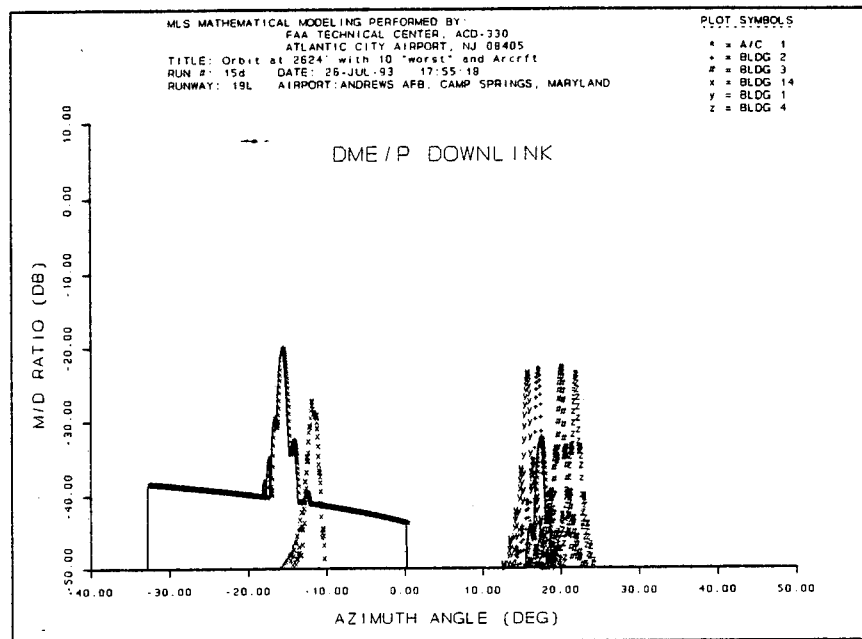
FIGURE C-33. DME/P DOWNLINK MULTIPATH RELATIVE MAGNITUDE PLOT FOR AN ORBITAL (2624' ABOVE REF.) FLIGHT PATH.
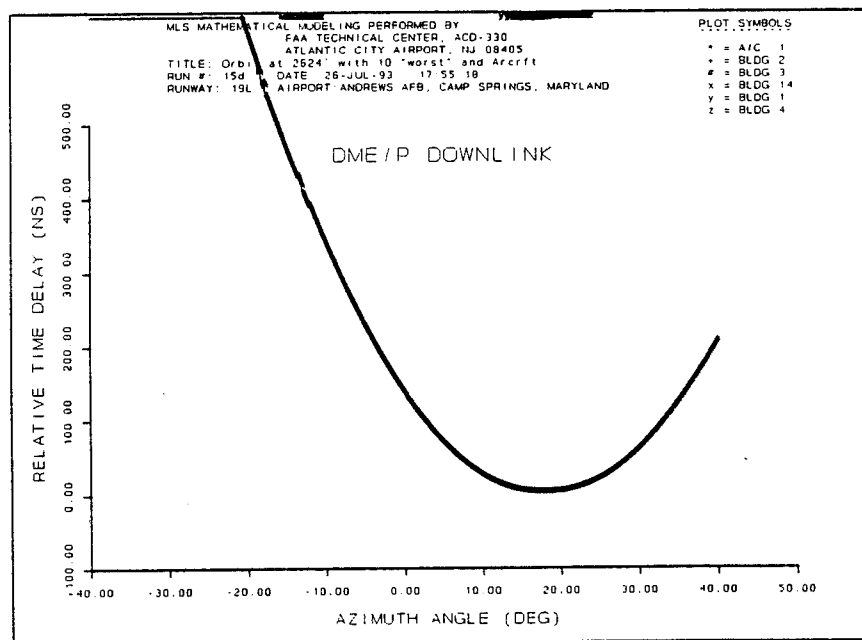
FIGURE C-34. DME/P DOWNLINK RELATIVE TIME DELAY PLOT FOR AN ORBITAL (2624' ABOVE REF.) FLIGHT PATH.
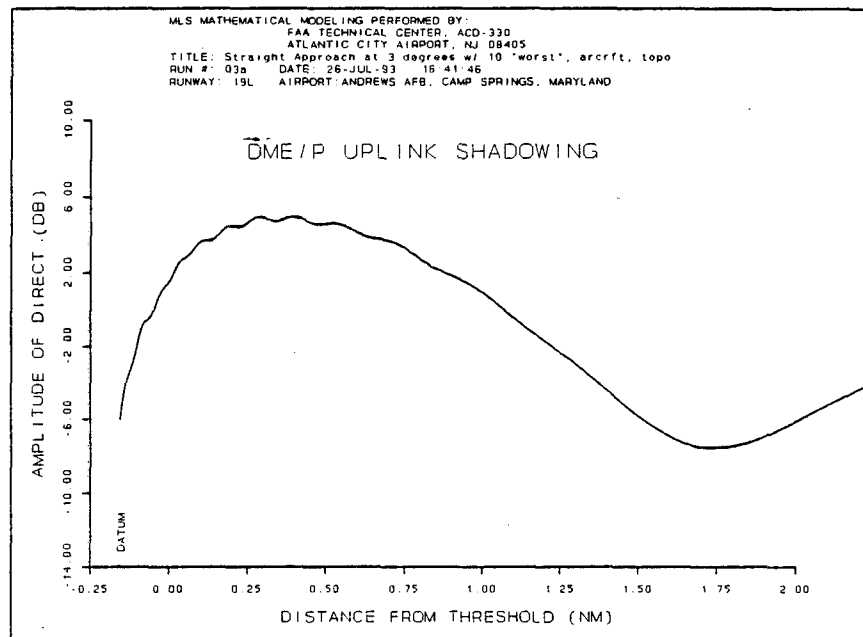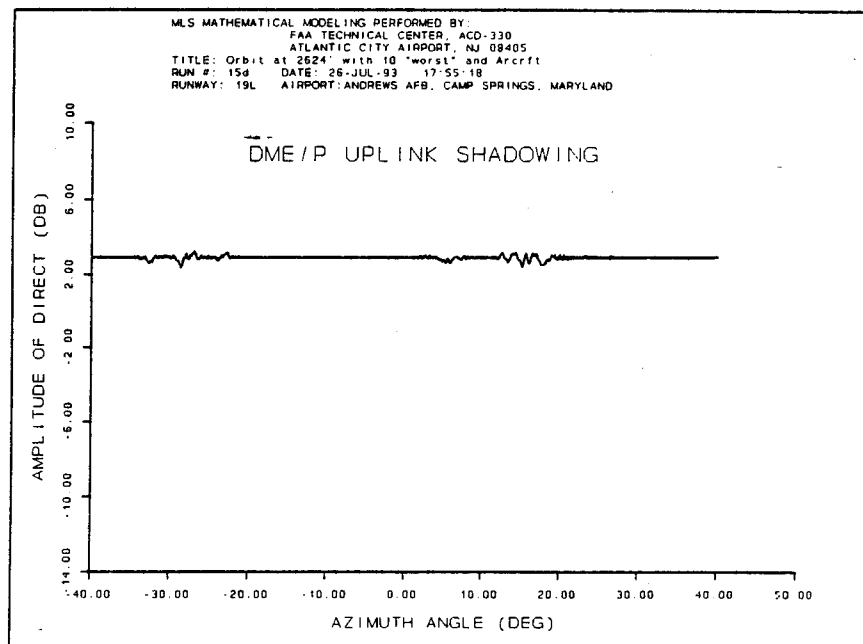
FIGURE C-35. DME/P UPLINK COMPOSITE MAGNITUDE PLOT
FOR AN ORBITAL (2624' ABOVE REF.) FLIGHT PATH.
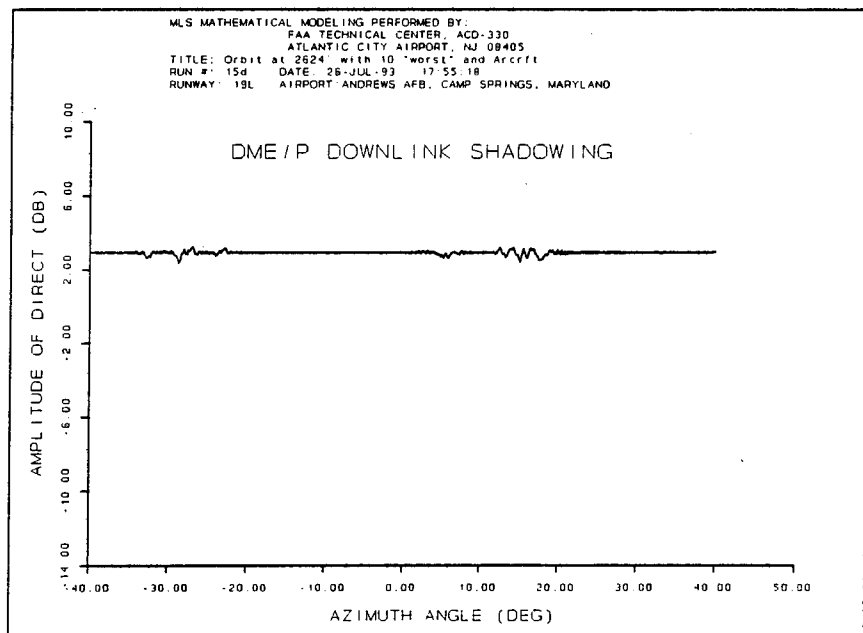
FIGURE C-36. DME/P DOWNLINK COMPOSITE MAGNITUDE
PLOT FOR AN ORBITAL (2624' ABOVE REF.) FLIGHT PATH.

MLS MATHEMATICAL MODELING PERFORMED BY:
FAA TECHNICAL CENTER, ACD-330
ATLANTIC CITY AIRPORT, NJ 08405
TITLE: Orbit at 2624' with 10 'worst' and Arcrft
RUN #: 15d   DATE : 26-JUL-93   18:00:24
RUNWAY: 19L   AIRPORT:ANDREWS AFB, CAMP SPRINGS, MARYLAND
ANTENNA: DMBN   PULSE: PCOC21200   DETECTOR:DAC   FILTER: NO FILTER

DME/P MEAN   STATIC

ERROR (FT)

AZIMUTH ANGLE (DEG)
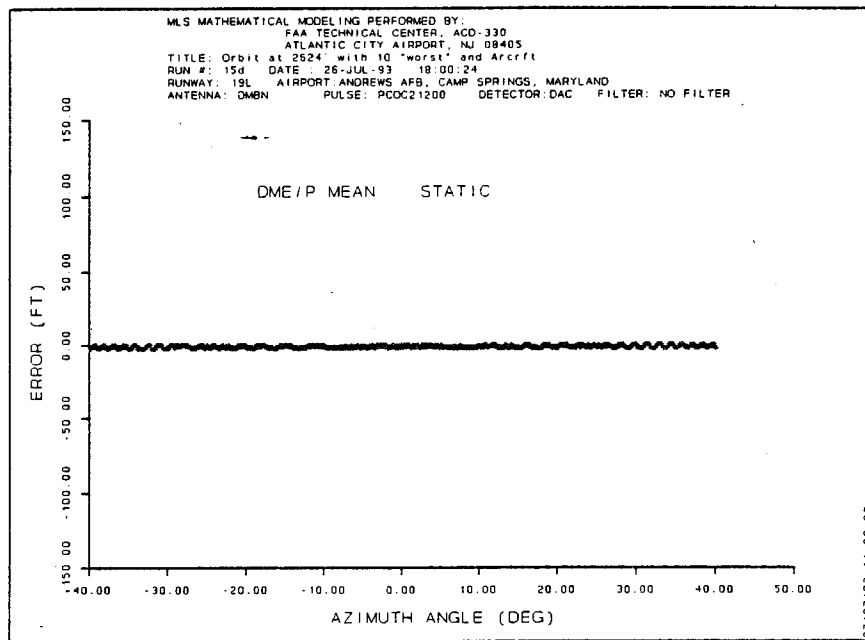
FIGURE C-37.. DME/P STATIC ERROR PLOT FOR AN ORBITAL (2624' ABOVE REF.) FLIGHT PATH.

MLS MATHEMATICAL MODELING PERFORMED BY:
FAA TECHNICAL CENTER, ACD-330
ATLANTIC CITY AIRPORT, NJ 08405
TITLE: Orbit at 2624' with 10 'worst' and Arcrft
RUN #: 15d   DATE   26-JUL-93   18:00:24
RUNWAY: 19L   AIRPORT:ANDREWS AFB, CAMP SPRINGS, MARYLAND
ANTENNA: DMBN   PULSE: PCOC21200   DETECTOR:DAC   FILTER: NO FILTER

DME/P MEAN   DYNAMIC

ERROR (FT)

AZIMUTH ANGLE (DEG)
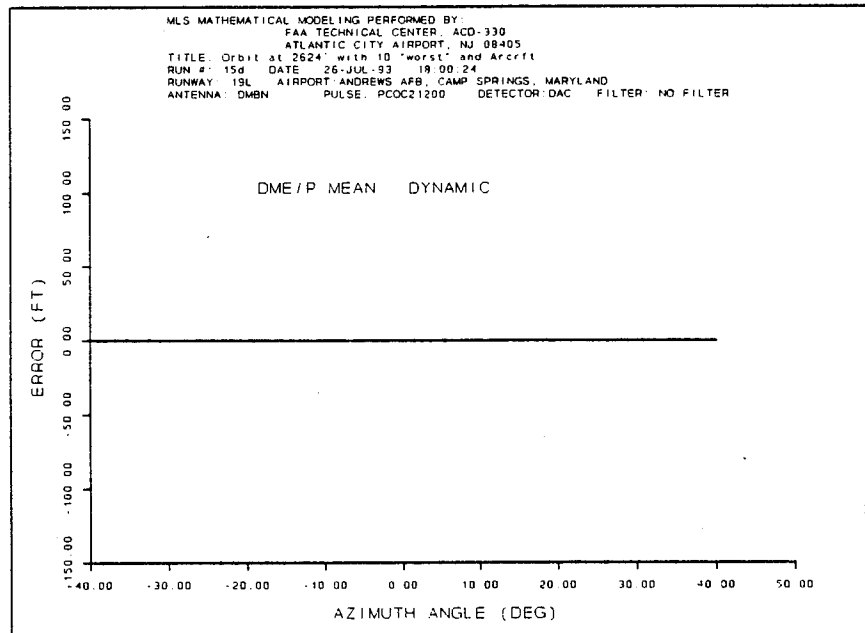
FIGURE C-38. DME/P DYNAMIC ERROR PLOT FOR AN ORBITAL (2624' ABOVE REF.) FLIGHT PATH.

MLS MATHEMATICAL MODELING PERFORMED BY:
FAA TECHNICAL CENTER, ACD-330
ATLANTIC CITY AIRPORT, NJ 08405
TITLE: Orbit at 2624' with 10 'worst' and Arcrft
RUN #: 15d   DATE : 26-JUL-93   18:00:24
RUNWAY: 19L   AIRPORT:ANDREWS AFB, CAMP SPRINGS, MARYLAND
ANTENNA: DMBN   PULSE: PCOC21200   DETECTOR:DAC   FILTER: NO FILTER
MEAN: 0.00   2*STD DEV: 0.00
TOLERANCE LIMITS VIOLATION (%): 0.00

DME/P MEAN   PFE
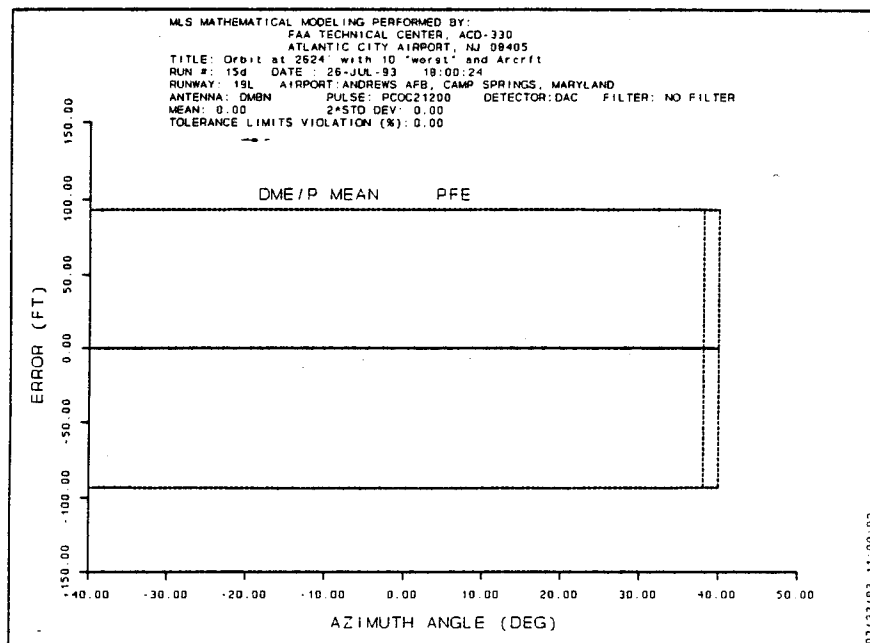
FIGURE C-39.   DME/P PATH FOLLOWING ERROR PLOT FOR AN ORBITAL (2624' ABOVE REF.) FLIGHT PATH.

MLS MATHEMATICAL MODELING PERFORMED BY:
FAA TECHNICAL CENTER, ACD-330
ATLANTIC CITY AIRPORT, NJ 08405
TITLE: Orbit at 2624' with 10 'worst' and Arcrft
RUN #: 15d   DATE   26-JUL-93   18:00:24
RUNWAY: 19L   AIRPORT ANDREWS AFB, CAMP SPRINGS, MARYLAND
ANTENNA: DMBN   PULSE: PCOC21200   DETECTOR:DAC   FILTER: NO FILTER
MEAN: 0.00   2*STD DEV: 0.00
TOLERANCE LIMITS VIOLATION (%): 0.00

DME/P MEAN   CMN
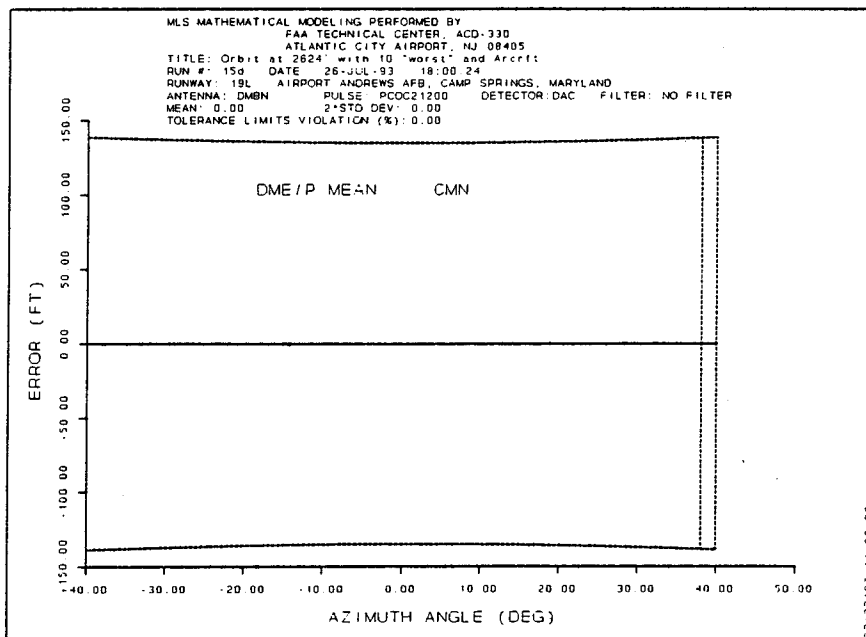
FIGURE C-40.   DME/P CONTROL MOTION NOISE PLOT FOR AN ORBITAL (2624' ABOVE REF.) FLIGHT PATH.

C-24
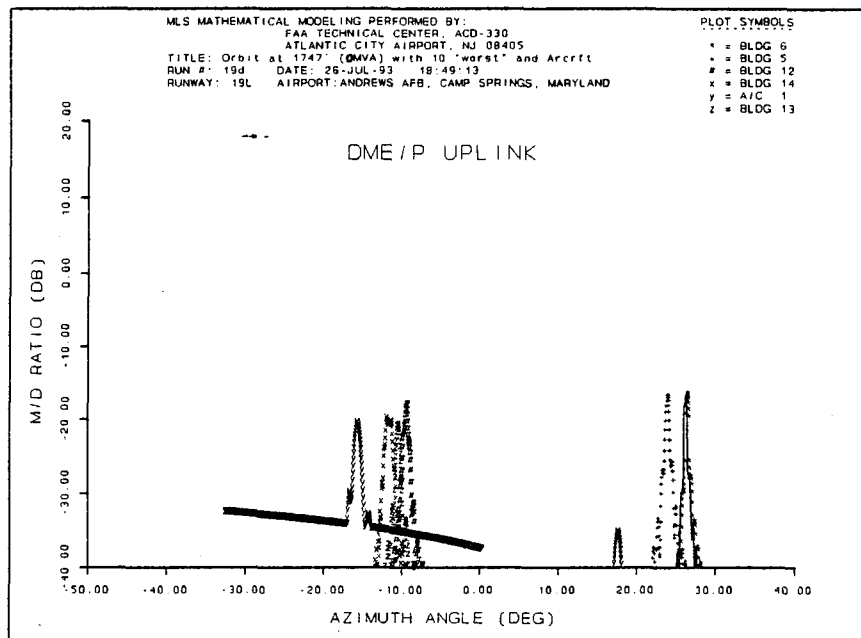
FIGURE C-41. DME/P UPLINK MULTIPATH RELATIVE
MAGNITUDE PLOT FOR AN ORBITAL (1747' ABOVE REF.)
FLIGHT PATH.
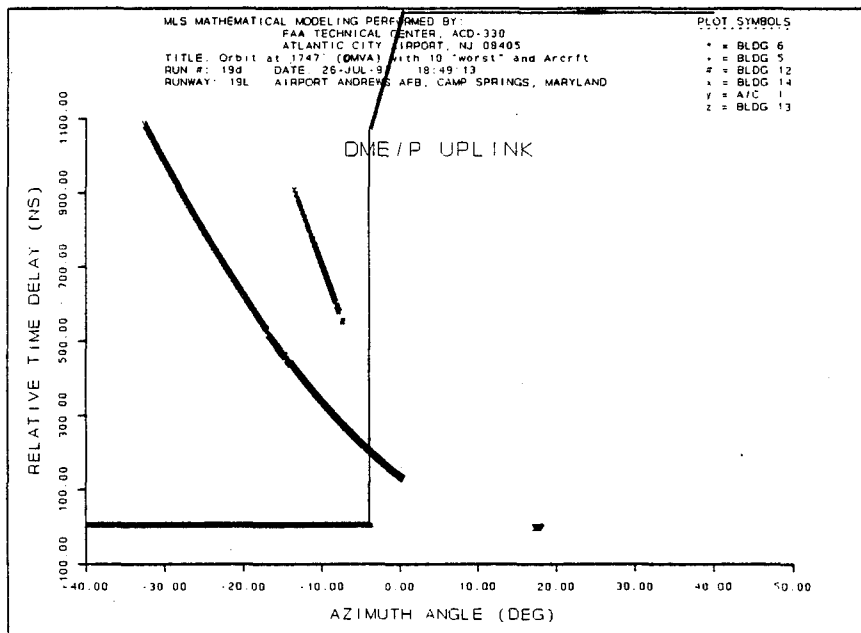
FIGURE C-42. DME/P UPLINK RELATIVE TIME DELAY PLOT
FOR AN ORBITAL (1747' ABOVE REF.) FLIGHT PATH.
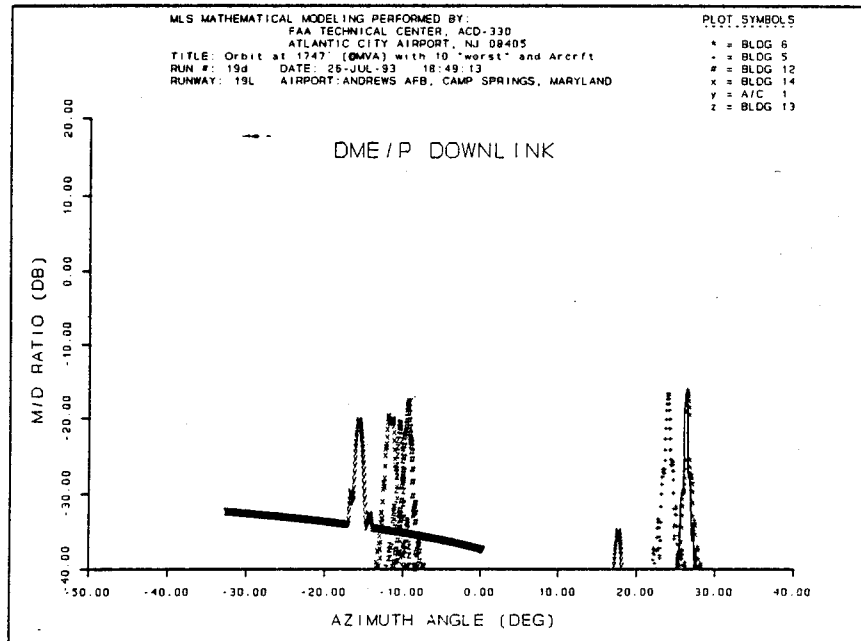
FIGURE C-43. DME/P DOWNLINK MULTIPATH RELATIVE
MAGNITUDE PLOT FOR AN ORBITAL (1747' ABOVE REF.)
FLIGHT PATH
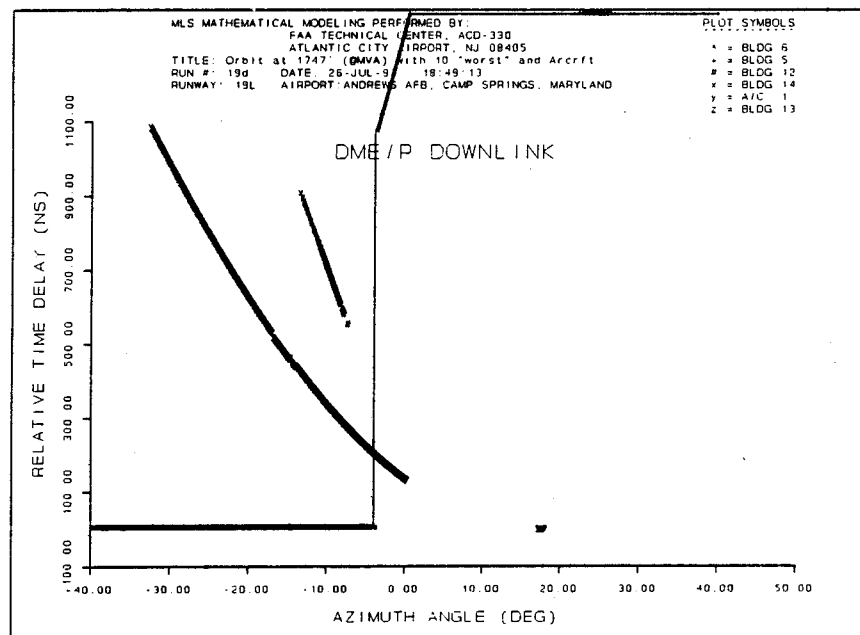
FIGURE C-44. DME/P DOWNLINK RELATIVE TIME DELAY
PLOT FOR AN ORBITAL (1747' ABOVE REF.) FLIGHT PATH.
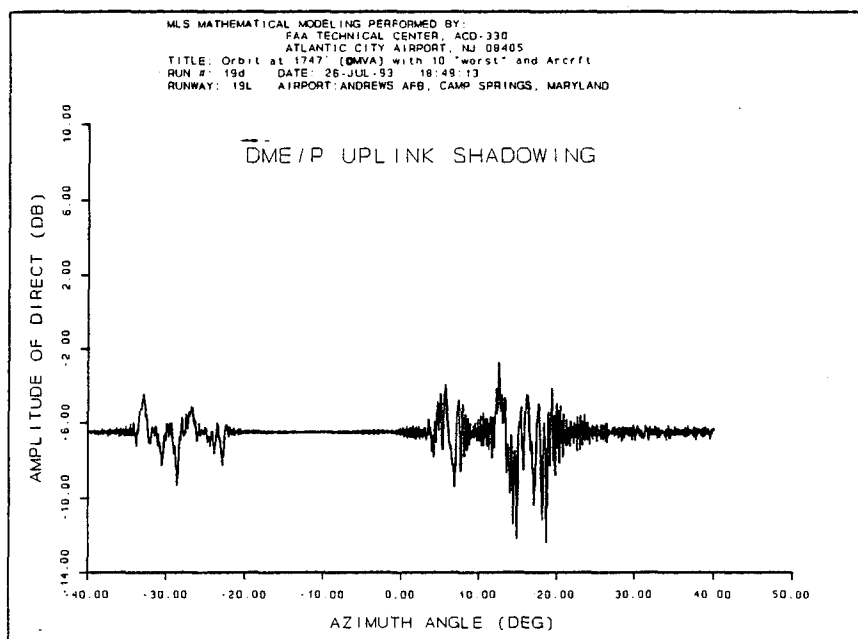
FIGURE C-45. DME/P UPLINK COMPOSITE MAGNITUDE PLOT
FOR AN ORBITAL (1747' ABOVE REF.) FLIGHT PATH.
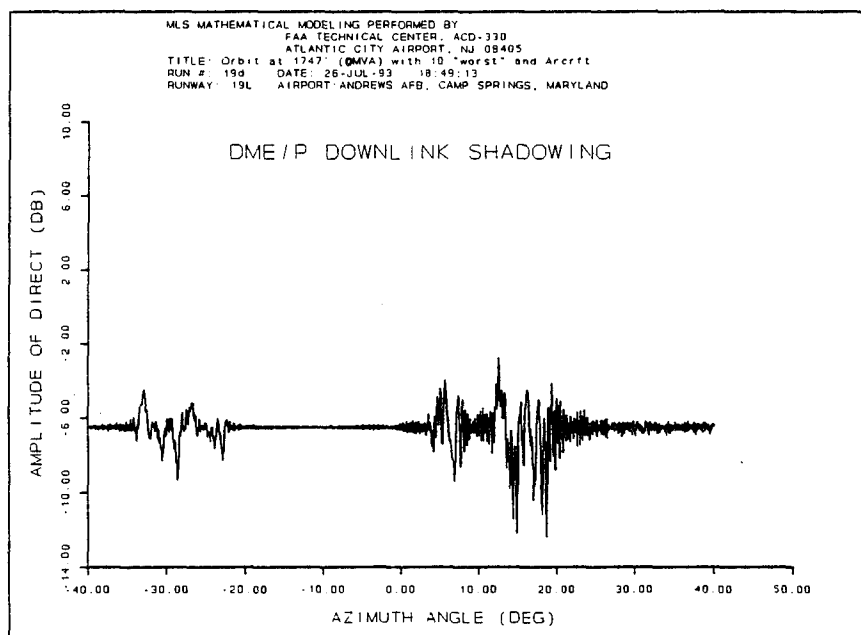
FIGURE C-46. DME/P DOWNLINK COMPOSITE MAGNITUDE
PLOT FOR AN ORBITAL (1747' ABOVE REF.) FLIGHT PATH.

C-27

MLS MATHEMATICAL MODELING PERFORMED BY:
FAA TECHNICAL CENTER, ACD-330
ATLANTIC CITY AIRPORT, NJ 08405
TITLE: Orbit at 1747' (OMVA) with 10 "worst" and Arcrft
RUN #: 19d   DATE : 26-JUL-93   18:54:27
RUNWAY: 19L   AIRPORT: ANDREWS AFB, CAMP SPRINGS, MARYLAND
ANTENNA: DMBN   PULSE: PCOC21200   DETECTOR:DAC   FILTER: NO FILTER

DME/P MEAN   STATIC
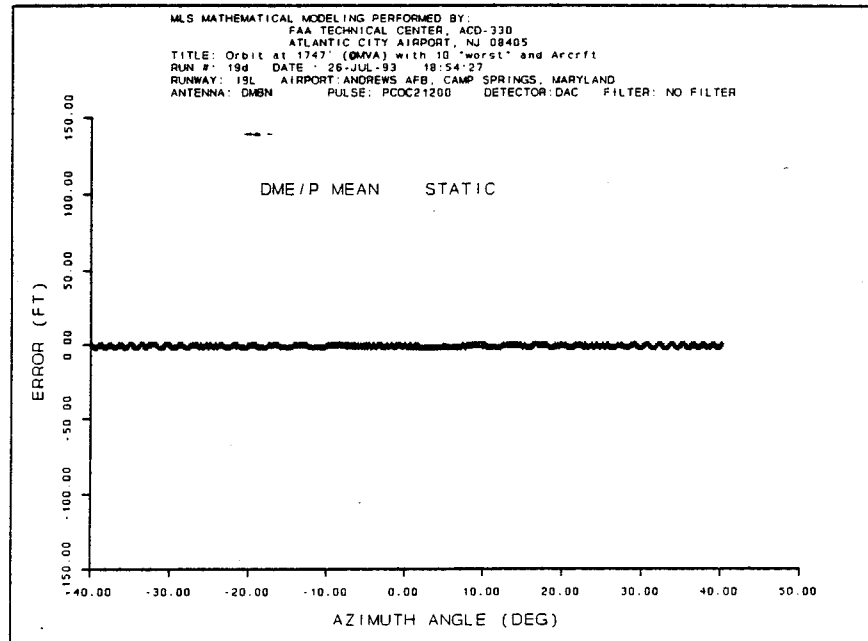
FIGURE C-47. DME/P STATIC ERROR PLOT FOR AN ORBITAL (1747' ABOVE REF.) FLIGHT PATH.

MLS MATHEMATICAL MODELING PERFORMED BY:
FAA TECHNICAL CENTER, ACD-330
ATLANTIC CITY AIRPORT, NJ 08405
TITLE: Orbit at 1747' (OMVA) with 10 "worst" and Arcrft
RUN #: 19d   DATE : 26-JUL-93   18:54:27
RUNWAY: 19L   AIRPORT: ANDREWS AFB, CAMP SPRINGS, MARYLAND
ANTENNA: DMBN   PULSE: PCOC21200   DETECTOR:DAC   FILTER: NO FILTER

DME/P MEAN   DYNAMIC
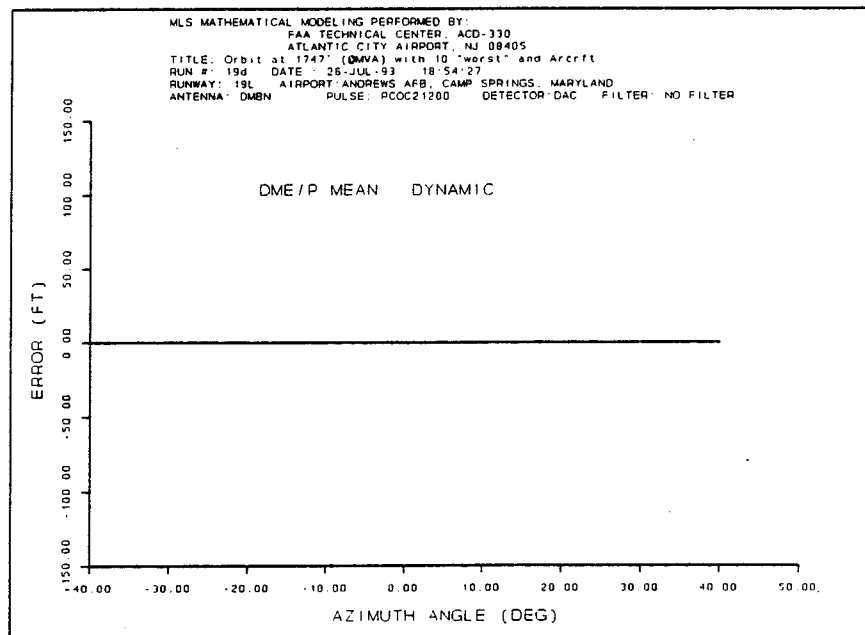
FIGURE C-48. DME/P DYNAMIC ERROR PLOT FOR AN ORBITAL (1747' ABOVE REF.) FLIGHT PATH.

C-28
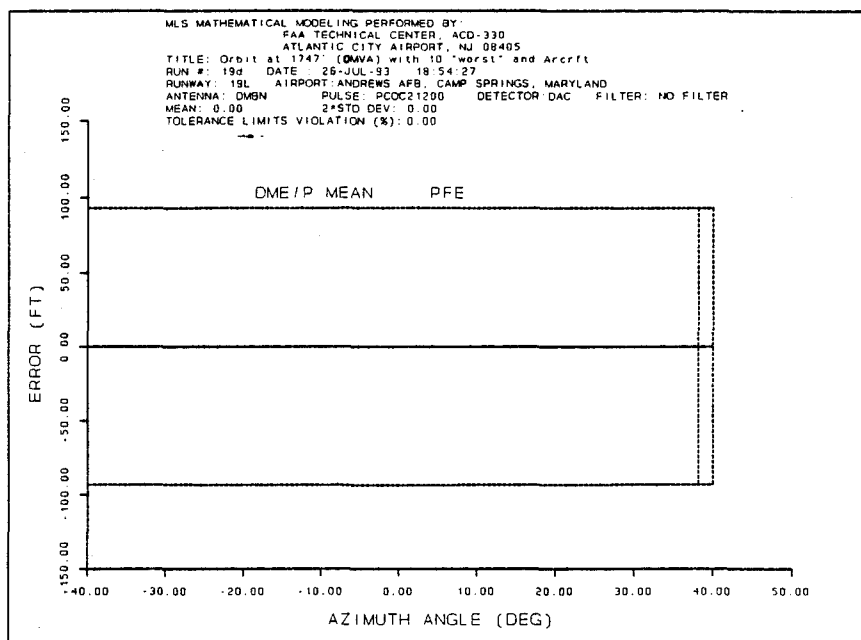
FIGURE C-49.   DME/P PATH FOLLOWING ERROR PLOT FOR AN
ORBITAL (1747' ABOVE REF.) FLIGHT PATH.
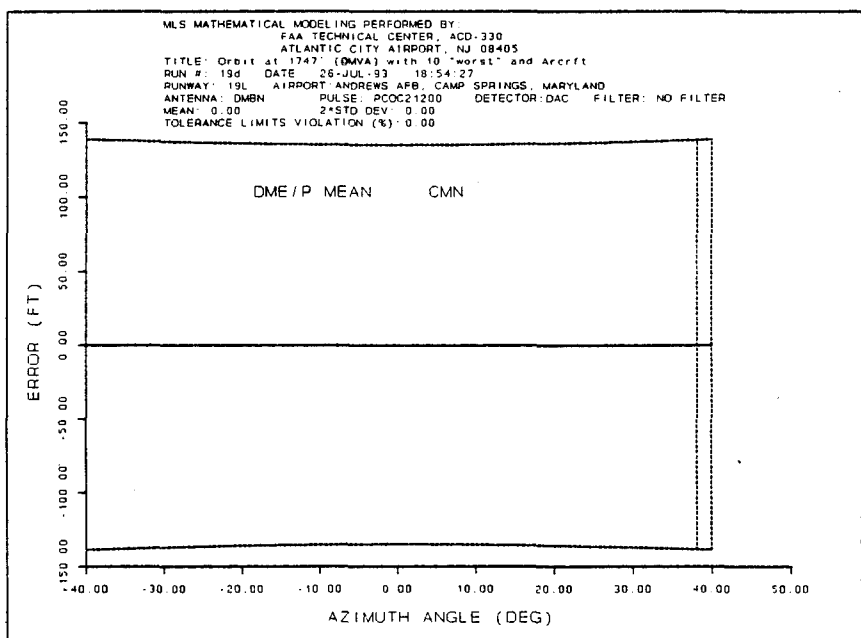
FIGURE C-50.   DME/P CONTROL MOTION NOISE PLOT FOR AN
ORBITAL (1747' ABOVE REF.) FLIGHT PATH.

C-29
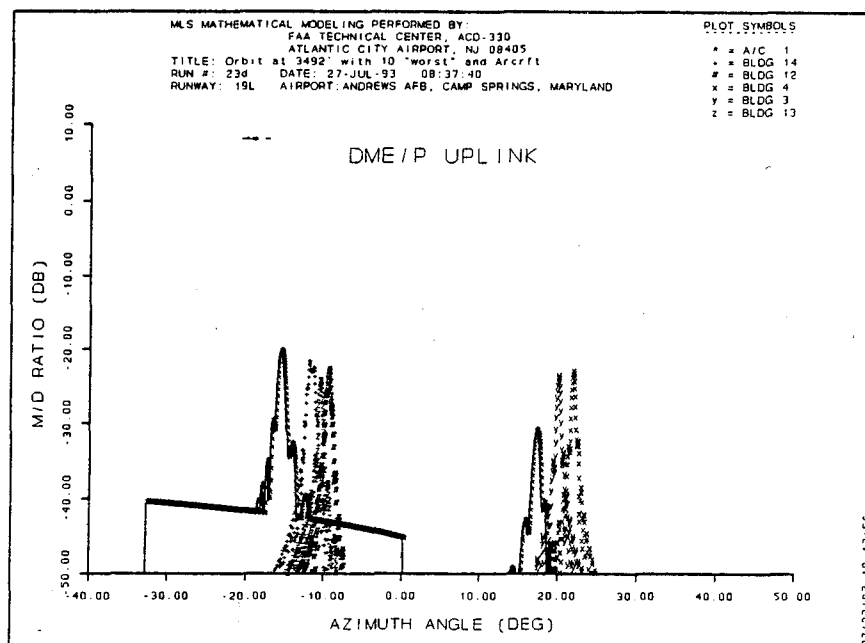
FIGURE C-51. DME/P UPLINK COMPOSITE MAGNITUDE PLOT FOR AN ORBITAL (3492' ABOVE REF.) FLIGHT PATH.
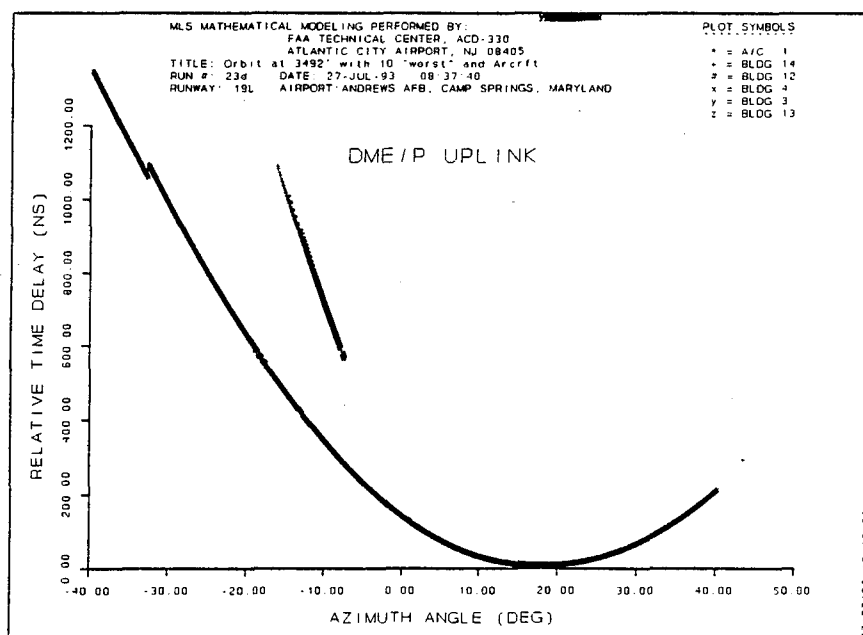
FIGURE C-52. DME/P UPLINK RELATIVE TIME DELAY PLOT FOR AN ORBITAL (3492' ABOVE REF.) FLIGHT PATH.

C-30
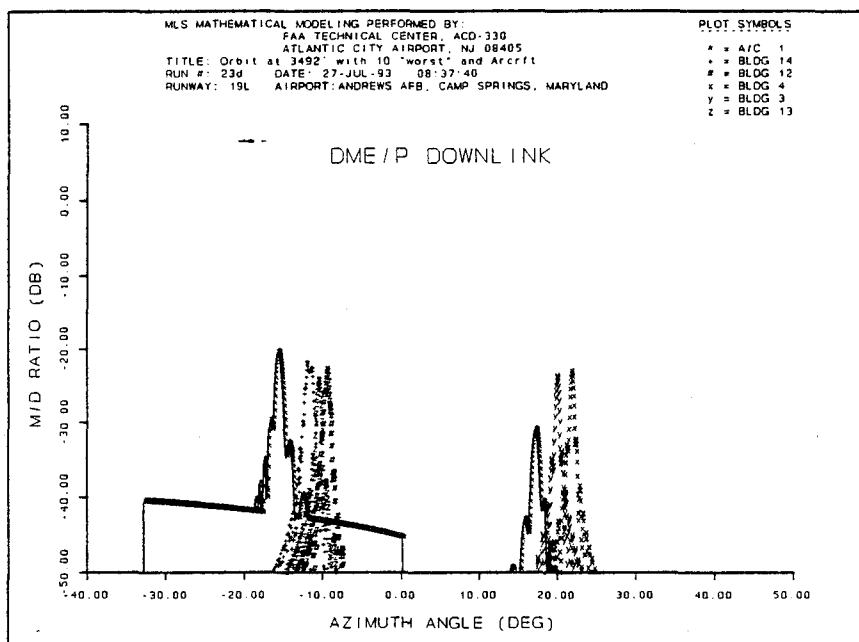
FIGURE C-53. DME/P DOWNLINK MULTIPATH RELATIVE MAGNITUDE PLOT FOR AN ORBITAL (3492' ABOVE REF.) FLIGHT PATH.
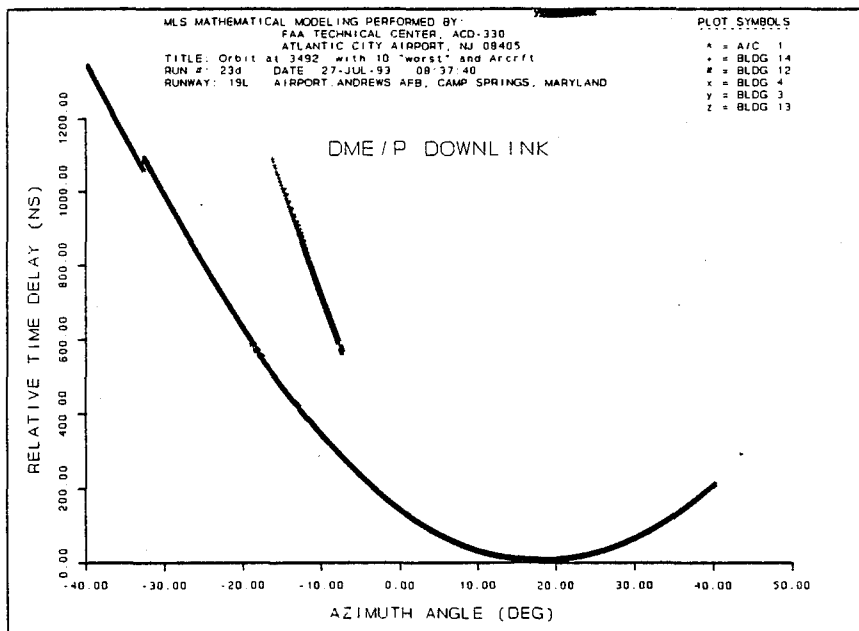
FIGURE C-54. DME/P DOWNLINK RELATIVE TIME DELAY PLOT FOR AN ORBITAL (3492' ABOVE REF.) FLIGHT PATH.

MLS MATHEMATICAL MODELING PERFORMED BY:
FAA TECHNICAL CENTER, ACD-330
ATLANTIC CITY AIRPORT, NJ 08405
TITLE: Orbit at 3492' with 10 "worst" and Arcrft
RUN #: 23d   DATE: 27-JUL-93   09:37:40
RUNWAY: 19L   AIRPORT:ANDREWS AFB, CAMP SPRINGS, MARYLAND

DME/P UPLINK SHADOWING

AMPLITUDE OF DIRECT (DB)

AZIMUTH ANGLE (DEG)
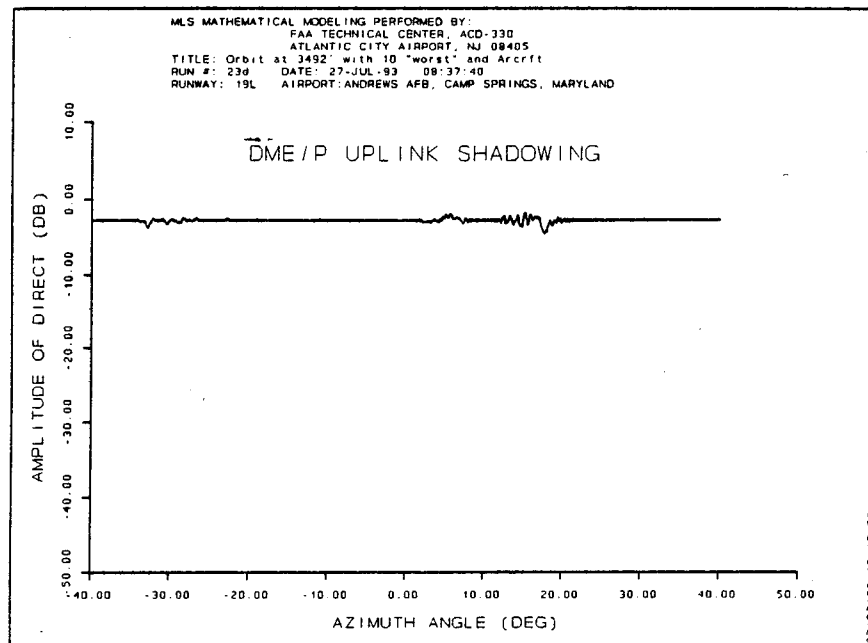
FIGURE C-55.   DME/P UPLINK COMPOSITE MAGNITUDE PLOT FOR AN ORBITAL (3492' ABOVE REF.) FLIGHT PATH.

MLS MATHEMATICAL MODELING PERFORMED BY:
FAA TECHNICAL CENTER, ACD-330
ATLANTIC CITY AIRPORT, NJ 08405
TITLE: Orbit at 3492' with 10 "worst" and Arcrft
RUN #: 23d   DATE: 27-JUL-93   09:37:40
RUNWAY: 19L   AIRPORT:ANDREWS AFB, CAMP SPRINGS, MARYLAND

DME/P DOWNLINK SHADOWING

AMPLITUDE OF DIRECT (DB)

AZIMUTH ANGLE (DEG)
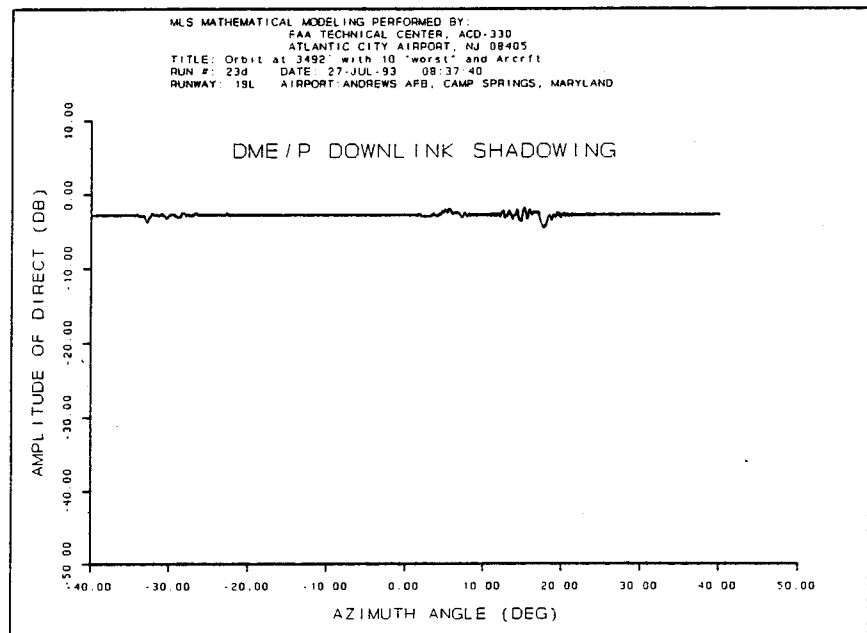
FIGURE C-56.   DME/P DOWNLINK COMPOSITE MAGNITUDE PLOT FOR AN ORBITAL (3492' ABOVE REF.) FLIGHT PATH.

C-32
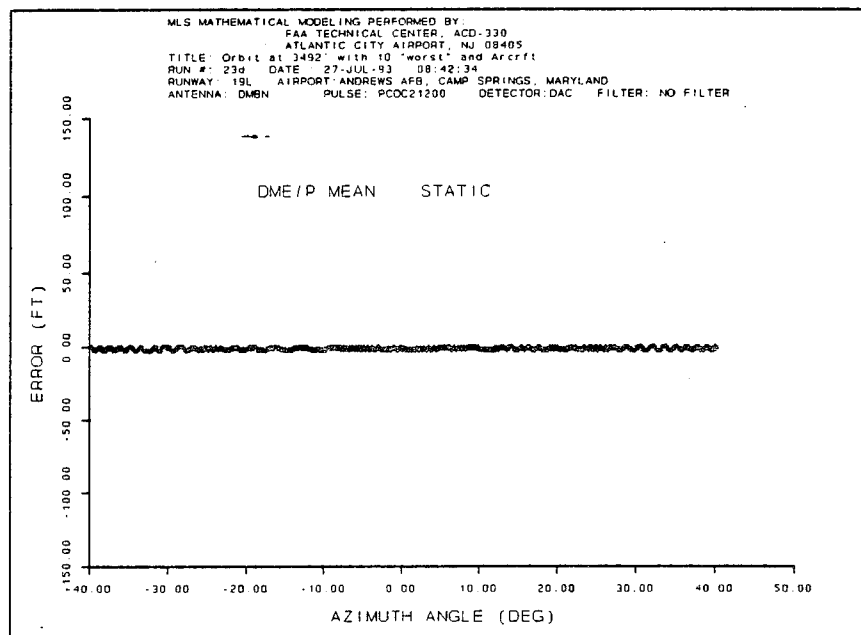
FIGURE C-57. DME/P STATIC ERROR PLOT FOR AN ORBITAL
(3492' ABOVE REF.) FLIGHT PATH.
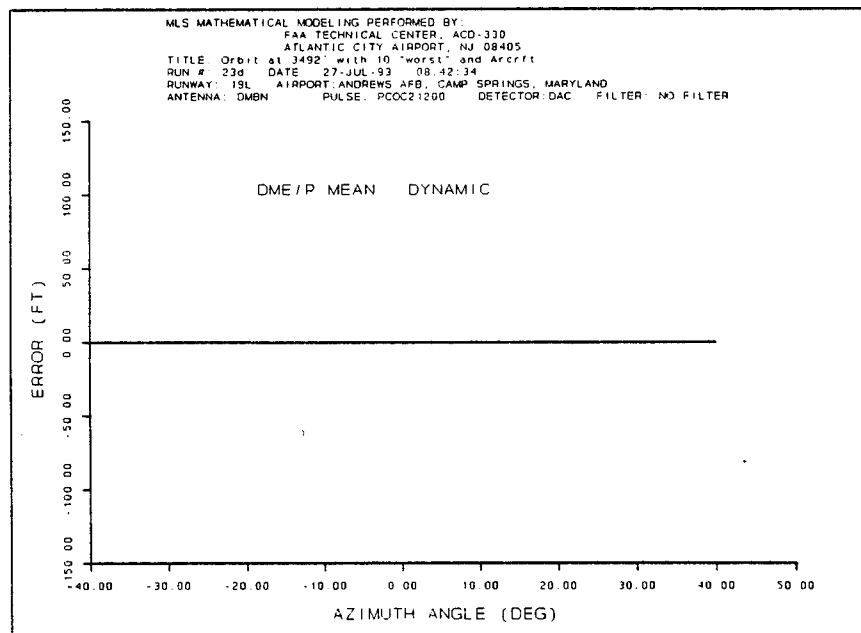
FIGURE C-58. DME/P DYNAMIC ERROR PLOT FOR AN
ORBITAL (3492' ABOVE REF.) FLIGHT PATH.

C-33

MLS MATHEMATICAL MODELING PERFORMED BY:
FAA TECHNICAL CENTER, ACD-330
ATLANTIC CITY AIRPORT, NJ 08405
TITLE: Orbit at 3492' with 10 "worst" and Arcrft
RUN #: 23d   DATE : 27-JUL-93   08:42:34
RUNWAY: 19L   AIRPORT:ANDREWS AFB, CAMP SPRINGS, MARYLAND
ANTENNA: DMBN   PULSE: PCOC21200   DETECTOR:DAC   FILTER: NO FILTER
MEAN: 0.00   2*STD DEV: 0.00
TOLERANCE LIMITS VIOLATION (%):0.00

DME/P MEAN   PFE
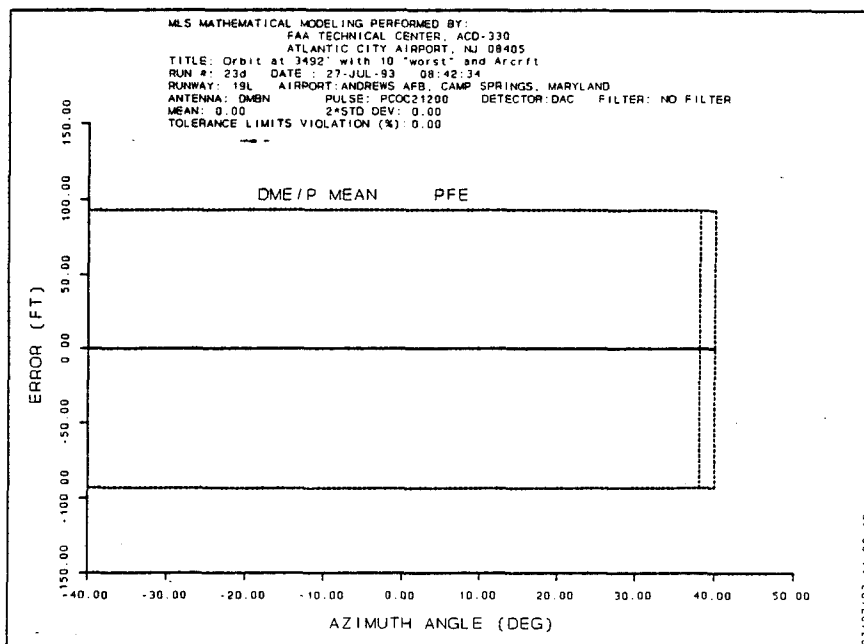
FIGURE C-59.   DME/P PATH FOLLOWING ERROR PLOT FOR AN
ORBITAL (3492' ABOVE REF.) FLIGHT PATH.

MLS MATHEMATICAL MODELING PERFORMED BY:
FAA TECHNICAL CENTER, ACD-330
ATLANTIC CITY AIRPORT, NJ 08405
TITLE: Orbit at 3492' with 10 "worst" and Arcrft
RUN #: 23d   DATE 27-JUL-93   08:42:34
RUNWAY: 19L   AIRPORT:ANDREWS AFB, CAMP SPRINGS, MARYLAND
ANTENNA: DMBN   PULSE: PCOC21200   DETECTOR:DAC   FILTER: NO FILTER
MEAN: 0.00   2*STD DEV: 0.00
TOLERANCE LIMITS VIOLATION (%): 0.00

DME/P MEAN   CMN
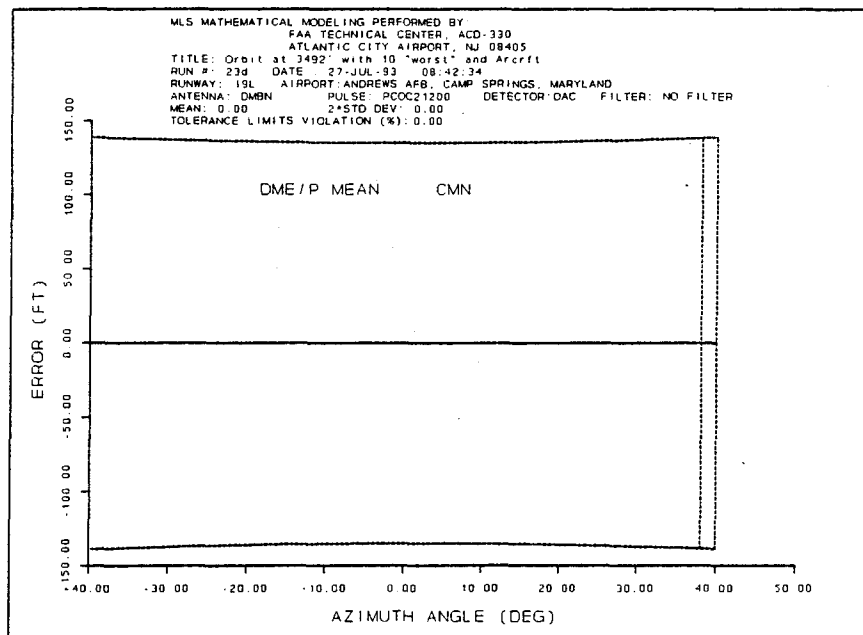
FIGURE C-60.   DME/P CONTROL MOTION NOISE PLOT FOR AN
ORBITAL (3492' ABOVE REF.) FLIGHT PATH.

C-34

Appendix D
Hangars and Buildings Modeled for Multipath Effects

Appendix D contains tables showing the structure of the data describing the hangars and buildings that were originally modeled for evaluation of multipath effects. These data represent part of the input files used to calculate the quality of guidance to be provided by the proposed MLS-DME/P installation. Some scatterers were modeled again in the third set of buildings to evaluate the effects of their roofs.

The first column contains the reference name and number used to identify the different scatterers that represent the selected hangars and buildings. The second through fifth columns contain the locations of the endpoints of the scatterers in the x-y plane of the model's reference coordinate system in feet. The "left" coordinates refer to the end of the current scatterer closest to the origin, while the "right" coordinates refer to the end of the current scatterer farthest from the origin. "ELV", in the sixth column, refers to the height of the base of the scatterer above the origin in feet. "HGT", in the seventh column, refers to the height of the top of the current scatterer above its base. "TLT", in the eighth column, refers to the angle between the surface of the scatterer and the reference Z axis in degrees. 0 degrees means that the scatterer stands straight up, with its surface parallel to the Z axis. "GRCORR", in the ninth column, is the elevation of the ground halfway between the scatterer and the transmitter. "CMP", in the last column, is the composition of the modeled scatterer.

SET #1

	##	X-LEFT	Y-LEFT	X-RGHT	Y-RGHT	ELV	HGT	TLT	GRCORR	CMP
hngr	01	7373.5	4149.8	7604.1	4149.8	15.8	75.2	0	8	METAL
hngr	02	6786.8	4154.5	7020.7	4154.5	15.8	75.2	0	8	METAL
hngr	03	5709.0	4147.2	5943.5	4147.2	15.8	75.2	0	8	METAL
hngr	04	5123.6	4146.0	5363.0	4146.0	15.8	75.2	0	8	METAL
hngr	05	4557.8	4143.5	4783.2	4143.5	21.3	20.8	0	10	METAL
hngr	06	3949.5	4147.0	4186.7	4147.0	17.8	75.0	0	9	METAL
hngr	10	8558.2	-1067.0	8866.0	-1067.0	24.0	53.0	0	12	METAL
hgr11	21	8010.8	-1070.6	8242.0	-1070.6	32.0	61.6	0	16	METAL
hgr11	22	7942.6	-1085.9	8010.8	-1085.9	32.0	61.6	0	16	METAL
hgr11	23	7881.2	-1065.9	7942.6	-1065.9	32.0	61.6	0	16	METAL

SET #2

	##	X-LEFT	Y-LEFT	X-RGHT	Y-RGHT	ELV	HGT	TLT	GRCORR	CMP
hngr	12	4977.6	-1652.3	5646.8	-1652.3	18.8	42.5	0	9	METAL
hngr	13	4552.7	-1655.9	4895.1	-1655.9	18.8	42.5	0	9	METAL
hngr	14	3824.5	-1657.2	4481.3	-1657.2	19.8	42.5	0	9	METAL
hngr	15	3574.4	-1656.4	3758.4	-1656.4	26.0	42.8	0	13	METAL
3629a	51	7563.6	-1072.5	7659.2	-1072.5	24.0	50.0	0	12	METAL
3629b	52	7518.8	-1125.7	7563.6	-1125.7	24.0	50.0	0	12	METAL
3001a	53	2057.1	-1127.9	2080.7	-1127.1	5.0	35.0	0	2	METAL
3001b	54	1964.7	-1137.6	2057.1	-1137.6	5.0	35.0	0	2	METAL
2487	55	1180.1	-1034.4	1265.2	-1034.4	5.0	25.0	0	2	METAL
1915	56	7930.0	4148.4	8168.4	4184.4	15.8	34.0	0	8	METAL

SET #3

	##	X-LEFT	Y-LEFT	X-RGHT	Y-RGHT	ELV	HGT	TLT	GRCORR	CMP
hngr	12	4977.6	-1652.3	5646.8	-1652.3	18.8	27.2	0	9	METAL
hgr rf	32	4977.6	-1648.3	5646.8	-1648.3	46.0	18.0	45	9	METAL
hngr	13	4552.7	-1655.9	4895.1	-1655.9	18.8	27.2	0	9	METAL
hgr rf	33	4552.7	-1651.9	4895.1	-1651.9	46.0	18.0	45	9	METAL
hngr	14	3824.5	-1657.2	4481.3	-1657.2	19.8	27.2	0	9	METAL
hgr rf	34	3824.5	-1653.2	4481.3	-1653.2	47.0	18.0	45	9	METAL
hngr	15	3574.4	-1656.4	3758.4	-1656.4	26.0	27.2	0	13	METAL
hgr rf	35	3574.4	-1652.4	3758.4	-1652.4	46.0	18.0	45	13	METAL

Appendix E
Aircraft Used for Multipath and Shadowing Effects

The table below shows the structure of the data describing the C5A Galaxy aircraft that was modeled for evaluation of multipath effects. This data represent another section of the input files used to calculate the quality of guidance to be provided by the proposed MLS-DME/P installation.

The first column contains the reference name and number used to identify the different modeled aircraft. The second through fifth columns contain the locations of the endpoints of the aircraft in the x-y plane of the model's reference coordinate system in feet. The "tail" coordinates refer to the location of the tail of the aircraft fuselage, while the "ckpt" coordinates refer to the location of the cockpit of the aircraft in the model's coordinate system. "ALT", in the sixth column, refers to the height of the center of the fuselage above the origin in feet. "AT", in the seventh column, is a reference number to the aircraft type being modeled (a C5A Galaxy). The representation of the aircraft (diameter of fuselage, height and shape of tail, etc.) changes with aircraft type to properly represent the profile of the desired aircraft. "GRCORR", in the eighth column, is the elevation of the ground halfway between the aircraft and the transmitter.

##	X-TAIL	Y-TAIL	X-CKPT	Y-CKPT	ALT	AT	GRCORR
01	523.5	-800.0	276.5	-800.0	0.	11	0.
02	2297.05	-487.3	2472.35	-312.7	23.583	11	5.
03	9728.5	-500.0	9481.5	-500.0	37.583	11	12.

Appendix F
Hangars and Buildings Modeled for Shadowing Effects

The table below shows the structure of the data describing the buildings that were originally modeled for evaluation of shadowing effects. These data represent part of the input files used to calculate the quality of guidance to be provided by the proposed MLS-DME/P installation.

The first column contains the reference name and number used to identify the different scatterers that represent the selected hangars and buildings. The second through fifth columns contain the locations of the endpoints of the scatterers in the x-y plane of the model's reference coordinate system in feet. The "left" coordinates refer to the end of the current scatterer closest to the origin, while the "right" coordinates refer to the end of the current scatterer farthest from the origin. "ELV", in the sixth column, refers to the height of the base of the scatterer above the origin in feet. "HGT", in the seventh column, refers to the height of the top of the current scatterer above its base.

	##	X-LEFT	Y-LEFT	X-RGHT	Y-RGHT	ELV	HGT
	01	7373.5	4149.8	7604.1	4149.8	15.8	75.2
	02	6786.8	4154.5	7020.7	4154.5	15.8	75.2
	03	5709.0	4147.2	5943.5	4147.2	15.8	75.2
	04	5123.6	4146.0	5363.0	4146.0	15.8	75.2
	05	4557.8	4143.5	4783.2	4143.5	21.3	20.8
	06	3949.5	4147.0	4186.7	4147.0	17.8	75.0
	10	8558.2	-1067.0	8866.0	-1067.0	24.0	53.0
	21	8010.8	-1070.6	8242.0	-1070.6	32.0	61.6
	22	7942.6	-1085.9	8010.8	-1085.9	32.0	61.6
	23	7881.2	-1065.9	7942.6	-1065.9	32.0	61.6

	##	X-LEFT	Y-LEFT	X-RGHT	Y-RGHT	ELV	HGT
	12	4977.6	-1652.3	5646.8	-1652.3	18.8	42.5
	13	4552.7	-1655.9	4895.1	-1655.9	18.8	42.5
	14	3824.5	-1657.2	4481.3	-1657.2	19.8	42.5
	15	3574.4	-1656.4	3758.4	-1656.4	26.0	42.8
3629a	51	7563.6	-1072.5	7659.2	-1072.5	24.0	50.0
3629b	52	7518.8	-1125.7	7563.6	-1125.7	24.0	50.0
3001a	53	2057.1	-1127.9	2080.7	-1127.1	5.0	35.0
3001b	54	1964.7	-1137.6	2057.1	-1137.6	5.0	35.0
2487	55	1180.1	-1034.4	1265.2	-1034.4	5.0	25.0
1915	56	7930.0	4148.4	8168.4	4184.4	15.8	34.0

Appendix G
Data Collected During Terrain Survey

The following tables list the original data collected during a site survey of the terrain, in the region of the proposed MLS EL station. The point numbers are used in reference to figure 6, an illustration of the surveyed data points. The first group lists the actual collected information. The second group lists the original information transformed into the reference coordinate system. Distances are in feet. Surveyed elevations (first group) are in feet relative to MSL.

Point Number	Distance from Threshold	Distance from Cntrln	Surveyed Elevation
1.	999.780	173.892	277.117
2.	1006.343	270.293	276.850
3.	1013.677	370.017	272.034
4.	1010.810	468.706	272.632
5.	1016.182	565.603	273.446
6.	918.119	563.412	271.832
7.	916.893	464.258	270.565
8.	913.199	364.049	270.518
9.	904.741	269.687	276.189
10.	806.953	266.910	276.148
11.	799.876	366.177	270.918
12.	791.626	463.641	269.181
13.	789.929	561.690	269.313
14.	688.497	552.957	268.342
15.	687.756	456.857	268.971
16.	684.611	356.646	275.261
17.	685.688	256.954	277.351
18.	586.433	244.236	277.856
19.	594.086	342.933	276.816
20.	591.687	441.659	272.693
21.	583.767	540.940	270.569
22.	231.120	536.260	272.734

Point Number	X	Y	Z
1.	8755.220	173.892	24.117
2.	8748.657	270.293	23.850
3.	8741.323	370.017	19.034
4.	8744.190	468.706	19.632
5.	8738.818	565.603	20.446
6.	8836.881	563.412	18.832
7.	8838.107	464.258	17.565
8.	8841.801	364.049	17.518
9.	8850.259	269.687	23.189
10.	8948.047	266.910	23.148
11.	8955.124	366.177	17.918
12.	8963.374	463.641	16.181
13.	8965.071	561.690	16.313
14.	9066.503	552.957	15.342
15.	9067.244	456.857	15.971
16.	9070.389	356.646	22.261
17.	9069.312	256.954	24.351
18.	9168.567	244.236	24.856
19.	9160.914	342.933	23.816
20.	9163.313	441.659	19.693
21.	9171.233	540.940	17.569
22.	9523.880	536.260	19.734

Appendix H
Data Used to Represent Terrain as Plates

The following tables show data used to develop mathematical modeling input files to represent the topographical structure in the region of the MLS EL station. These data were extracted from the topographical information collected during the site survey and listed in appendix G. The resulting representation of the terrain, using the plates described below, is illustrated in figure 5. Each plate requires three points to define its size, location, and orientation. Table H-1 lists the plate identification and the coordinates of the three corners input to the model. Table H-2 identifies the survey points used for each of the plates that were input to the model.

##	X-VALU	Y-VALU	Z-VALU
plate05	8850.259	269.687	23.189
	8841.801	364.049	17.518
	8955.124	366.177	17.918
plate06	8841.801	364.049	17.518
	8838.107	464.258	17.565
	8963.374	463.641	16.181
plate07	8838.107	464.258	17.565
	8836.881	563.412	18.832
	8965.071	561.69	16.313
plate08	8948.047	266.91	23.148
	8955.124	366.177	17.918
	9070.389	356.646	22.261
plate09	8955.124	366.177	17.918
	8963.374	463.641	16.181
	9067.244	456.857	15.971
plate10	8963.374	463.641	16.181
	8965.071	561.69	16.313
	9066.503	552.957	15.342
plate11	9069.312	256.954	24.351
	9070.389	356.646	22.261
	9160.914	342.933	23.816
plate12	9070.389	356.646	22.261
	9067.244	456.857	15.971
	9163.313	441.659	19.693
plate13	9067.244	456.857	15.971
	9066.503	552.957	15.342
	9171.233	540.94	17.569
plate17	9168.567	244.236	24.856
	9171.233	540.94	17.569
	9523.88	536.26	19.734

Table H-1

Plate Number	Corners Used
plate 05	7, 6,13
plate 06	8, 7,12
plate 07	9, 8,11
plate 08	10,11,16
plate 09	11,12,15
plate 10	12,13,14
plate 11	15,14,21
plate 12	16,15,20
plate 13	17,16,19
plate 17	18,21,22

Table H-2

Appendix I
An Introduction to MLS
List of Illustrations

The following sections explain the function of the theory of operation of MLS and the subsystems that are used to implement these theories. The discussion is divided into an explanation of the angular and range measurements, followed by some site issues and problems that may occur with a particular installation regarding signal multipath and shadowing.

I.1 ANGULAR MEASUREMENTS.

I.1.1 AZ.

The AZ antenna generates a narrow, vertical, fan-shaped beam and sweeps it across the coverage area, as shown in figure I-1. At the beginning of the AZ time slot, the AZ preamble is transmitted. This sets up the processor in the receiver to decode AZ angle data. The "TO" scan starts. At the end of the scan, there is a pause before the "FRO" scan starts.

During a single scanning cycle, the aircraft receiver detects a "TO" and a "FRO" pulse, and measures the time between the two pulses. As shown in figure I-1, it is the elapsed time between receipt of the TO and FRO pulses that determines the angular location of the aircraft, and thus, its displacement from the selected course.

The antenna can actually scan out to +/- 62°, but courses within 2° of the edges of the service area are not used, in order to avoid losing the signal and having to go through the acquisition cycle again. The normal scan of most installations is +/- 40°. Some locations may require a 60° scan to serve an additional runway or heliport, or to support curved approaches. On the other hand, some may scan as low as +/- 10° at locations where special site or multipath problems exist.

I.1.2 EL.

The same angular measurement principle used for determining azimuth, is used for determining the elevation angle. The EL antenna generates a narrow horizontal fan-shaped beam and sweeps it up and down through the coverage area shown in figure I-2.

During the elevation scan cycle, the aircraft receiver detects a "TO" pulse from the upward scan and a "FRO" pulse from the downward scan. The elapsed time between the two pulses establishes the elevation angle of the aircraft, and thus its displacement from the glide path angle selected by the pilot.

Because the aircraft flight control system is considerably more responsive to changes in elevation than to changes in azimuth, the elevation scan cycle is repeated 39 times per second, as compared to 13 times per second for the azimuth cycle.
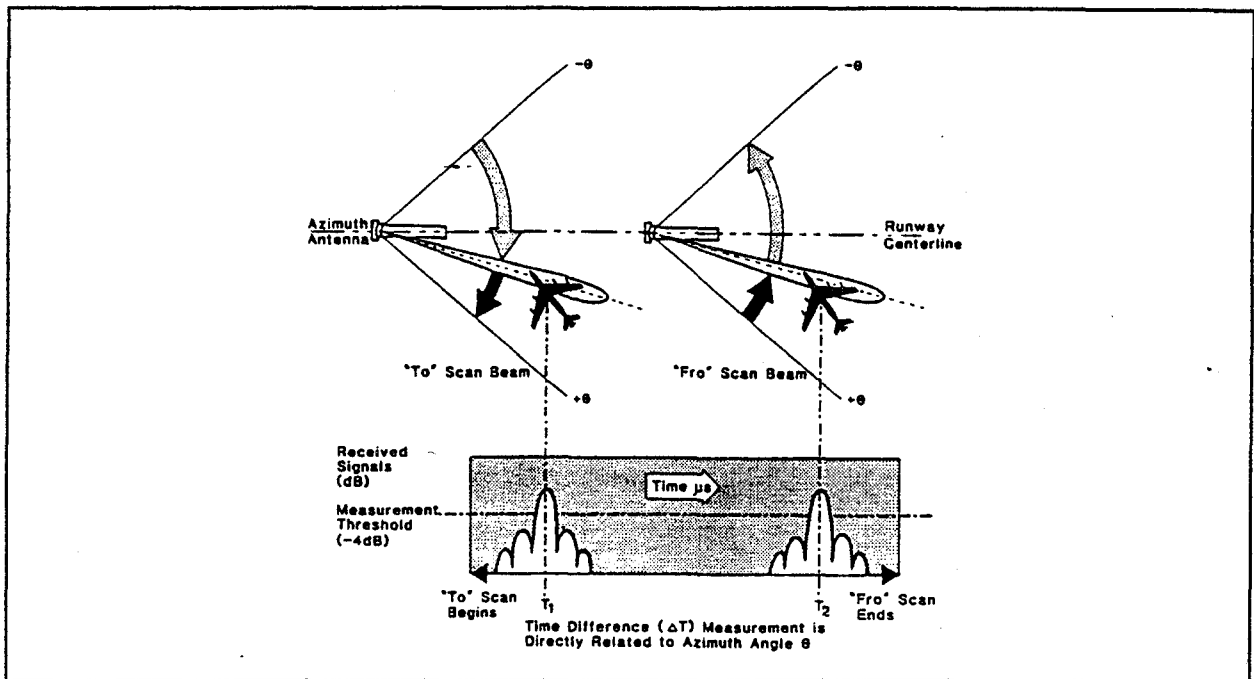
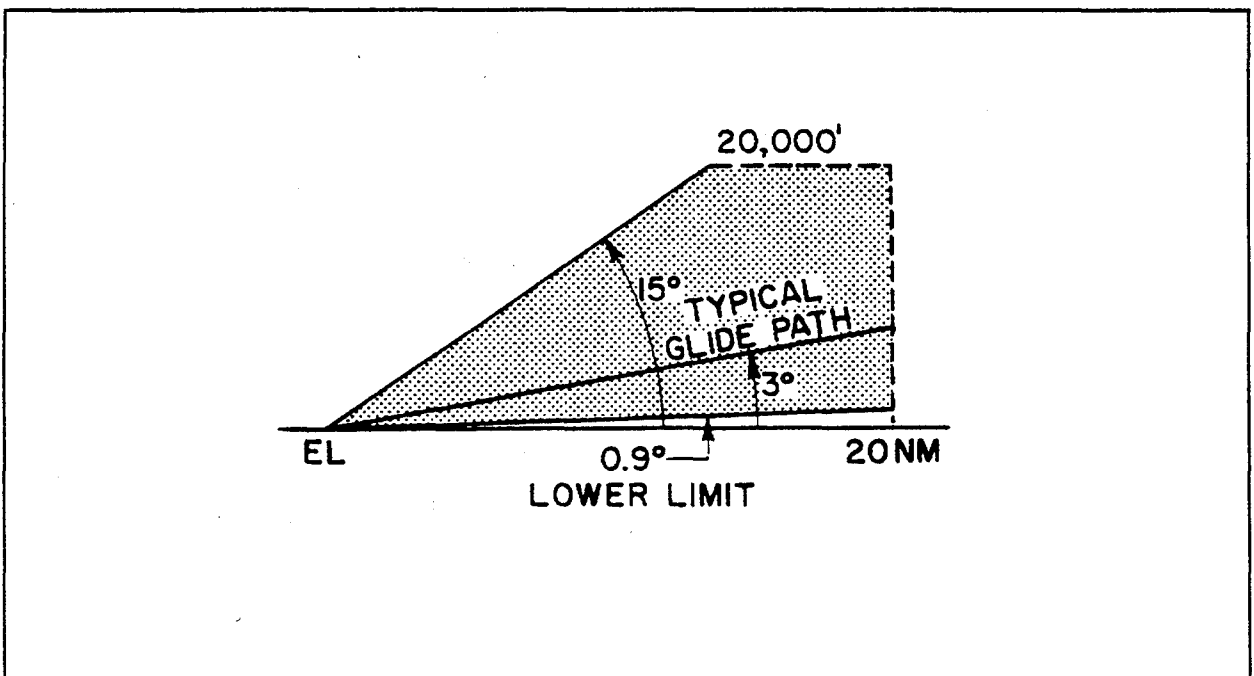FIGURE I-1.   ANGULAR MEASUREMENT PRINCIPLE.

FIGURE I-2.   ELEVATION COVERAGE.

I.2 FACILITY SITING CONSIDERATIONS.

I.2.1 General.

The electronic equipment for the AZ and back azimuth (BAZ) stations are mounted inside the antenna enclosures. The EL and DME/P stations are contained in weatherproof enclosures.

I.2.2 AZ.

The desired location for the AZ will be on the extended runway centerline between 1000 and 1500 feet beyond the stop end of the runway, as shown in figure I-3. If a location on the centerline is not feasible, the AZ station should be located within the alternate siting area shown in figure I-3. The penalty will be a slightly higher decision height. Care must be taken to keep the AZ station clear of jet blast areas.

I.2.3 EL.

The desired location for the EL station is 400 feet offset from the runway centerline. The range of offset distances for Cat I facilities is from a minimum of 250 feet to a maximum of 600 feet. At Cat II and III locations, the EL station must not be closer than 325 feet. As shown in figure I-4, the longitudinal displacement distance from the threshold of the landing runway is chosen to provide an threshold crossing height (TCH) of 50 feet.

Like the ILS glide path, the MLS glide path has a conical characteristic. Because the elevation station is offset from the runway centerline, the glide path along the runway centerline is a hyperbolic curve, which flares slightly above the straight line path along the boresight of the antenna. This effect increases if the offset distance is increased, or if a higher glide path angle is selected for the MLS approach.

To minimize shadowing and multipath effects, the EL station should, if possible, be sited on the opposite side of the runway from the entry taxiway, as shown in figure I-4.

I.2.4 DME/P.

The preferred location of the DME/P is at the AZ site. However, the antenna can be moved up to 450 feet, if necessary, to avoid penetration of obstacle clearance surfaces, and approach light planes. MLS facility configurations can be varied to meet operational requirements. For example, an MLS has been installed at Jasper, Alberta, Canada, with the DME element collocated with the EL, instead of the AZ element, in order to reduce the shadowing effects of a nearby mountain. MLS installations for heliports may have their AZ, EL, and DME elements collocated.
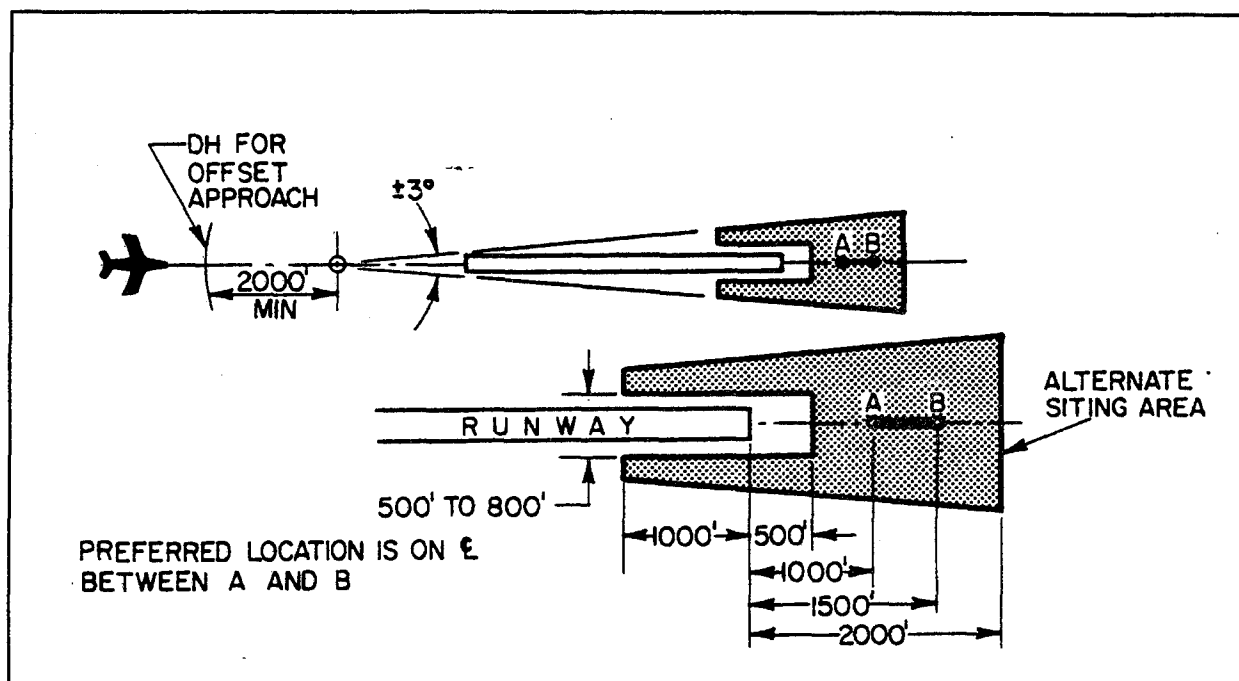
I-4

FIGURE I-3.   PREFERRED AND ALTERNATE LOCATIONS FOR THE APPROACH
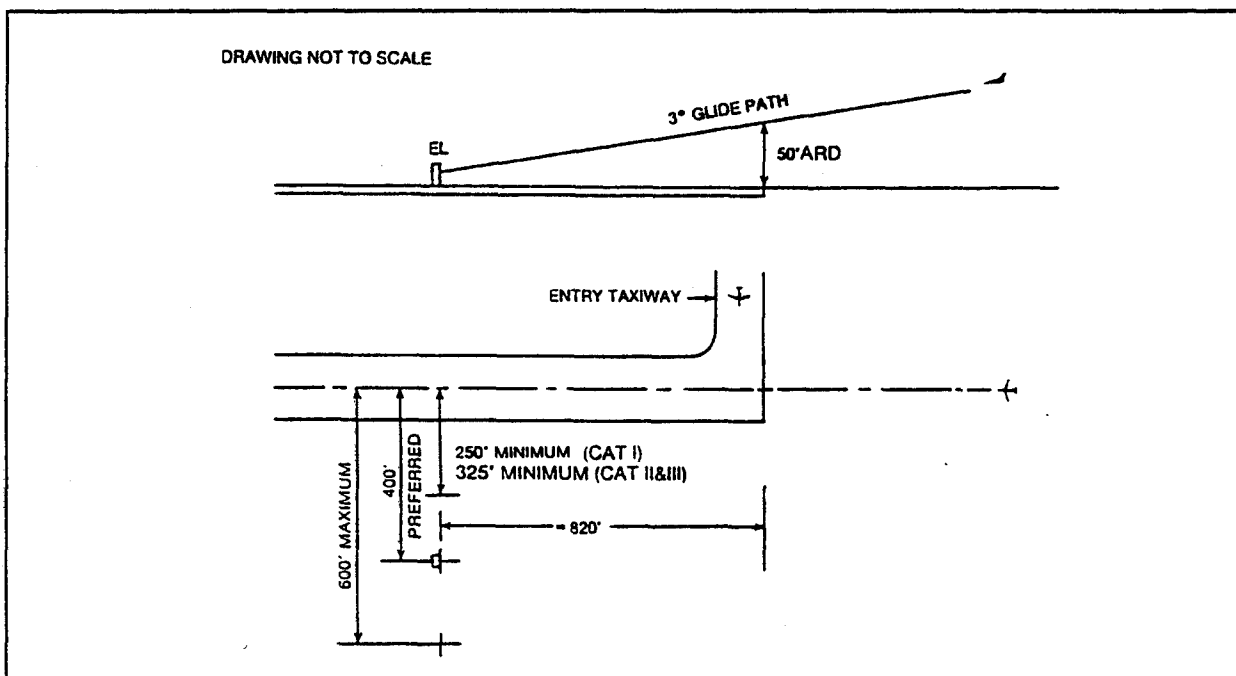AZIMUTH STATION.

FIGURE I-4.   PREFERRED AND ALTERNATE LOCATIONS FOR ELEVATION
STATION.

I-5

I.2.5 BAZ.

The siting criteria for the BAZ is the same as that shown for the AZ in figure I-3.

I.2.6 Out-of-Coverage Indication (OCI) Signals.

It is desirable for the MLS cockpit display to show a flag warning whenever the aircraft is outside of the normal service volume of the MLS. However, in some out-of-coverage areas, spurious MLS signals caused by terrain reflections, or other anomalies, may still be present. To prevent false guidance from this cause, provision is made to transmit OCI pulses from directional antennas. This will result in a flag warning on the deviation indicator in the cockpit. OCI signals can be provided up to eight regions outside the azimuth service volume, and two regions outside the EL service volume, as needed.

Figure I-5, which is a magnified view of the AZ time slot, shows the location of the AZ OCI pulses within this time slot. When the aircraft receives an OCI pulse, which is stronger than the scanning signal, a flag warning indication appears on the MLS cockpit display.

The OCI feature is intended to be implemented only as needed, on a case-by-case basis. Figure I-6 shows a typical scenario where AZ OCI signals might be required.

I.2.7 Clearance Guidance Signals

Although most MLS facilities will have a proportional coverage of +/- 40° in azimuth, a minimum installation would cover only +/- 10°. For any AZ equipment which provided less than +/- 40° of proportional coverage, clearance guidance (fly left/fly right) signals will be provided to produce a minimum guidance sector of +/- 40°, as shown in figure I-7.

Within a clearance guidance sector, the azimuth guidance is not proportional to the angular displacement of the aircraft from the approach course. It is a full-scale left or right indication of which way the approaching aircraft should turn in order to enter the proportional coverage region.

The clearance signals are comprised of four pulses, two of which are transmitted in pairs from directional antennas, into the fly-left and fly-right clearance sectors. Figure I-8 shows the location of the clearance pulses within the AZ function time slot, adjacent to the TO and FRO scanning beams. Pulses No. 1 and No. 4 are transmitted into Sector A. The wide time spacing between these two pulses produces a fly-left indication on the cockpit display. Pulses 2 and 3 are transmitted into Sector C. Their narrow time spacing produces a fly-right indication on the display.
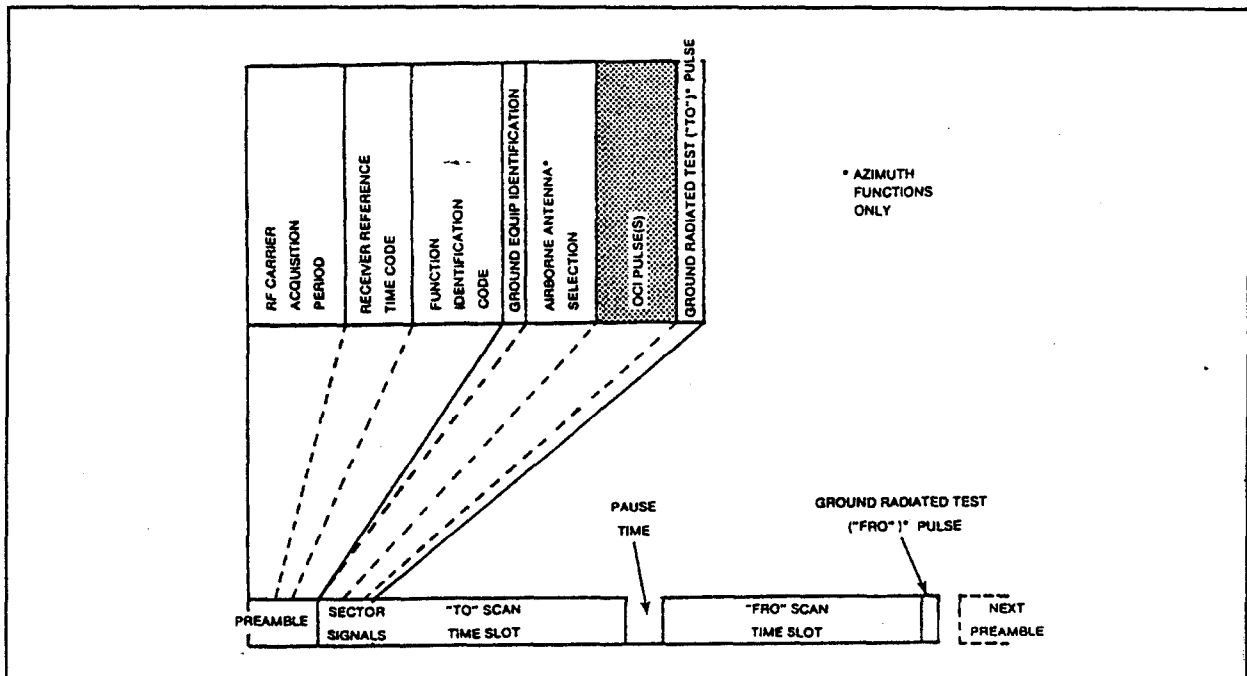
Figure I-5.   LOCATION OF OCI PULSES IN AZIMUTH TIME SLOT.
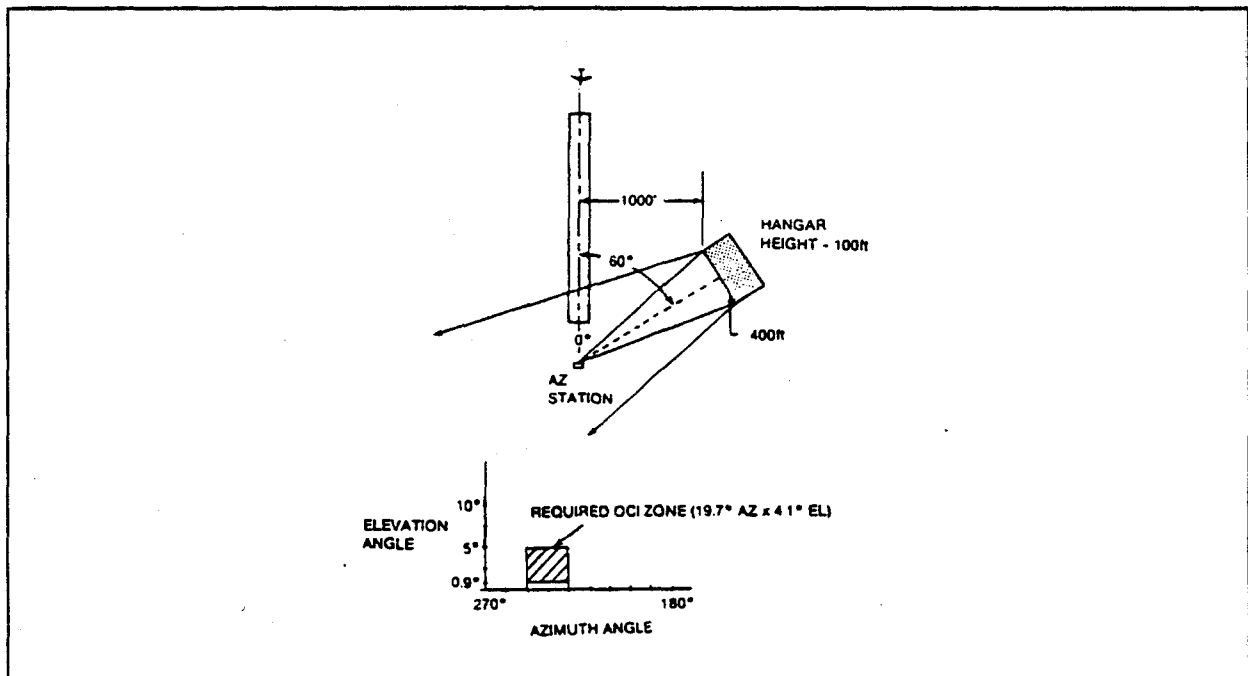
FIGURE I-6.   NEED FOR OCI SIGNALS.

I-7

A - CLEARANCE GUIDANCE SECTOR
(FLY LEFT)

B - PROPORTIONAL GUIDANCE SECTOR

C - CLEARANCE GUIDANCE SECTOR
(FLY RIGHT)
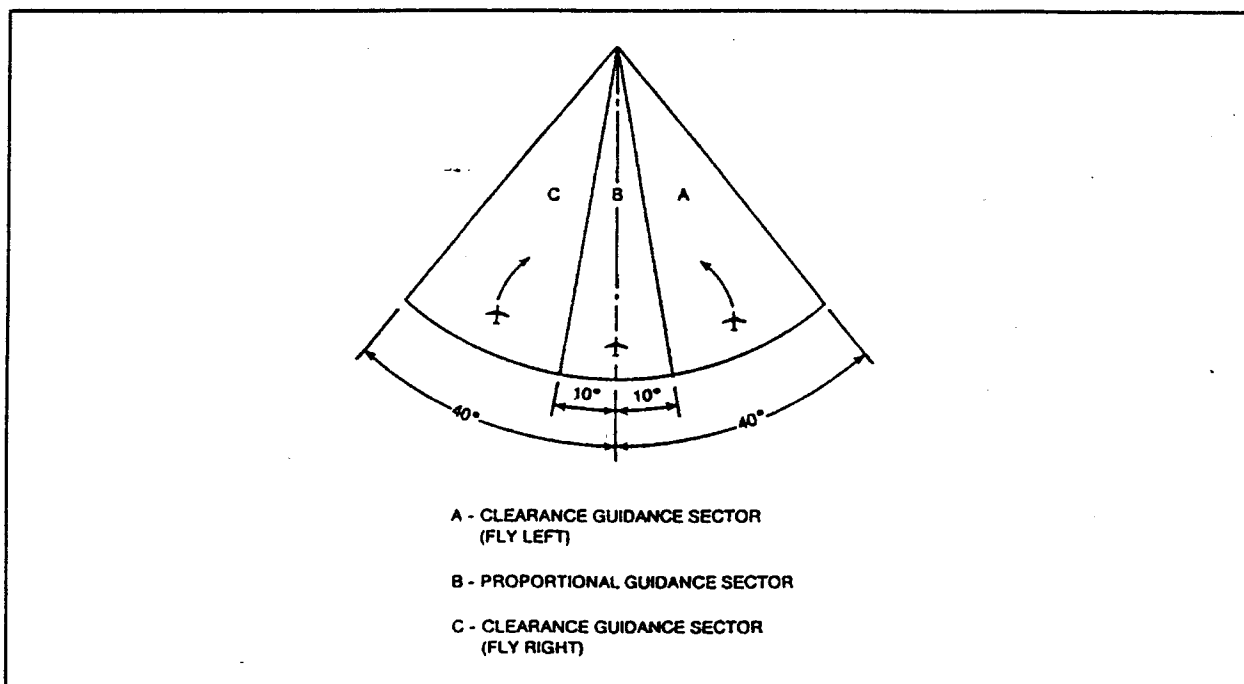
FIGURE I-7.   CLEARANCE GUIDANCE SECTORS.

I.2.8   Critical Areas

Critical areas are regions around the MLS stations wherein objects, vehicles, or aircraft may cause serious signal degradation as a result of multipath or shadowing.   Care must be taken that roads and taxiways do not pass through these critical areas unless it has been determined that the vehicular traffic will not interfere with the transmitted signals.   If the traffic is proven to interfere and cannot be rerouted, traffic can be restricted during instrument approach operations.   Definitions for MLS critical areas are now being developed.

I.2.9   Shadowing

To minimize the effects of shadowing of the EL beam by aircraft awaiting takeoff clearance, it is usually desirable to site the EL station on the opposite side of the runway from the entry taxiway, as shown in figure I-4.   Another factor which should be considered is the shadowing of the EL beam by nearby buildings or other obstacles, as shown in figure I-9.   In some cases the effects of shadowing can be reduced by adjustment of the EL station location in order to place the shadows in a non-critical portion of the coverage area.   The simplicity of siting an EL station facilitates this solution.

FIGURE I-8.   CLEARANCE GUIDANCE SIGNALS.

FIGURE I-9.   SHADOWING AND MULTIPATH AREAS.

I-9

I.2.10 Multipath.

The MLS has to operate in an airport environment that is subject to
multipath (reflections) from hangers, aircraft, and other objects
in the vicinity. Potentially, these effects can introduce errors
in the guidance signals. Therefore, careful attention has been
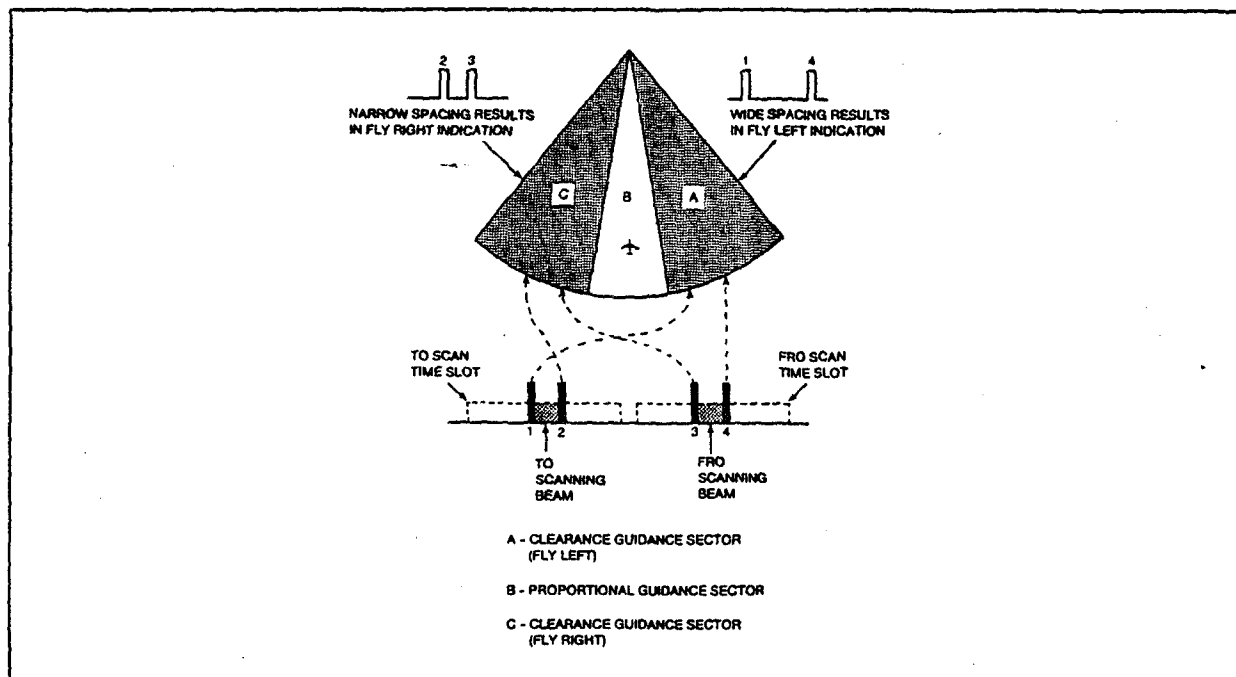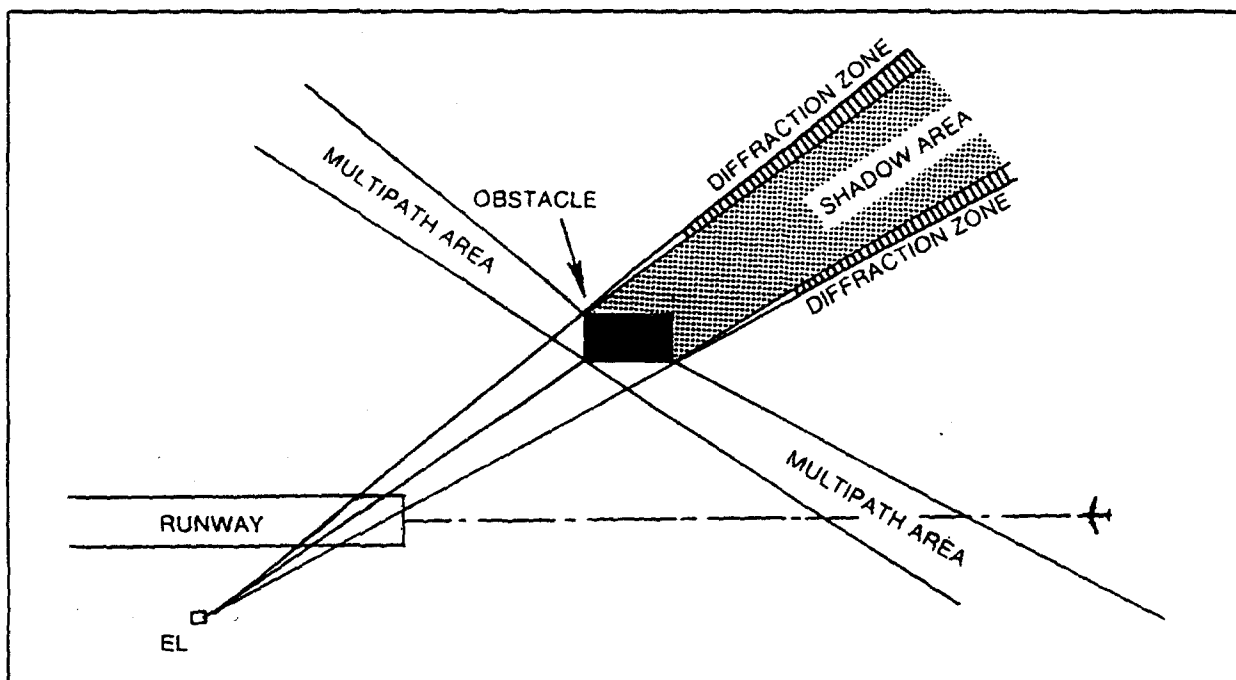given in the design of the system, to resist the effects of
multipath.

Because of the short wavelengths used by the MLS, relatively small
flat surfaces can produce specular (mirror-like) reflections of
high intensity. However, these reflections are highly variable in
amplitude, phase, and duration. The MLS angle (azimuth and
elevation) receiver is designed with acquisition and validation
circuits, to select and process the strongest and most persistent
signal. This allows the receiver to operate in strong multipath
environments.

Three basic principles are used in the system design to reduce the
effects of multipath:

    a.   Try to keep multipath signals from arriving in the
         receiver at the same time as the scanning beams.

    b.   If multipath signals do arrive at the same time, reduce
         multipath signal magnitude to a negligible value.

    c.   Average rapidly varying signal components.

The received MLS scanning beam may be distorted if interfering
signals are present at the same time the direct scanning beam is
received. This situation, known as in-beam multipath, is shown in
figure I-10. It can occur if the separation angle between the
aircraft and the reflecting object is within 1.7 beamwidths.

However, if the separation angle is more than 1.7 beamwidths, the
reflected signal will arrive at a different time than the direct
signal, and therefore will not distort the beam envelope, or cause
a guidance error. This situation, which is shown in figure I-11,
is known as out-of-beam multipath. One way to reduce in-beam
multipath effects is to use an antenna with a narrower beam width.
Another way to reduce multipath effects is to design the antenna
patterns with the lowest possible sidelobe levels.

The vertical pattern of the AZ antenna is designed with a rapid
reduction in amplitude (a sharp cutoff) on the lower side. The
reduction is approximately 6 dB per degree below the horizontal.
This ensures that close-in reflections, from the ground in front of
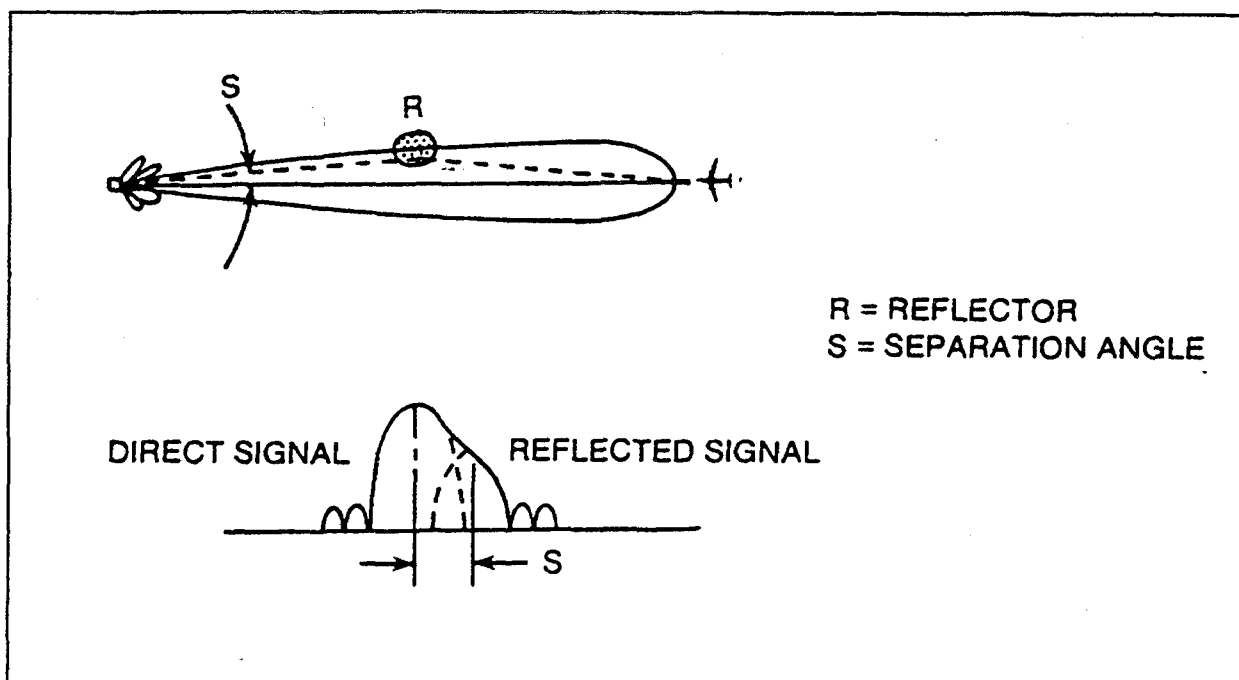the antenna, are much weaker than the direct signal received in the
aircraft.

R = REFLECTOR
S = SEPARATION ANGLE

DIRECT SIGNAL   REFLECTED SIGNAL

FIGURE I-10.   IN-BEAM MULTIPATH.

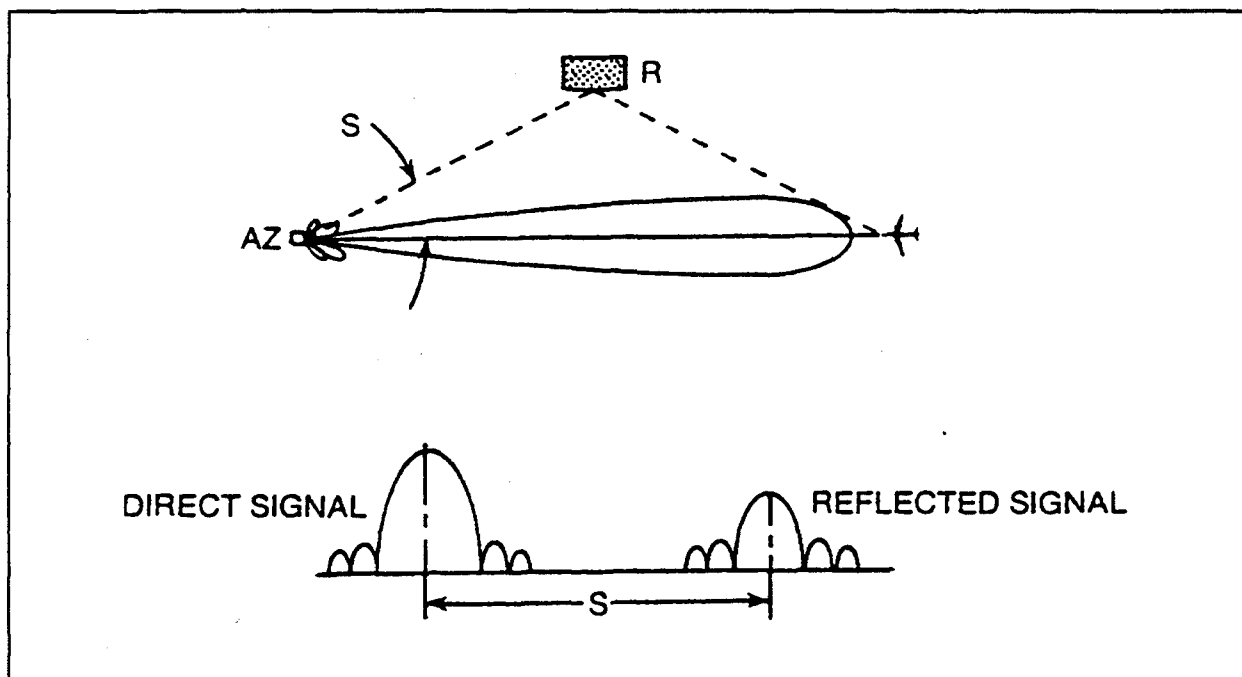DIRECT SIGNAL   REFLECTED SIGNAL

FIGURE I-11.   OUT-OF-BEAM MULTIPATH.

If there is a strong reflector on one side of the final approach course (i.e. mountain range), the scan of the azimuth antenna can be tailored to not illuminate the mountain (see figure I-12). The horizontal pattern of the elevation antenna is designed with a rapid reduction in amplitude beyond 40° from the centerline.

Although multipath can be strong for short periods, it is not persistently stronger than direct signals. Fortunately, the high data rates (13 scans-per-second for azimuth and 39 scans-per-second for elevation) make it possible to average the direct and multipath signals. Averaging by the receiver filter serves to reduce the rapidly varying azimuth and elevation errors as the aircraft flies through the multipath interference region.

The distance-measuring portion of the MLS is designed to resist multipath effects which would otherwise introduce range errors. This is of particular interest when the aircraft gets down to a low altitude in the final part of the approach where range accuracy is most important. For this reason, the DME/P of the MLS uses a very accurate pulse processing method, more resistant to multipath effects, when operating within 7 nautical miles of the ground station. This mode of operation is called the Final Approach (FA) Mode.
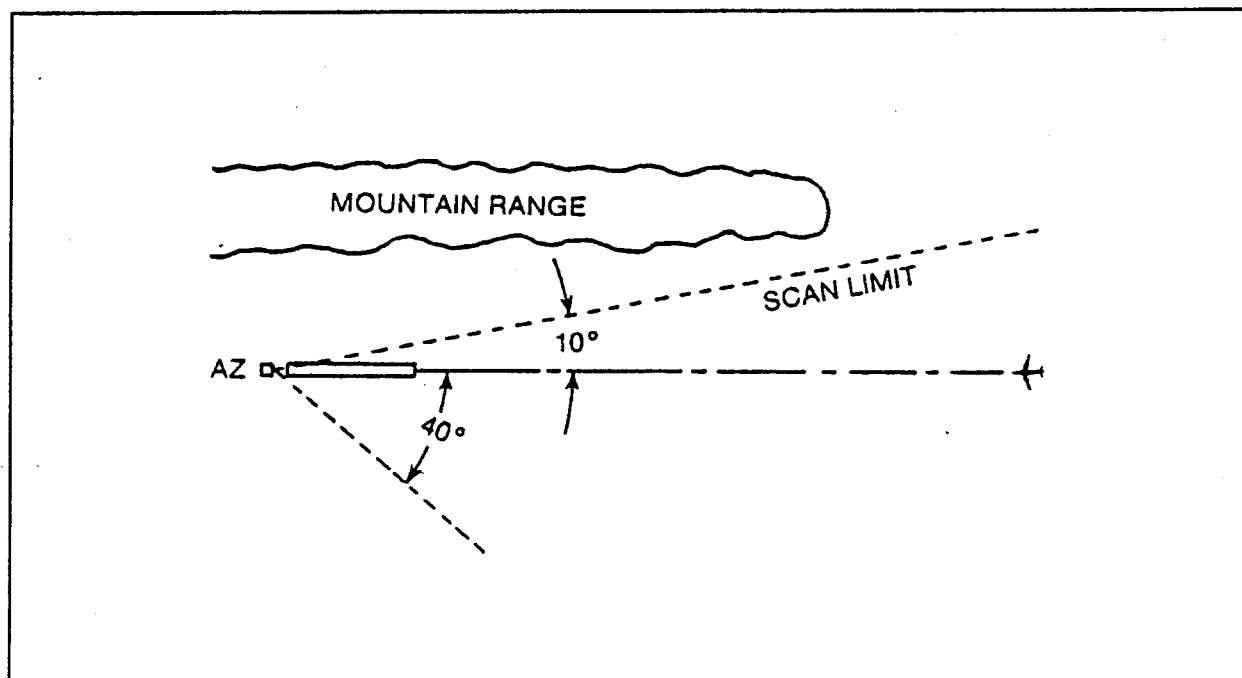

FIGURE I-12. SCAN LIMITED TO AVOID MULTIPATH.

Appendix J
An Introduction to the MLS Math Model

J.1 PURPOSE.

This section introduces the Microwave Landing System (MLS) Mathematical Model for interested persons not familiar with the model's purpose and features. It discusses the format of the model, the input and output parameters, and additions and improvements planned for future versions of the model.

J.2 INTRODUCTION.

The MLS Mathematical Model is a computer simulation of the effects of an airport environment on the MLS signal. It is used to provide guidance in the selection of MLS and siting configuration for a specific airport environment, by predicting the errors due to multipath in that environment.

J.3 THE MODEL SOURCE CODE.

The complete model consists of four computer programs. The flow diagram shows the relationships among these four programs. The source code, about 40,000 lines, is written in ANSI standard FORTRAN-77, and has been successfully implemented on a variety of mainframe and personal computers.

A complete site simulation is performed in two stages. The first stage is the execution of program BMLST. This is the propagation (or transmitter) model, a simulation of the signal in space as it interacts with objects in the airport environment. Output from BMLST is written to two files. One file provides plotting information to BPLOTT, a program that plots the multipath and shadowing effects on the signal from each of the ground stations--- AZ, EL and DME/P. The second file is the input file to the second stage of simulation.

In this second stage, program BMLSR simulates the behavior of an MLS receiver. At each point along the flight path, the system (or receiver) model evaluates the signal it is receiving in order to distinguish the direct beam from any caused by multipath. Once the receiver is confident that it has acquired the direct signal, it compares this MLS angle with the true position of the aircraft (as defined by the flight path coordinates, discussed in the section on input parameters). The angular difference between these positions is the error at that flight path point for that system (AZ or EL). This error is written to an output file, which is used by program BPLOTR to plot the error data. BPLOTR also filters the error data with both path following error (PFE) and control motion noise (CMN)

with both path following error (PFE) and control motion noise (CMN) algorithms, and plots the filtered data with appropriate error tolerances (discussed in the section on output). These plots allow the user to evaluate the receiver errors and determine whether or not they fall within acceptable tolerance limits.

J.4 INPUT PARAMETERS.

The model accepts input from an ASCII text input file consisting of 13 sections of input data. The input data fall roughly into three categories: (1) a description of the airport environment, (2) the configuration of the MLS and DME/P systems, and (3) a specification of the flight path of the receiver.

The airport environment is described by coordinate information relative to the runway. The coordinate system assumes an origin at the centerline of the stop end of the runway. It is a right-handed coordinate system. The positive X axis lies along centerline points toward the threshold and the positive Z axis points up. Each obstacle must be identified in separate sections of the input file as to its potential effect on the MLS signal---reflective (scattering) or diffractive (shadowing). Obstacles that can be defined include buildings, aircraft (shadowing aircraft can be moving), terrain features, and a runway hump. Obstacles are represented by simple geometric shapes, such as rectangles, triangles, and cylinders. User input defines the location of the object, and whatever additional information is required (vertical orientation, surface characteristics, velocity, etc.).

For the configuration of the ground systems, the user specifies the location and type of each transmitter. The user can also indicate a frequency and scan angle limits for each transmitter. The appropriate data for representing the specified transmitter type are loaded into memory by program BMLSR, and are used in the evaluation of the signal at the receiver. The receiving antenna is assumed omnidirectional. The propagation portion of the model (BMLST) assumes an omnidirectional transmitter pattern in its operation, and does not consider the characteristics of the receiver other than its location in space.

Currently, the path of the receiver is represented as a set of 2 to 36 coordinate triplets (X, Y, Z), which define the locations of the flight path waypoints. Multipath calculations are made for points between the waypoints depending on the velocity (in feet/second) and distance increment (in feet) defined by the user. These latter values are constrained by the model's assumption of a data rate of 5 hertz for the PFE and CMN filter algorithms.

J.5   OUTPUT.

Output from the math model is provided in graphic form by the two plotting programs (BPLOTT for the propagation model, BPLOTR for the system model). Output from BPLOTT includes tables of data and plots (flight path plots, airport map) that allow the user to verify the input data. In addition, a multipath plot shows the multipath/direct ratio in decibels, for each point along the flight path, for each of the six highest multipath sources in the environment. This is accompanied by a plot of the separation angle in degrees (for AZ and EL), or the time delay in nanoseconds (for DME/P). If the user has specified shadowing obstacles, a shadowing plot shows the effect of the simulated shadowing obstacles on the magnitude of the direct signal. For both scattering and shadowing, each transmitter is plotted separately, as requested by the user.

The output from BPLOTR is a plot of the angle error, in degrees, for each system. The DME/P interrogator is not implemented by the system model at this time. Error plots are provided in four formats. The static error shows the raw error at each receiver point. The dynamic error also shows the raw error with account taken of the movement of the receiver. PFE and CMN plots show the error as filtered by these algorithms, respectively. In addition, tolerance and coverage limits are calculated, based on (FAA) specifications, and are displayed on the filtered error plots. The user can then see, at a glance, whether or not the MLS signal goes out of tolerance at any point along the flight path. If it does not, it is reasonable to conclude that the airport environment, as defined, will not adversely effect the MLS signal.

J.6   THE FUTURE OF THE MLS MATH MODEL.

The model, as described above, is the current version distributed by the FAA to users throughout the world. However, the model is not considered to be in final form. Plans are being made to release version 3.0 of the model, which will include the following features:

a. Implementation, in the system model, of a DME/P interrogator.

b. Implementation of a measured flight path. This option will permit the model to read flight path coordinates from a separate input file, which might be created from actual flight data.

c. Inclusion of additional transmitter antenna patterns.

d. Assignment of specific dielectric constants, for each possible surface material, for scattering building plates.

Additions and improvements to the model will continue after the release of version 3.0. These additions and improvements will include implementation of an orbit flight path option, improved algorithms for simulating runway hump shadowing and ground plate scattering, the addition of the ability to simulate shadowing by trees, and other features, as required.